

**THE IMPACT OF FEMALE SEX HORMONES ON CIGARETTE SMOKE-INDUCED
AIRWAY REMODELLING AND MUCUS PRODUCTION**

by

ANTHONY TAM

B.Sc., The University of British Columbia, 2009

A THESIS SUBMITTED IN PARTIAL FULFILLMENT OF
THE REQUIREMENTS FOR THE DEGREE OF

DOCTOR OF PHILOSOPHY

in

THE FACULTY OF GRADUATE AND POSTDOCTORAL STUDIES

(Experimental Medicine)

THE UNIVERSITY OF BRITISH COLUMBIA

(Vancouver)

December 2015

© Anthony Tam, 2015

Abstract

Adjusting for amount of smoking, women have a 50% increased risk of COPD compared with men. It is not known what the anatomic basis/mechanism(s) of these sex-related differences in COPD might be. The main objective of this study is to characterize the impact of female sex hormones on chronic cigarette smoke-induced airway remodelling and emphysema in a murine model of COPD. We showed here for the first time that smoke-induced COPD in female compared to male mice have increased small airway remodelling, and may be biologically driven by estrogen through down-regulation of antioxidant defences and activation of TGF β 1 signalling, resulting in increased expression of collagen matrix in the airway walls. These effects can be ameliorated by ovariectomy before smoke exposure or use of the estrogen antagonist, tamoxifen, during smoke exposure, suggesting that estrogen is involved in this process.

Using the flexiVent system to assess the functional relationship with the observed structural changes, we showed evidence of cigarette smoke-induced lung abnormalities. Tissue damping (G), and complex input resistance of the respiratory system (Zrs) at low oscillating frequency were elevated in female compared to male mice after smoke exposure, and this effect was attenuated after ovariectomy. Quasistatic pressure-volume curve revealed a decrease in inspiratory capacity in female mice but not in male mice after smoke exposure, and this effect was attenuated after ovariectomy. Chronic smoke exposure did not increase goblet cell expression in the distal airways of all groups, suggesting that the increase in distal airway resistance in smoke-exposed female mice is unlikely to be derived from luminal exudates.

Finally, using a human bronchial epithelial cell culture model in air liquid interface, we showed that transfection with nuclear factor of activated T-cell (NFAT)c1 or NFATc2 siRNA blunted estrogen or progesterone-induced increase in MUC5AC mRNA expression, respectively.

Collectively, our data showed that estrogen may be involved in the excess risk for small airways disease in a mouse model of COPD, and MUC5AC expression is regulated by estrogen and progesterone via NFATc1 and NFATc2 in normal human bronchial epithelial cells.

Preface

The following articles have been incorporated in part or in whole into chapters in this thesis:

Tam A, Wadsworth SJ, Dorscheid DR, Man SFP, Sin DD. Airway epithelium – More than just a structural barrier. *Therapeutic Advances and Respiratory Diseases*. 2001 5:255 (PMID: 21372121). I wrote the first draft of this review article. All authors have read and participated in critical revision of the paper.

Part of this published reviewer article is in chapter 1.

Tam A, Wadsworth SJ, Dorscheid DR, Morrish D, Man SFP, Sin DD (2011). The role of female sex hormones on lung function chronic lung diseases. *BMC Women's Health* 11:24 (PMID: 21639909). I wrote the first draft of this review article. All authors have read and participated in critical revision of the paper.

Part of this published reviewer article is in chapter 1.

Tam A, Sin DD (2012). Pathobiologic mechanisms of chronic obstructive pulmonary disease. *Medical Clinic of North America* (PMID: 22793938). I wrote the first draft of this review article. All authors have read and participated in critical revision of the paper.

Part of this published reviewer article is in chapter 1.

Tam A, Sin DD (2013). Why are women more vulnerable to chronic obstructive pulmonary disease? *Expert Review Respiratory Medicine* 7(3), 197-199 (PMID: 23734641). I wrote the first draft of this review article. All authors have read and participated in critical revision of the paper.

Part of this published reviewer article is in chapter 1.

Tam A, Churg A, Wright JL, Zhou S, Kirby M, Coxson HO, Lam S, Man SFP, Sin DD. Sex differences in airway remodeling in a mouse model of chronic obstructive pulmonary disease. *American Journal of Respiratory and Critical Care Medicine*. 2015 (PMID: 26599602). (Epub ahead of print).

Reprinted with permission of the American Thoracic Society. Copyright © 2015 American Thoracic Society.

Andy Churg and Joanne Wright quantified the linear mean intercepts and airway wall area from histologic sections. Jason Hua was responsible for cigarette exposure to the animals and regular health maintenance. Steven Zhou performed gene expression experiments and 3-nitrotyrosine ELISA measurements. Miranda Kirby, Harvey Coxson and Stephen Lam performed airway wall thickness quantification by optical coherence tomography. I was involved in the remaining portions of the experiments. All authors have read and participated in critical revision of the paper. This study was approved by the Animal Care Committee from the University of British Columbia (A11-0149).

Part of this published research article is in chapter 2, 3 and 4.

Tam A, Bates JHT, Churg A, Wright JL, Zhou S, Man SFP, Sin DD. Sex-related differences in pulmonary function measurements following 6 months of cigarette exposure: Implications for sexual dimorphism in mild COPD.

Data presented in chapter 3 was conducted in collaboration with Andy Churg and Joanne Wright. Jason Hua was responsible for cigarette exposure to the animals and regular health maintenance. Dr. Yuki Hirano assisted in all surgical procedures and tissue extractions. I was involved in conducting lung function measurement using the FlexiVent, and analyzing all data. Jason Bates was involved in interpreting the data with critical revisions. All authors have read and participated in critical revision of the paper. This study was approved by the Animal Care Committee from the University of British Columbia (A11-0149).

Part of this unpublished research article in preparation is in chapter 3.

Tam A, Wadsworth SJ, Dorscheid DR, Man SFP, Sin DD (2014). Estradiol enhances mucus synthesis in human bronchial epithelium. PloS ONE (PMID: 24964096).

I conducted all experiments, analysis and wrote the first draft of this manuscript. All authors have read and participated in critical revision of the paper. Research conducted in this chapter was approved by the University of British Columbia/Providence Health Care Research Ethics Board (Number H11-02151 and A13-0207).

Part of this published research article is in chapter 5.

Tam A, Wadsworth SJ, Dorscheid DR, Hackett TL, Man SFP, Sin DD. Silencing NFATc2 by siRNA blunted progesterone-induced increase in MUC5AC synthesis in human bronchial epithelial cells.

Tillie Hackett provided the paraffin-embedded human tissue sections and Furquan Shaheen provided assistance on immunohistochemical staining procedures. I conducted all experiments, analysis and wrote the first draft of this manuscript. All authors have read and participated in critical revision of the paper. Research conducted in this chapter was approved by the University of British Columbia/Providence Health Care Research Ethics Board (Number H11-02151 and A13-0207).

Part of this unpublished research article in preparation is in chapter 6.

Table of Contents

Abstract.....	ii
Preface.....	iv
Table of Contents.....	vi
List of Tables	xii
List of Figures.....	xiii
List of Abbreviations	xvi
Acknowledgements.....	xvii
Dedication.....	xviii
Chapter 1 : Introduction.....	1
1.1 Epidemiology on sex differences in COPD	1
1.2 Phenotypes of COPD	2
1.3 Structure and function of the respiratory system	4
1.4 Clinical measurement of lung function	5
1.5 Animal model of COPD.....	7
1.6 Lung function measurements in murine models	9
1.7 Structure of airway mucosa.....	11
1.7.1 Airway epithelium	13
1.7.2 Mucociliary clearance and regulation of air surface liquid	15
1.7.3 Airway wall.....	17
1.8 Properties of female sex hormones	19
1.8.1 Sex hormone receptors: lung physiology.....	19
1.8.2 Sex hormones and menstrual cycle.....	21
1.8.3 Delivery of sex hormones to target tissues	21
1.8.4 Sex hormone receptor activation	22

1.9	Effects of cigarette smoke on the airway mucosa	23
1.9.1	Cigarette smoke and oxidant/antioxidant imbalance	23
1.9.2	Xenobiotic metabolism	23
1.9.3	Oxidative stress and airway remodelling	25
1.9.4	Cigarette smoke and inflammation in the lungs	27
1.9.5	Structural damage and tissue repair/remodelling.....	27
Chapter 2 : Sexual Dimorphism in Structural Differences in a Mouse Model of Chronic Obstructive Lung Disease		29
2.1	Introduction	29
2.2	Materials and methods	30
2.2.1	Animal smoke exposure.....	30
2.2.2	Morphometric measurements.....	30
2.2.3	Immunohistochemical staining for neutrophils and macrophages.....	31
2.2.4	Immunofluorescence staining for Ki67 protein	31
2.2.5	Statistics	32
2.3	Results	32
2.3.1	Female mice showed greater morphologic small airway remodelling than male and ovariectomized mice after smoke exposure.....	32
2.3.2	Distal airways in female mice have greater epithelial cell count and Ki67-positive cells than male and ovariectomized mice after smoke exposure.....	36
2.4	Discussion	39
Chapter 3 : Sex-Related Differences in Pulmonary Function Measurements Following 6 Months of Cigarette Exposure: Implications for Sexual Dimorphism in Mild COPD		42
3.1	Introduction	42
3.2	Materials and methods	43
3.2.1	Animals.....	43
3.2.2	Smoke exposure	43

3.2.3	Pulmonary function test	43
3.2.4	Statistics	45
3.3	Results	45
3.3.1	Female mice have increased tissue damping than male and ovariectomized mice after smoke exposure.	45
3.3.2	Female mice have greater respiratory resistance than male and ovariectomized mice after smoke exposure.	45
3.3.3	Female mice have lower inspiratory capacity than male and ovariectomized mice after smoke exposure.	49
3.3.4	Inspiratory capacity does not depend on whole body weight of mice	49
3.4	Discussion	52
Chapter 4 : Female Mice Have Increased Oxidative Stress and Airway Remodelling After Chronic Smoke Exposure: Implication for Sexual Dimorphism in Mild COPD.....		
4.1	Introduction	55
4.2	Materials and methods	56
4.2.1	Animal smoke exposure.....	56
4.2.2	Laser-capture micro-dissection and real time PCR	56
4.2.3	Trolox-equivalent antioxidant capacity	57
4.2.4	Dihydroethidium labelling	58
4.2.5	ELISA assays for 3-nitrotyrosine and active TGF β 1.....	58
4.2.6	Immunofluorescence staining for active TGF β 1	59
4.2.7	Isolation of primary fibroblasts and bronchial epithelial cell culture	59
4.2.8	Uteri epithelial thickness.....	60
4.2.9	Statistics	60
4.3	Results	60

4.3.1	Increased small airway remodelling was associated with impaired antioxidant gene expression in response to cigarette exposure in female mice, and this effect was attenuated by ovariectomy.	60
4.3.2	Female mice showed greater pulmonary oxidative stress than male mice, and this effect was attenuated by ovariectomy.	63
4.3.3	Female mice showed greater airway-specific active TGF β 1 protein and downstream signalling compared to male or ovariectomized mice	65
4.3.4	Tamoxifen attenuated smoke-induced increase in Cyp1a1 mRNA expression in the airways of female mice after 1 month of smoke exposure	67
4.3.5	Tamoxifen attenuated smoke-induced increase in Nox4 mRNA expression in the airways of female mice after 1 month of smoke exposure	69
4.3.6	Estrogen differentially enhanced smoke-induced increase in Cyp1a1 but not Cyp1b1 and Nqo1 mRNA expression in normal human bronchial epithelial cells.....	71
4.4	Discussion	73
Chapter 5 : Estrogen Increases Mucus Synthesis in Bronchial Epithelial Cells.....		77
5.1	Introduction	77
5.2	Materials and methods	78
5.2.1	Cell cultures	78
5.2.2	Histological staining	79
5.2.3	Transcription factor activation protein array	80
5.2.4	Real time PCR.....	80
5.2.5	Western blot analysis	81
5.2.6	Small interfering RNA treatment.....	82
5.2.7	DNA gel	82
5.2.8	Cytotoxicity.....	83
5.2.9	Statistical analyses	83
5.3	Results	84
5.3.1	Estrogen receptor beta is the predominant form in the human airway epithelium .	84

5.3.2	Estradiol increases PAS-positive cell count in ALI cultures.	87
5.3.3	Estradiol increases MUC5AC expression in ALI cultures	89
5.3.4	Estradiol increases nuclear factor of activated protein c1 (NFATc1).....	91
5.3.5	NFATc1 siRNA attenuated estradiol-induced increase in MUC5AC expression ..	94
5.4	Discussion	98
Chapter 6 : Silencing NFATc2 by siRNA Blunted Progesterone-Induced Increase in MUC5AC Synthesis in Human Bronchial Epithelial Cells.....		
		102
6.1	Introduction	102
6.2	Methods.....	103
6.2.1	Cell cultures	103
6.2.2	Histological staining	104
6.2.3	Transcription factor activation protein array	105
6.2.4	Real time PCR.....	105
6.2.5	Western blot analysis	105
6.2.6	Small interfering RNA treatment.....	106
6.2.7	DNA gel	106
6.2.8	Statistical analysis.....	107
6.3	Results	107
6.3.1	Progesterone receptor expression in human airway tissues and ALI cultures	107
6.3.2	Mifepristone attenuated progesterone-stimulated increase in PAS-positive cell staining in ALI cultures	109
6.3.3	Progesterone increases nuclear factor of activated T- cell protein (NFAT)	111
6.3.4	Progesterone differentially increased NFATc2 mRNA in 1HAE ₀ cells	114
6.3.5	NFATc2 siRNA blunted progesterone-induced increase in MUC5AC mRNA ...	114
6.4	Discussion	117
Chapter 7 : Conclusion.....		
		121

7.1	Limitations and strengths of the studies	123
7.2	Future directions.....	124
	Bibliography	126
	Appendices.....	142

List of Tables

Table 1.1: Female hormone levels throughout the menstrual cycle	21
---	----

List of Figures

Figure 1.1: Lung volume compartments	6
Figure 1.2: Cellular composition in the human airway muscosa.....	12
Figure 2.1: Female mice show greater morphologic small airway remodelling (dark red = total collagen) after cigarette smoke (CS) exposure than male mice, and this effect can be prevented by ovariectomy before smoke exposure.	33
Figure 2.2: 6 months of cigarette exposure increased mean linear intercept, but no sexual dimorphism was present.	34
Figure 2.3: Absence of PAS-positive cells in the distal airways of mice after 6 months of cigarette exposure.	35
Figure 2.4: 6 months of cigarette exposure increased total airway epithelial cell count and Ki67-positive cells in female but not male mice, and these effects were attenuated in ovariectomized mice.....	37
Figure 2.5: Morphologic differentiation between ovary-intact and ovariectomized mice, and airway-specific sex hormone receptor mRNA expression.....	38
Figure 3.1: Female mice have greater tissue damping than male mice after smoke exposure, and these effects were abolished with ovariectomy.	47
Figure 3.2: Female mice have greater Zrs than male mice after smoke exposure, and this effect was abolished after ovariectomy.....	48
Figure 3.3: Female mice have lower inspiratory capacity than male mice after smoke exposure, and this effect was abolished with ovariectomy.	50
Figure 3.4: Inspiratory capacity does not depend on whole body weight of mice.	51
Figure 4.1: Female mice have an impaired antioxidant gene response to cigarette smoke compared to male mice or ovariectomized mice.	62
Figure 4.2: Female mice have increased nitrosative and oxidative stress, and increased active TGFβ1 protein expression.....	64
Figure 4.3: Female mice have increased expression of active TGFβ1 protein and TGFβ1-responsive genes in airway tissues.....	66
Figure 4.4: Tamoxifen attenuated smoke-induced increase in <i>Cyp1a1</i> mRNA expression in the airways of female mice.	68

Figure 4.5: Tamoxifen attenuated smoke-induced increase in Nox3 and Nox4 mRNA expression in the distal airways of female mice.	70
Figure 4.6: Estradiol differentially enhanced smoke-induced increase in Cyp1a1 but not Cyp1b1 and Nqo1 mRNA expression in normal human bronchial epithelial (NHBE) cells.	72
Figure 5.1: Determining the specificities for estrogen receptors and goblet cell expression	85
Figure 5.2: Estrogen receptor expression in human female airway tissues and NHBE cells in air liquid interface.	86
Figure 5.3: Effect of estradiol on periodic acid schiff (PAS)-positive cell staining in air liquid interface (ALI) cultures.....	88
Figure 5.4: Effects of estradiol on MUC5AC mRNA and protein expression in ALI cultures....	90
Figure 5.5: Transcription factor expression panel demonstrates increased total nuclear factor of activated T-cell (NFAT) protein in the nuclear fraction of primary female NHBE cells after 10^{-7} M estradiol treatment for 24h.	92
Figure 5.6: NFAT mRNA and protein expression in ALI cultures after 2 weeks of estradiol treatment.	93
Figure 5.7: Characterization of NFATc1-4 mRNA expression and effect of estradiol in 1HAE ₀ cells.	95
Figure 5.8: Effects of estradiol and NFATc1-specific siRNA on NFATc1 and MUC5AC mRNA expression in 1HAE ₀ cells.	96
Figure 5.9: NFATc1 siRNA attenuated estradiol-induced increase in NFATc1 and MUC5AC protein expression in 1HAE ₀ cells.	97
Figure 6.1: Progesterone receptor antibody specificity and protein expression in human airway epithelium.	108
Figure 6.2: Mifepristone attenuated progesterone-stimulated increase in PAS-positive cell count in ALI cultures.	110
Figure 6.3: Progesterone increases nuclear factor of activated T-cell protein (NFAT).....	112
Figure 6.4: Progesterone differentially increased NFATc2 mRNA expression in ALI cultures.	113
Figure 6.5: Progesterone stimulation transiently and differentially increased NFATc2 mRNA expression in 1HAE ₀ cells.....	115

Figure 6.6: NFATc2 siRNA blunted progesterone-induced increase in NFATc2 and MUC5AC mRNA expression. 116

List of Abbreviations

Abbreviation	Definition
1HAE ₀	human airway epithelial cell line
ALI	air liquid interface
CF	cystic fibrosis
COPD	chronic obstructive pulmonary disease
CS	cigarette smoke
CYP	cytochrome P450
DAB	3,3'-Diaminobenzidine
DMEM	Dulbecco's Modified Eagle Medium
E2	estradiol
EGF	epidermal growth factor
ER	estrogen receptor
Hmox-1	heme oxygenase
HPRT1	hypoxanthine phosphoribosyltransferase 1
HRE	hormone response element
HRP	horseradish peroxidase
IL	interleukin
LPS	lipopolysaccharride
MPP	estrogen receptor alpha antagonist [1,3-Bis(4-hydroxyphenyl)-4-methyl-5-[4-(2-piperidinylethoxy)phenol]-1H-pyrazole dihydrochloride]
MUC5AC	mucin 5AC
MUC5B	mucin 5B
NFAT	nuclear factor of activated T-cell
NHBE	normal human bronchial epithelial cells
NO	nitric oxide
NRF2/NFE2L2	nuclear factor (erythroid-derived)-like 2
NQO-1	NADPH oxidoreductase
PAS	periodic acid schiff
PHTPP	estrogen receptor beta antagonist [4-[2-Phenyl-5,7-bis(trifluoromethyl)pyrazolo[1,5-a]pyrimidin-3-yl]phenol]
PR	progesterone receptor
SEM	standard error of the mean
SHBG	sex hormone binding globulin
siCon	scramble control silencing RNA
siRNA	silencing RNA
TAM	tamoxifen
TNF	tumor necrosis factor
WB	western blot

Acknowledgements

I offer my enduring gratitude to the faculty and staff at UBC, and my previous co-operative placement internship supervisors, who have inspired and led me into the department of experimental medicine. I owe particular thanks to my primary supervisor Dr. Don Sin, co-supervisor Dr. Delbert Dorscheid, and supervisory committee member Dr. Paul Man, whose penetrating questions taught me to question more deeply in the field of pulmonary diseases and to translate basic science into the clinical settings. I thank my mentor, Dr. Samuel Wadsworth, for enlarging my vision of science and providing me advice in all aspects such as experimental designs and conducting experimental techniques at the highest quality and standard, Dr. Yuexin Li and Sheena Tam for teaching me the ELISA technique and keeping everything in order at the highest level of proficiency, and David Ngan for his assistance in the formatting of my thesis. Thank you Dr. Andy Churg and Dr. Joanne Wright for providing the smoke exposure system for our mouse model of COPD, and Steven Zhou, Jason Hua, Yeni Oh and Dr. Yuki Hirano for their technical support. I would like to extend my appreciations to Crystal Leung, Amrit Samra, Furquan Shaheen, Dr. Tillie Hackett and Dr Mark Elliott from the human tissue Biobank at the Centre for Heart and Lung Innovation for tissue processing and sectioning the ALI culture inserts for immunohistochemistry, optimizing and validating all tissue staining. I would also like to recognize the Canadian Institute of Health Research (CIHR), the Institute of Gender and Health from CIHR, and Dr. Don Sin's grant stipend for their financial support and travel awards.

Dedication

Special thanks are owed to my parents for their unconditional support, both morally and financially.

Chapter 1: Introduction

1.1 Epidemiology on sex differences in COPD

Chronic obstructive pulmonary disease (COPD) is a silent but growing epidemic in both men and women. More than 70% of COPD patients have a long standing history of cigarette smoking, accounting for 5-15% of the population 45 years of age and older across the world. More than 200 million individuals are affected by COPD and approximately 3 million die annually, making COPD the fourth leading cause of death in the world. It has been projected that by 2020, COPD will become the third leading cause of death, trailing behind ischemic heart disease and stroke [1]. COPD has long been known to be a lung disease that is more prevalent in men. Although cigarette smoking was rare among women in the early 20th century, the number of female smokers started to increase soon after the creation of Virginia Slims that specifically targeted women on their weight and body physique [2]. In 2000, the number of COPD deaths in women has surpassed that of men for the first time [3]. The diverging death rates marked the beginning of the rising COPD burden in women. The US National Institutes of Health (NIH) Act required NIH-funded clinical studies the inclusion of female participants [4], as some publications continued to neglect sex-based considerations and analyses [5, 6]. This is particularly concerning because emerging clinical studies revealed that women may be biologically more susceptible to the toxic effects from cigarette smoke, and have proposed that circulating female sex hormones, estrogen in particular, may play an important role in these processes [7-10].

The prevalence, morbidity, and mortality in COPD are increasing disproportionately in women than in men [11]. Using histological data from the National Emphysema Treatment Trial (NETT), Martinez and colleagues showed that women with severe COPD have thickened airway

walls but less severe emphysema than men [12], suggesting a sexual dimorphism in the manifestation of these phenotypes. In a large meta-analysis, female smokers experienced a greater decline in lung function compared to male smokers after 45 years of age [13, 14]. Women smoke fewer numbers of cigarettes per lifetime on average [15], have more symptoms, greater risk of exacerbations [16] and are two to three times more likely to be hospitalized from COPD complications compared to men [13]. According to data from the National Health Interview Survey (NHIS), chronic bronchitis is also more prevalent in women than in men [17].

In line with these clinical data, several studies [13, 18-20] have also reported that women may be biologically more vulnerable to cigarette smoke. These observations have prompted much interest in studying the biological factors in explaining sex differences in cigarette smoke-induced airways disease. The majority of the work in this thesis is based on chronic smoke-induced airway remodelling in a mouse model of COPD, and the effect of estrogen and progesterone on mucus synthesis in a human bronchial epithelial cell culture model. To begin, we will describe the clinical and biological manifestations of the three important phenotypes of COPD.

1.2 Phenotypes of COPD

COPD is characterized by progressive airflow limitation that is not fully reversible [21]. COPD is composed of three major clinical phenotypes: (1) emphysema, (2) chronic bronchitis, and (3) small airways disease. Emphysema is a pathologic diagnosis, defined by abnormal enlargement of airspaces distal to terminal bronchioles that is permanent and accompanied by destruction of alveoli, resulting in a loss of lung elastic recoil pressure without obvious fibrosis, and gas exchange abnormalities such as hypoxemia and hypercapnia [22]. In normal lungs, expiration is passive. During expiration, the stored mechanical energy generated in the alveolar

walls propels air out of alveoli and into proximal airways. However, in emphysema, there is premature closure of the small airways because of a loss in elastic recoil pressure and increased lung compliance, which leads to overinflation, gas trapping, dynamic hyperinflation, and expiratory flow limitation [23].

Mucus hypersecretion is a hallmark of chronic bronchitis, which is caused by mucus gland hypertrophy and goblet cell metaplasia in the airway epithelium. Clinical phenotype of chronic bronchitis is defined by a productive cough of at least 3 months for 2 consecutive years [24]. Patients with chronic bronchitis account for approximately 50% of all smokers. Some have normal lung function, whereas others have airflow limitation in the absence of mucus hypersecretion, which makes chronic bronchitis a distinct phenotype of COPD. Mucus hypersecretion is one the most prominent features in COPD, and mucus plugging of the airways is the single most powerful histological predictor of mortality in severe COPD [25]. Two primary functions of the airway epithelium are mucus production and mucociliary transport where mucous cells and ciliated epithelial cells work in collaboration to trap and remove inhaled foreign materials from the airways [26]. However, patients with chronic bronchitis have altered airway mucus viscoelasticity properties and fluid lining properties, which impact the process of normal ciliary clearance.

Small airway remodelling is another important cause of airflow limitation and a major site of airflow resistance in patients with COPD that is not completely reversible [27]. The concept of smoke-induced airway remodelling was first established in the 1960s when Hogg and colleagues found that the distending pressure of the lungs was not associated with lung resistance, suggesting that it was the abnormalities of the airways rather than the parenchyma that was responsible for the increase in airflow resistance in emphysematous lungs [27].

Histologic findings revealed an increase in volume fraction of adventitia, lamina propria and smooth muscles in the sub-epithelial walls of the small airways (< 2mm in diameter) by 50% in moderate to severe COPD patients [28]. This observation positively correlated with disease severity and negatively with force expiratory volume in 1s (FEV1) [28]. Several independent studies revealed that female smokers have an accelerated decline in lung function than men after controlling for pack years of smoking [13, 29]. In healthy subjects, studies showed that women have significantly reduced cross-sectional area by 29%, and narrower conducting airways compared to men [30, 31]. Using lung tissue obtained at lung volume reduction surgery, Martinez and colleagues have shown that women with severe COPD have smaller airway lumen and disproportionately thicker airway walls compared to those men [12]. These data suggest that women may naturally be at increased risk for cigarette smoke-related airflow limitations. A vast majority of the literature has studied the pathogenesis of emphysema, while smoke-derived mechanism on small airway remodelling has received less attention.

The majority of the work in this thesis will explore the biological mechanism on sex differences in chronic smoke-induced airway remodelling in a mouse model of COPD.

1.3 Structure and function of the respiratory system

The respiratory system is generally divided into two major zones: 1) the conducting zone and 2) the respiratory zone. The conducting zone includes the trachea, bronchi, bronchioles and terminal bronchioles, whereas the respiratory zone consists of the respiratory bronchioles, alveolar ducts and alveolar sacs. The human lung is a dichotomous branching system that consists of approximately 23 airway generations. Each generation refers to a branch point that bifurcates into smaller but roughly equal luminal cross-sectional area within each airway generation before reaching the terminal alveoli where the site of gas exchange occurs. As the

number of airway branches exponentially increases, the total cross-sectional area also increases. According to Bernoullie's Principle, airway resistance is proportional to the inverse of the radius to the fourth power. In normal lungs, the total airway resistance measured at each generation decreases exponentially with increasing airway bifurcations. However, in the lungs of COPD patients, airway resistance increases. Increases in airway resistance may be a composite of various factors including airway wall remodelling accompanied by reductions in luminal area, mucus secretion and inflammatory exudates.

1.4 Clinical measurement of lung function

Spirometry is a physiological test that measures the flow of air in and out of the lungs over time. This is an invaluable tool for clinician to detect lung abnormalities. A normal set of lungs contains on average 6L of air and the lung volumes can be divided into several compartments as indicated in a schematic diagram in figure 1.1. In normal resting lungs, the function residual capacity (FRC) is centered at approximately 50% predicted total lung capacity (TLC) [32]. After a normal tidal inspiration, the lungs tend to return to a resting volume termed the functional residual capacity (FRC). When performing a lung function test, our lungs inflate to total lung capacity (TLC), followed by maximal exhalation; this volume of air is termed vital capacity (VC). In the detection for airflow obstruction, the two most important clinical parameters are forced expiratory in the first second (FEV1) and forced vital capacity (FVC). The presence of a post-bronchodilator FEV1/FVC ratio < 0.70 confirms the presence of airflow limitation in the lungs of patients with COPD [33], however, this fixed ratio may "over-diagnose" some elderly subjects as lung function naturally declines with aging [34].

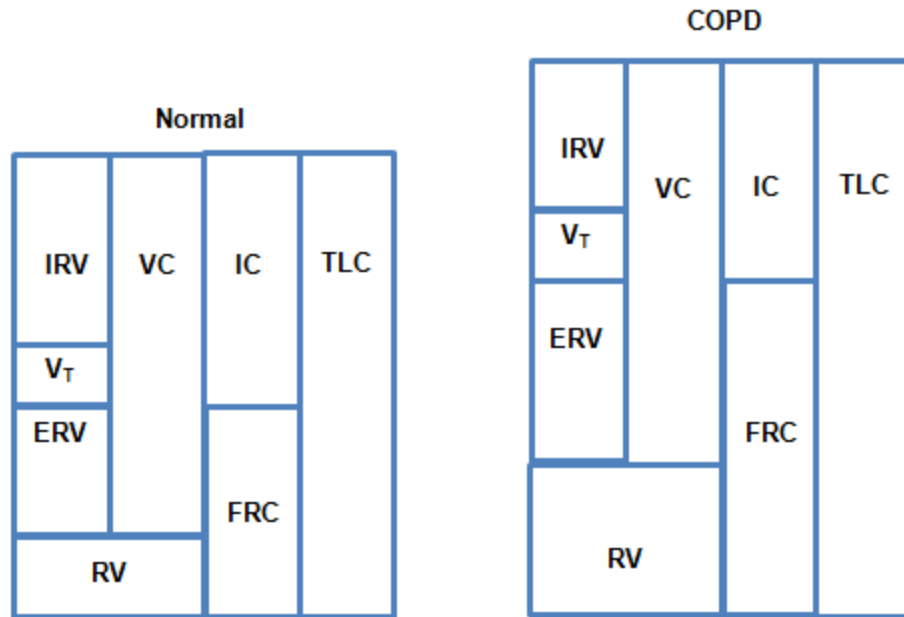


Figure 1.1: Lung volume compartments

Our lungs can be divided into unique compartments including tidal volume (V_T), inspiratory and expiratory reserve volume (IRV, ERV), residual volume (RV), vital capacity (VC), inspiratory capacity (IC), functional residual capacity (FRC), and total lung capacity (TLC). In emphysema patients with dynamic hyperinflation, RV, FRC and TLC increase as a functional consequence of reduced elastic recoil pressure.

Some degree of hyperinflation in the lungs is usually present in patients with COPD. Hyperinflation is characterized by elevated levels of FRC and RV from normal resting values [32]. Both static and dynamic rhythm of breathing contributes to hyperinflation in patients with COPD. Static hyperinflation results from reduced elasticity of the lung parenchyma associated with destruction of the alveoli units and connective tissues that tether the airways open during exhalation. The reduction in lung recoil alters the relationship between lung volume and distending pressure in a typical pressure volume loop; thus requiring a greater volume (FRC) to balance the recoil pressure of the chest wall [35].

Dynamic hyperinflation occurs when the subject begins to inhale before complete exhalation from the previous breath. Consequently, air traps within the lungs with successive breaths, resulting in elevation in FRC. Although FEV1/FVC is the gold standard in detecting airflow obstruction, it does not provide measurable evidence of hyperinflation in patients in COPD. Other groups have shown that hyperinflation expressed as RV/TLC or IC/TLC to be important predictors of COPD mortality [36, 37].

1.5 Animal model of COPD

Much of our understandings on the functional physiology in respiratory diseases were derived from animal models such as guinea pigs, pigs, rabbits, dogs, rats and mice. Although some believe that animal models do not completely reflect human diseases, Morissette and colleagues demonstrated greater similarities in transcriptomic response in lungs of human and mice exposed to cigarette smoke at the pathway and functional levels rather than the single gene level [38], suggesting that the use of a more integrative approach is essential in improving the translational potential.

To study the pathogenesis of COPD, it is important to have an animal model that possesses some degree of lung-architectural and mechanical homology, such that chronic smoke exposure can recapitulate emphysematous-like lesion, small airway remodelling and chronic bronchitis. Mice have been widely used to model the pathogenesis of diseases because of their well-understood immunologic system, a large repertoire of antibodies and reagents, short reproductive cycle, fully-sequenced genome, and well-developed transgenic technology [39, 40]. Mice have been shown to reproduce emphysematous-like lesion and small airway remodelling after 6 months of daily cigarette smoke exposure [41-44]. Genetic modification via over-expression or knockout of particular gene has provided important advances in the understanding

of the pathogenesis of COPD. For examples, genetic deficiency in MMP12 [45], neutrophil elastase (NE) [46], IL1R and TNFR [47] were partially or completely protective from chronic smoke-induced emphysema in murine models of COPD. Despite advantages in the use of mice as a model of COPD, it is important to point out several limitations as there is no perfect model of COPD. Genetic deficiency or constitutive over-expression of a particular gene can interfere with proper lung development, which may be misinterpreted as emphysema. One such example is ER α and ER β knockout mice, which result in abnormal numbers of alveoli per surface area and elastic tissue recoil pressure in the lungs [48, 49]. To overcome problems associated with developmental effects, researchers have elegantly produced an inducible model where animals are fed with doxycycline, which drives the gene of interest with a lung-specific promoter in mature animals. However, there may be small amounts of "leakage" of the transgene even in the absence of doxycycline and that the expression of the reverse tetracycline-transactivator gene can cause airspace enlargement in mice [50]. Doxycycline may also present potential off target effects because it is a matrix metalloproteinase inhibitor that inhibits MMP2 and MMP9, which are thought to be involved in COPD pathogenesis [51].

Unlike human, rodents have less extensive airway branching [52] and near absence of membranous and respiratory bronchioles, and yet the targets of smoke-induced small airway remodelling and emphysema are believed to occur at the membranous and respiratory bronchioles [53]. The production of emphysema and airway remodelling requires many months (usually on the order of 6 months), which presents a considerable amount of time and cost. Regardless of the species and how long the animals are exposed to cigarette smoke, the disease they produce is usually mild and is probably equivalent to human GOLD stage 1 or 2 [54]. The majority of morbidity and mortality occurs in patients with more severe form of COPD, and

these types of severe emphysema and small airway remodelling simply cannot be reproduced in mice after chronic smoke exposure. Furthermore, COPD frequently progresses even after smoking cessation in human, whereas cessation of smoke exposure in mice results in stabilization of emphysema [55]. Furthermore, mice do not develop considerable goblet cell metaplasia after smoke exposure because of the absence of submucosal glands in the airways with the exception in the first few airway generations [53].

1.6 Lung function measurements in murine models

To demonstrate whether certain histological changes in a mouse produce any function changes in the distal airways, we can use the FlexiVent system to measure lung mechanics. Although this method is invasive and terminal, the FlexiVent system offers the greatest degree of accuracy, specificity and reproducibility because the breathing frequency, tidal volume and the volume history are under fixed experimental conditions [56]. After mice are connected to the mechanical ventilation via tracheostomy, a series of manoeuvres are applied on the lungs to obtain volume, pressure and flow measurements. Complex mathematical formulas are used to model different aspects of lung mechanics but will not be discussed because this is beyond the scope of this thesis. Instead, we will discuss the meaning and function of each manoeuvres with respect to lung mechanics.

The total lung capacity (TLC) in mice is approximately 1ml compared to 6000ml in an average human being. To obtain accurate measurement of IC from FRC in mice, the lungs are slowly inflated from a positive end-expiratory pressure (PEEP) of 3cmH₂O to 30cmH₂O by convention to model "physiologic" TLC. The simplest model of lung mechanic is a single compartment model consisting of a single elastic balloon with elastance (E) connected to a single airway and ventilated at a single breathing frequency [57]. When a single frequency forced

oscillation manoeuvre is applied on the lungs, the resulting pressure, flow and volume signals are fitted to a single compartment model using linear regression to assess the level of constriction or resistive behavior (R-resistance), elastic rigidity or the stiffness (E-elastance) and C-compliance of the total respiratory system. Given the heterogeneity of lung abnormalities such as COPD, values obtained from the single compartment model does not provide the exact source of airflow limitation. Therefore, a broadband forced oscillation manoeuvre containing a range of frequencies below and above the subject's breathing frequency to partition the respiratory mechanics into Newtonian resistance (R_n), tissue damping (G) and tissue elastance (H). R_n represents the resistance of the central airways, whereas G is a measure of the degree to which energy is dissipated in the respiratory tissue as lung volume increases and decreases. Similarly, H is a measure of the elastic stiffness of the tissues that opposes expansion as lung volume increases.

Furthermore, to improve the approximation of the location of lung abnormalities, a broad-spectrum oscillation of pseudorandom frequencies (1.0 - 20.5 Hz) can be applied on the lungs, and the data generated from pressure, flow and volume are computed by Fourier transformation with ratios generating the real and imaginary parts of respiratory impedance (Z_{rs}). The real part of the Z_{rs} measures the resistance of the respiratory system at each frequency, whereas the imaginary part of Z_{rs} reflects the respiratory compliance below 20.5Hz in a mouse [57]. The higher frequencies are influenced by large and central airways, whereas lower frequencies are heavily influenced by small airways and parenchymal tissue [58]. This mechanical behaviour in a homogeneous model was previously described using a single airway coupling to a Kelvin body, which consists of two springs and a dashpot to account for the viscoelastic behavior of the lung [57]. At low oscillating frequency, the dashpot is given enough

time to move under the influence of the spring attached to it. As the spring becomes stretched, it exerts a force on the dashpot, which in turn dissipates this energy by sliding toward the force in order to eliminate this; and thus, the tissues exhibit resistance. In contrast, at high oscillating frequency, the dashpot is not given enough time to dissipate this energy; therefore, as frequency increases, tissue resistance diminishes to zero and this resistance essentially reflects those of the central airways.

After a brief understanding of the pulmonary physiology, we will next explore the structure and biology of the airway mucosa that coat the lumen of the airways as these are the primary line of defence against the environmental insults including cigarette smoke.

1.7 Structure of airway mucosa

The airway epithelium is the first line of defence in protecting our lungs from small particles in the air such as dust, cigarette smoke and pathogens from the trachea to the alveoli. The airway epithelium is a pseudo-stratified layer that is composed of specialized cells such as ciliated, mucous, basal, and club cells in the bronchial epithelium (Figure 1.2). The airway epithelium is in dynamic equilibrium between mucus production and mucociliary clearance, which is one of the most important features in maintaining normal airway function. However, in patients with COPD, mucus cell hyperplasia (cellular division) and metaplasia (trans-differentiation) can contribute to excessive sputum production [59]. Excess mucus production by the airway epithelium can overwhelm the normal mucociliary clearance mechanism and lead to partial or complete plugging of the airways, which can lead to morbidity and mortality [60].

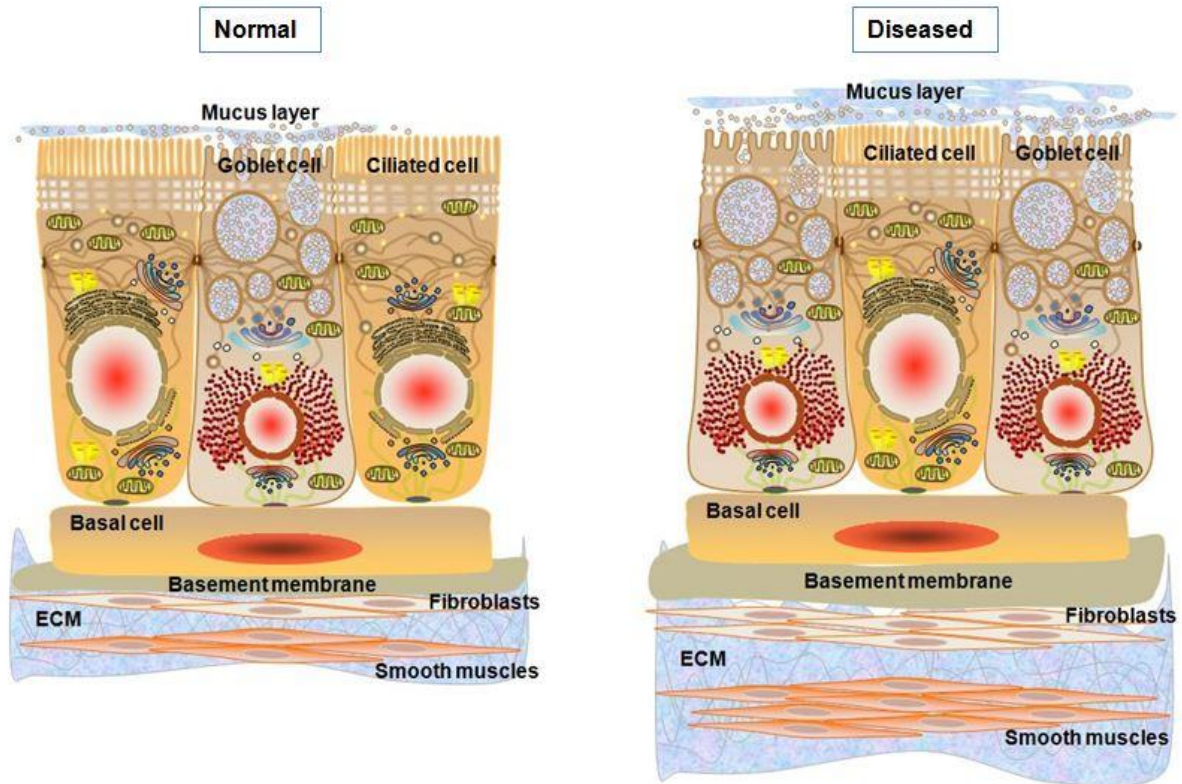


Figure 1.2: Cellular composition in the human airway mucosa.

The airway mucosa consists of a layer of pseudostratified epithelium containing basal cells, goblet cells, and ciliated cells, all of which sit on a dense layer of extracellular matrix protein called the basement membrane. A thin sheet of mucus layer produced by goblet cells lies on the apical cell compartment that traps and removes particles that enter our lungs. Fibroblasts and smooth muscle cells are found in the sub-epithelial compartment bathed in extracellular matrix (ECM). In a diseased epithelium, an increase in goblet cells and mucus secretion alters the efficiency of the mucociliary transport system. Sub-epithelial thickness increases as the ECM protein synthesis increases.

1.7.1 Airway epithelium

Basal cells - Basal cells (BCs) account for approximately 31% and 6% of airway epithelial cells in the large and small airways, respectively [61]. They are relatively undifferentiated and characteristically express transcription factor Trp-63 (p63) and cytokeratins 5 and 14 (Krt5/14) [62]. BCs have sparse electron-dense cytoplasm and appear to be the only cells that express hemidesmosomes, which are firmly attached to the basement membrane via integrins ($\alpha6\beta4$) [63]. In rodents, BCs are populated among ciliated and secretory cells in the trachea [64], whereas BCs in the human lungs are present throughout the airways including the bronchioles [62]. There is a positive correlation between the number of basal cells attached to the basement membrane and airway size [65, 66]. BCs are relatively undifferentiated and possess stem cell-like properties that can give rise to secretory and ciliated epithelial cells in response to epithelial injury [67].

Club cells - In humans, Club cells contain electron-dense granules and are found in the small airways [66]. The regulation of the activity of potentially harmful proteinases secreted by neutrophils during inflammation is important for the prevention of excessive tissue damage [68]. To regulate bronchiolar epithelial integrity and immunity, Club cells have been shown to produce bronchiolar surfactants and specific antiproteases such as secretory leukocyte protease inhibitor [69]. In addition, Club cells can produce p450 mono-oxygenases [69], which are able to metabolize xenobiotic compounds such as aromatic hydrocarbons, which are found in cigarette smoke. Recent evidence has suggested that these cells may also possess important stem cell potential and may act as progenitors for both ciliated and mucus-secreting cells [70].

Columnar ciliated epithelial cells - Ciliated epithelial cells account for over 50% of all epithelial cells within the human airways [71] and characteristically express an f-box transcription factor (Foxj1), which is involved in the synthesis of cilia precursor proteins [72]. They are believed to be terminally differentiated cells that arise from either basal or secretory cells [73]. Typically, these cells possess up to 300 cilia per cell and a large number of mitochondria are found immediately beneath the apical surface, which are responsible for providing energy to the cilia for mucous clearance up and out of the airways via co-ordinated ciliary beating [74].

Mucus-producing cells - Mucus cells, also known as goblet cells, are defined by electron-lucent acidic-mucin granules that secrete mucus into airway lumen to trap foreign objects such as pathogens and dust particles [75]. In normal human trachea, it is estimated that there are up to 6800 mucous-secreting cells / mm² of surface epithelium [59]. As the predominant form of mucin in the human airway, MUC5AC is produced mainly in goblet cells in the surface epithelium, while MUC5B is produced mainly by submucosal glands located below the airway epithelium [76]. MUC5AC may be an acute response mucin responding directly to environmental insults, whereas MUC5B may play a more prominent role in responding to chronic infection and inflammation [77]. The mucus layer present in the airway from the level of the trachea to the bronchioles consists of a mixture of highly glycosylated mucin proteins. Mucins that are present in goblet cells are among the largest molecules in nature with a mass of up to 2-40MDa [78]. The mucin protein backbone accounts for ~20% of its weight, whereas the remaining 80% of the structure are carbohydrate [79]. These oligosaccharide side chains are linked to serine and threonine residues via O-glycosidic bonds, which are presented in linear or

branched moieties with varying length (2-20 monosaccharides long). Mucins confer a polyanionic character owing largely to the presence of sulphate and sialic acid. Mucus condensation is characterized by tightly packing of mucins that is accompanied by high concentration of calcium ions, which acts to neutralize the repulsive forces of the anionic property of mucins [79]. Secretion of mucins opens up the lipid bilayer between the intragranular space and the extracellular space, thereby, permitting the influx of water and the efflux of calcium ions for rapid expansion of the tightly packed mucins within tens of milliseconds [79].

1.7.2 Mucociliary clearance and regulation of air surface liquid

Two primary functions of the airway epithelium are mucus production and mucociliary transport where mucus cells and ciliated epithelial cells work in collaboration to trap and remove inhaled foreign materials from the airways [26]. According to the mucociliary transport model proposed by Yates et al. in 1980 [80], a visco-elastic layer of mucus floats on the periciliary layer tethered to the apical cell surface by mucins 1, 4 and 16 and glycolipids [81]. Hydration of the apical epithelial surface has been shown to be regulated by the release, metabolism and retention of nucleotides on airway surfaces [82]. The mucus layer acts as a fluid reservoir by accepting or donating liquid to maintain normal air surface liquid (ASL) level that approximates the height of the outstretched cilia (6-7 μ m) [83]. To ensure correct mucus movement in the airway, cilia beat in a highly co-ordinated fashion. During the effective stroke, the ciliary tips penetrate into the mucus layer, and during the recovery stroke, they withdraw from this layer [80]. Reverdin et al. have demonstrated the presence of actin in the basal body region of ciliated cells in rat trachea [84], suggesting that this contractile protein may participate in the ciliary movement and in the coordination of the ciliary beat. Cilia are anchored to the apical surface of ciliated cells via specialized structures known as basal bodies. The presence of claw-like

structures on the cilia have been suggested to serve as a special anchorage device for pushing the entrapped particulate matter on the mucus sheet towards the pharynx [85].

Despite normal ciliary function, mucociliary clearance may be compromised if mucus is not adequately hydrated. The lung fluid lining is an aqueous lining that consists of two distinct components: the mucus layer and the periciliary liquid layer [86]. The respiratory fluid lining is a thin layer of aqueous fluid at the interface between the airway epithelium and the air space. This liquid component contains ions, glycoproteins such as mucins, and antimicrobial proteins such as lactoferrin, defensins, lysozyme, IgA, surfactant proteins and secretory leukoprotease inhibitor, which provides a suitable chemical environment and physical barrier for mucociliary clearance, bacterial killing and epithelial homeostasis. Regulation of airway surface liquid is critical in maintaining normal airway function. In normal airways, the cystic fibrosis transmembrane conductance regulator (CFTR) and the epithelial Na^+ channel (ENaC) (that coexist in the apical plasma membrane of airway epithelial cells with Ca^+ -activated chloride channel (CaCC), outwardly rectifying Cl^- channel (ORCC), and Cl^- channel 2 (CLC2)) are fully functional [87]. The combination of Cl^- secretion and reduced Na^+ reabsorption favors a healthy ion composition and depth of airway surface liquid, which enables effective ciliary beat for proper mucociliary clearance [87]. In chronic airway diseases such as cystic fibrosis, CFTR is absent or dysfunctional and ENaC is no longer regulated, leading to hyperabsorption of Na^+ and an increased driving force for fluid reabsorption [87]. The airway surface liquid depth is reduced, the mucosal glands are hypertrophied and excessive mucus is secreted. The excessive production of viscous mucus impairs mucociliary clearance, resulting in airflow obstruction and bacterial colonization of the lungs [87].

1.7.3 Airway wall

Beneath the airway epithelium lies the sub-epithelial compartments containing fibroblasts, smooth muscles and extracellular matrix protein. The dense basement membrane of extracellular matrix (ECM) molecules beneath the airway epithelium has several important roles in maintaining epithelial integrity: (i) it acts as an anchor facilitating adhesion of epithelial cells; (ii) it establishes and maintains correct cellular polarity, (iii) it acts as a barrier between the surface epithelium and the underlying mesenchymal compartment, and (iv) it provides essential survival signals to the epithelium [88-90]. The upper layer of the basement membrane, the lamina densa, consists of type IV collagen and laminin (predominantly type V) secreted by epithelial cells [66] (Figure 2.2). The lower lamina reticularis layer consists of type III and V collagen and fibronectin and is synthesized by subepithelial fibroblasts [91]. The interstitium is composed of two main types of fibroblast; the first is associated with fibrous connective tissues and is oriented parallel to the epithelium, whereas the second type is a myofibroblast that is perpendicular to the epithelium [92] and can generate high levels of contractile forces [93, 94]. Myofibroblasts express higher levels of myosin light chain kinase than naive fibroblasts [95]. There are two major populations of pulmonary fibroblasts: Thy1 (+) and Thy1 (-). Thy-1 (CD90) is a membrane-bound glycoprotein expressed on the outer leaflet of the lipid bilayer on human fibroblasts, neurons, blood stem cells, endothelial cells and T-cells [96-99]. A loss of Thy1 in fibroblasts exhibits profibrotic phenotype with increased proliferative capacity and stronger contraction on collagen gels compared to Thy1 (+) fibroblasts [100]. The increase in contractility in myofibroblasts has been shown to be associated with TGF β -mediated increase in alpha smooth muscle actin (α -SMA), suggesting that α -SMA is a marker of myofibroblast differentiation from naive fibroblasts [101].

Similar to myofibroblasts, α -SMA is also a marker of airway smooth muscle cells (ASM) [102]. Extending beyond the action of bronchoconstriction and relaxation, ASM is a rich source of cytokine, extracellular matrix protein, matrix metalloproteinases (MMPs) and growth factors [103]. Hogg and colleagues have identified that the smooth muscle thickness is increased by approximately 50% in the small airways of COPD patients at GOLD stage 3-4 [28], suggesting the contribution of ASM in airway remodelling and airway flow limitation. ASM is capable of producing IL-6 and -8 (a potent neutrophil chemoattractant); monocyte chemoattractant protein -1, -2, and -3, and granulocyte-macrophage colony-stimulating factor [104, 105]. The presence of surrounding extracellular matrix can influence ASM function such as proliferation and apoptosis [106]. For example, the presence of fibronectin and collagen-1 can increase mitogen-induced proliferation compared to ASM grown on plastic [107]. N-acetylcysteine significantly reduces cigarette smoke extract-induced increase in cellular proliferation (cyclin E and PCNA) on bovine tracheal smooth muscles [108]. Interaction of surface integrins α 5 and β 2 on the ASM and collagen IV/V, laminin and fibronectin provide important antiapoptotic signals to the ASM [109]. However, the secretion of serine proteases from neutrophils such as neutrophil elastase can degrade and disrupt the interaction between surface integrins on ASM and fibronectin, thereby, leading to apoptosis of ASM [110].

Large epidemiologic studies revealed that female patients with asthma, COPD, and CF generally have more symptoms and poorer prognosis than male patients [111, 112]. However, the exact biological mechanism for the sexual dimorphism in chronic lung diseases and whether female sex hormones contribute to disease pathogenesis are largely unknown. In the next section, we will describe more closely the relevance of female sex hormones in the mammalian lungs.

1.8 Properties of female sex hormones

1.8.1 Sex hormone receptors: lung physiology

For many years, we have known that estrogen and progesterone receptors are responsible for sexual development [113] but their effect beyond the reproductive system is becoming increasingly recognized. There are two types of estrogen receptors (ER) and two types of progesterone receptors (PR): ER- α , ER- β , PR-A and PR-B, all of which are expressed in rats [114], mouse [115], and humans [116]. While androgen receptor (AR) is expressed primarily in mammalian reproductive tissues [117], ER- α , ER- β , PR-A and PR-B expression have been noted in mammalian female and male reproductive tracts, female mammary glands, bone, the cardiovascular tissues, lung, and the brain [118] [113]. In the lungs, the expression of ER- β protein is twice as that of ER- α [119]. Most of the expression is found in the cytoplasm but minor expression has also been noted in the mitochondria and nucleus [119]. ER- α and ER- β belong to a super-family of nuclear hormone receptors, many of which are ligand-activated transcription factors that regulate gene expression by binding to the promoter region of genes [113]. These receptors contain an N-terminal DNA binding domain and a C-terminal ligand binding domain (LBD) for estrogen [113].

Accumulating data suggest that mammalian lung development is regulated by sex hormones before and during the neonatal period. Studies in mice in which ER- α and ER- β were deleted revealed that both types of ER are required for the formation of complete alveolar units in females. ER- α ensures that the lungs differentiate properly during development, leading to normal numbers of alveoli per surface area. ER- β , on the other hand, modulates the development of extracellular matrix, leading to normal elastic tissue recoil pressure in the lungs [48, 49]. In

human, The presence of estrogen accelerates alveolar maturation in female neonates with the production of lung surfactants compared to male neonates [120]. The delay in lung maturation in male neonates can be partially explained by an inhibitory effect of androgen on epidermal growth factor and transforming growth factor- β (TGF- β) [121]. The early appearance of lung surfactant in females may partially explain the higher airflow rate and lower airway resistance than in male neonatal lungs [122]. On average, the female lungs are smaller and lighter than those of males and contain few respiratory bronchioles at birth [123]. The number of alveoli per unit area and alveolar volume do not differ between boys and girls, but boys have larger lungs than girls [123].

Steroid hormones are primarily synthesized in the gonads, adrenal glands, and the fetoplacental unit [124]. Cholesterol is the common precursor of all sex hormones where it is first converted to pregnenolone by P450-linked side chain cleaving enzyme (P450_{ssc}). Pregnenolone is then converted to progesterone, which is used to synthesize androgens and estrogens [125]. Estrogens are derived from androgens by the addition of an aromatic A ring, through a reaction that is catalyzed by the enzyme aromatase [125, 126]. Estrogen and progesterone are multi-ringed structures with distinct functional groups. Unlike progesterone, there are three major naturally occurring estrogens in women: 1) estriol, 2) estradiol, and 3) estrone. In humans, estriol is the predominant estrogen in pregnant women, while estradiol is the predominant form in the non-pregnant premenopausal women and estrone is the predominant estrogen in the menopausal females. Sex hormones act via their own unique receptors: estrogen receptor (ER- α or ER- β), progesterone receptor (PR-A or PR-B), and an androgen receptor (AR) [127]. Estradiol binds with a higher affinity to ER than its metabolic products such as estrone and estriol [128]. All sex hormone receptors have been shown to be expressed in lung tissues [118, 129].

1.8.2 Sex hormones and menstrual cycle

Four main hormones characterize the menstrual cycle: estradiol, progesterone, luteinizing hormone, and follicle stimulating hormone. On average, the menstrual cycle is 28 days and is divided in two phases: the follicular (Day 1-13) and the luteal phase (Day 14-28). The onset of ovulation is defined by a surge in estradiol on day 14. Menstruation and the late luteal phase are characterized by low serum levels of estradiol (~0.15nM) and progesterone (~9.54-31.81nM); whereas ovulation is marked by high circulating levels of estradiol (~0.37-1.47nM) and low levels of progesterone (~0.95-9.54nM) (Table 1.1). During the luteal phase, estradiol levels range from 0.15-0.92nM, whereas progesterone levels increase from 9.54-31.81nM and drop back to lower levels prior to menstruation. However during menopause, estradiol and progesterone levels are significantly reduced to levels below those in the menstruation phase.

Table 1.1: Female hormone levels throughout the menstrual cycle

Phases	17 β -estradiol (nM)	Progesterone (nM)
Day 1-13 (follicular)	~0.15-0.37 (40-100pg/ml)	~0.95 (300pg/ml)
Day 14 (Ovulation)	~0.37-1.47 (100-400 pg/ml)	~0.95-9.54 (300-3000pg/ml)
Day 15-28 (luteal)	~0.15-0.92 (40-250pg/ml)	~9.54-31.81 (3000-10,000pg/ml)

1.8.3 Delivery of sex hormones to target tissues

Sex hormone binding globulin (SHBG) is an important steroid hormone binding protein in human plasma and regulates sex hormone delivery to tissues and cells [130]. Plasma SHBG is produced primarily in hepatocytes, which is a glycosylated isoform of SHBG [131] and is produced by the Sertoli cells [132]. In biological fluids, SHBG exists as a homodimer with a separate steroid-binding pocket and a calcium-binding site in each monomer [133] and binds to

both androgens and estradiol with nanomolar affinities [134]. In normal men and women, between 40-65% of circulating testosterone and between 20-40% of circulating estradiol is bound to SHBG [135]. SHBG regulates tissue delivery of sex hormones by binding them and retaining them in the circulatory pool, where they are relatively inert. However, once the sex hormones dissociate from SHBG, they can escape the bloodstream, and bind with the intracellular androgen or estrogen receptors, causing changes in gene expression of cells [130]. It is thus generally accepted that only the unbound hormone is biologically active [136].

1.8.4 Sex hormone receptor activation

The exact mechanism by which estrogen modulates cell signalling pathways is not completely known and there may be multiple cell signalling pathways by which sex hormones affect gene regulation and expression. According to the free hormone hypothesis, unbound sex hormones freely diffuse across cell surface membranes [136]. Binding of estrogen to the ligand binding domain of the ER causes a conformational change in the receptor, which results in dimerization of ER and translocation to the nucleus [113]. The activated receptor/DNA complex then binds to specific promoter sequences of DNA called hormone response elements (HREs) and recruits other cofactors to the nucleus, which results in transcription of DNA downstream from the HRE [113]. An alternate hypothesis suggests that even estrogens bound to SHBG are metabolically active. It is now well recognized that sex hormones target tissues containing membrane-binding sites that can bind with SHBG [137]. In prostate [138] and breast cancer cells, it has been shown that by binding to this site, SHBG triggers cAMP-dependent signalling causing upregulation of adenylyl cyclase and other downstream signalling molecules. It is important to note that these data were generated in vitro using isolated epithelial cells and not in

the context of these cells *in vivo*. Thus, the exact cell signalling pathway of sex hormones is incompletely known.

1.9 Effects of cigarette smoke on the airway mucosa

1.9.1 Cigarette smoke and oxidant/antioxidant imbalance

Cigarette smoking is an important cause of COPD. Cigarette smoke (CS) exists as a gaseous and a particulate phase, producing more than 4,000 chemicals and more than 10^{14} reactive oxygen species per puff. CS consists of side-stream and main-stream smoke. Side-stream smoke is produced by the tips of cigarettes, while main-stream smoke is produced by inhaling the mouth end of the cigarettes [139]. The gaseous phase is composed predominantly of carbon monoxide, ammonia, dimethylnitrosamine, formaldehyde, hydrogen cyanide and acrolein. The main components of the particulate phase are nicotine, tar, and aromatic hydrocarbons including benzene, benzo(a)pyrene (BP) and naphthalene. In the next following sections, we will explore how these toxic gases from the combustion of cigarette give rise to airway remodelling and dysregulation of pulmonary function in the mammalian lungs.

1.9.2 Xenobiotic metabolism

After inhalation, these chemicals are initially metabolized by Phase I enzymes and conjugated by Phase II enzymes. Phase I reaction is largely mediated by cytochrome P450 (CYP) enzymes, which is a family of xenobiotic enzymes that are responsible for hydroxylation of aromatic hydrocarbons into intermediate metabolites. Transcription of these CYP genes is controlled by ligand-mediated activation of aromatic hydrocarbon receptors (AHR) that bind on target genes containing xenobiotic response elements (XRE). These intermediate metabolites are in turn conjugated by Phase II enzymes, the rate-limiting step reaction in most cases, and

excreted out of the body. Because some intermediate metabolites may be more toxic than their parent constituents, lungs may suffer oxidant damage through a process called bioactivation unless there is excellent co-ordination of Phase I and Phase II enzymes. Reactive oxygen species (ROS) can be generated exogenously as by-products from the combustion of cigarettes, and endogenously from activated macrophages and neutrophils [140]. ROS such as superoxide can react with nitric oxide to produce a highly reactive substance called peroxynitrite. Protein nitrosylation by peroxynitrite can form 3-nitrotyrosine that can render antioxidant enzyme catalase inactive [141]. Long-lived semiquinone radicals present in the tar phase of cigarette smoke can react with superoxide to form hydroxyl radical and hydrogen peroxide [142]. Although catalase and superoxide dismutase can metabolize hydrogen peroxide and superoxide, respectively, over-production of these products can overwhelm the antioxidant system and result in a build up of oxidative stress.

A variety of animal models have been used to examine potential sex-related differences in the risk of oxidant-related lung diseases. For instance, Van Winkle et al. showed that the lungs of female mice were more susceptible to naphthalene, a prominent component of side stream cigarette smoke, compared to male mice [143]. Female lungs of rats had higher expression of CYP enzymes and demonstrated increased accumulation of potent oxidant intermediates from naphthalene metabolites [144]. Some of these xenobiotic enzymes also contain estrogen-responsive elements, which may be additive upon cigarette smoke exposure in female biological system [145]. For example, estradiol can up-regulate CYP enzymes without necessarily altering the expression of Phase II enzymes, making the female lungs more susceptible to oxidant damage in response to cigarette smoke. Interestingly, in humans, the two CYP enzymes that are up-regulated by cigarette smoke are CYP1A1 and CYP1B1, which are regulated by ER- α [145].

Smokers smoking an average of 10.7 cigarettes/day has a saliva cotinine level of 113ng/ml, and for the same number of cigarettes smoked per day, saliva cotinine level is greater in men than in women [146], suggesting that women have acceleration metabolism of cotinine. This was confirmed by Benowitz and colleagues that normal healthy women intravenously infused with deuterium-labeled nicotine and cotinine had faster clearance of both nicotine and cotinine, and greater conversion of nicotine to cotinine [147]. Interestingly, women on estrogen-only birth control pill had greater ratio of hydroxycotinine to cotinine than women not on any hormonal supplements [147].

1.9.3 Oxidative stress and airway remodelling

Oxidative stress has been shown to be important in the pathogenesis of COPD, but the precise mechanism by which this occurs is not clearly known [148]. Early evidence by Barcello-Hoff and colleagues demonstrated that reactive oxygen species generated from irradiation (50-200Gy of $^{60}\text{Co}\gamma$) can activate the release of TGF- β protein *in-vitro* [149]. Recent evidence revealed a direct activation of TGF- β protein in air-exposed control rat tracheal explants and from recombinant TGF- β latency-associated peptide by cigarette smoke via an oxidative mechanism [150]. This provides direct evidence of smoke-induced increase in collagen in the large airways where inflammation is not required for this process. However, this is an acute explant model and may not reflect small airway wall thickening *in-vivo*. Churg and colleagues have showed that *Coll*, *Ctgf* and *TGF- β* mRNA expression in isolated bronchiole tissues were increased after 6 months of smoke exposure in C57BL/6 mice [41]. Furthermore, in support for the role oxidative stress on airway remodelling, Rubio and colleagues demonstrated a 25% increase in wall area of small bronchi in rats after 10 weeks of cigarette smoke exposure, and this effect was prevented by the administration of N-acetylcysteine [151].

TGF- β receptor activation and its downstream signalling mechanism have been well-characterized and are associated with airway remodelling [152]. The TGF- β family consists of at least three isoforms (TGF- β 1, TGF- β 2, TGF- β 3) that are important growth cytokines responsible for bone development, growth differentiation, wound healing, tumour-cell growth and inhibition [152, 153]. All three isoforms of TGF- β are expressed throughout our body including the lungs, and stored in the extracellular matrix as latent complexes. Latent TGF- β can be activated *in-vivo* by a variety of mechanisms including direct proteolytic action of plasmin [154, 155], thrombospondin-1 [156], MMP2 and 9 [157, 158], and interaction of the α_v integrin with a triamino acid peptide arginine-glutamate-aspartate (RGD) sequence on the surface of the latent protein complex with a contractile force generated by α -SMA in myofibroblasts [149]. In addition to the activation of latent TGF- β by various proteolytic mechanisms, sequestration of TGF- β by decorin, a matrix proteoglycan, appears to play a role in TGF- β signaling by binding TGF- β and sequestering it to the matrix [159-161]. Decreased sequestration of TGF- β by decorin may be another method by which matrix synthesis can be increased [162].

First, TGF- β heterodimerizes to TGF- β R1/RII and triggers the phosphorylation of Smad-2 and -3 (pSMAD2/3), which are key protein mediators in the TGF- β signalling cascade. Direct binding of pSMAD2/3 to its response element up-regulates α -sma, collagen-1 (*Col1*), *Col3* and NAPDH-oxidase (*Nox4*) mRNA expression [163-165]. The first three genes have been implicated in airway wall thickening [166], whereas NOX4 mRNA and protein expression were increase in lung tissues of patients with idiopathic pulmonary fibrosis and in bleomycin-induced mouse model of lung injury [167, 168], suggesting a positive feedback loop between TGF- β signaling and oxidative stress. Collectively, these data provided a suggestive mechanistic link between cigarette smoke-induced oxidative stress and airway remodelling.

1.9.4 Cigarette smoke and inflammation in the lungs

The classical theory for the pathogenesis of smoke-induced emphysema is the protease-antiprotease hypothesis where smoke elicits an inflammatory response, which drives the release of proteases from inflammatory cells and overwhelms the antiproteolytic defense, leading to proteolytic breakdown of matrix protein [1, 169]. Although infiltration of immune cells such as neutrophils, macrophages and CD8+ T lymphocytes are consistently shown to be present in the small airways of cigarette smokers [28, 170], Hogg and colleagues showed that the strongest histological associations with airflow limitation were luminal mucus and airway wall thickness [28]. Col1 mRNA is increased in airways tissues as soon as 2h post smoke exposure [41], whereas smoke-induced inflammatory response does not increase until 24h [171], suggesting that an inflammatory response is not required, however may enhance the profibrotic effects of smoke-induced airway remodelling. Interestingly, C57BL/6 mice with genetic deficiencies in IL1 β or TNF α receptor are completely protective from chronic smoke-induced airway remodelling [47].

1.9.5 Structural damage and tissue repair/remodelling

Cigarette smoke can induce structural damages in the airway epithelium by unleashing proteases and oxidants and disrupting the barrier function of the airway [172]. Cells in the airway epithelium are held together by tight gap junctions that play important roles in maintaining structural integrity. When the airway epithelium is damaged, tissue repair becomes critical in re-establishing the integrity of the damaged tissue. However, the precise mechanisms by which the epithelium repairs itself are still controversial. In an *in vivo* study where the tracheal epithelium of guinea pig was wounded, epithelial cells including the secretory and ciliated cells near the damaged area began to dedifferentiate, flatten and migrate over the denuded area after 15

minutes [173]. The damaged area then becomes covered by a tight layer of flattened undifferentiated epithelium before epithelial redifferentiation restores the functional integrity of the tissue [173]. These data suggest that the lung epithelium is capable of self-renewal and proliferation after injury. Increased expression of specific integrins such as $\alpha v\beta 1$ and $\alpha v\beta 6$ are present on the basal surface of regenerating epithelium to promote regeneration of the physical barrier [174]. In addition, there is increased expression of fibronectin, collagen IV and laminin in bovine tracheal epithelial cell culture lesions, which promote the restoration of the basement membrane matrix and allow epithelial cell migration [175]. Furthermore, Park and colleagues demonstrated that acute exposure of naphthalene triggered ciliated bronchial epithelial cells to undergo squamous cell metaplasia at the site of injury, which was then followed by dynamic repair through redifferentiation via increased expression of transcription factors including β catenin, Foxa2, Foxj1, and Sox family members (Sox17 and Sox2) [176]. In chronically injured airways by cigarette smoke, there is also a marked distortion of the sub-epithelial fibroblast architecture and disappearance of the basal laminar layer [177]. This process may be mediated by increased synthesis of TGF- β , which in turn upregulates Smad-2, -3, and -4-mediated signaling, and reduced expression of Smad-7 [178]. Finally, cigarette smoke may trigger neutrophil infiltration in the airway walls, neutrophil elastase and cathepsin G released from neutrophils can induce fibronectin degradation with the disruption of integrin binding, leading to apoptosis of ASM [109]. The regulation of proliferative and apoptotic mechanism in ASM by neutrophils and extracellular may determine the overall ASM mass. In Chapter 2, we will first determine whether there is potential sexual dimorphism on airway remodelling, emphysema and mucus production in a well-established mouse model of COPD. We hypothesize that estrogen drives airway remodelling but not emphysema in smokers.

Chapter 2: Sexual Dimorphism in Structural Differences in a Mouse Model of Chronic Obstructive Lung Disease

2.1 Introduction

This chapter explores two important anatomic lesions in a mouse model of COPD. COPD is a complex disease that is characterized anatomically by small airway remodelling and emphysema, but these pathologic changes may be influenced by sex. In patients with very severe COPD, women have anatomically smaller airway lumens and thicker airway walls compared to men [12]. Female smokers in their 40's and 50's demonstrate faster declines in lung function compared with male smokers, and experience a 50% increased risk of COPD, following adjustments for pack-years of smoking [13, 29]. In the United States (US), where smoking rates between men and women are similar, the number of females dying from COPD surpassed the number of males dying of COPD in 1999 [179]; and in 2010, 60% of all COPD hospitalizations occurred in female patients [180]. However, the mechanisms behind these differences in COPD risk between men and women are largely unknown.

Although some believe that animal models do not completely reflect human diseases, Morissette and colleagues have shown translational potential of animal models by demonstrating similar genes, pathways and biological functions affected by cigarette smoke in the lungs of mice and human [38]. To our knowledge, there have been no previous studies which have systematically evaluated the effects of cigarette smoke in male and female mice with and without intact ovaries on small airway remodelling and emphysema. The primary goal of this study was to determine whether there is any significant sexual dimorphism in the anatomic phenotypes of COPD and whether female sex hormones play any role in COPD pathogenesis following 6 months of cigarette exposure in mice, which are commonly used to model COPD.

2.2 Materials and methods

2.2.1 Animal smoke exposure

Adult male (N=20), female (N=20) and ovariectomized (N=20) C57BL/6 mice (12 weeks old) were obtained from Charles River (Montreal, PQ, Canada). Surgical ovariectomy of female mice was performed at Charles River four weeks prior to cigarette smoke exposure. 1R1 and 2R4F research grade cigarettes were obtained from the University of Kentucky (Lexington, KY). Experimental groups consisted of six groups of ten mice per group (male control, male smoke-exposed, female control, female smoke-exposed, ovariectomized control, and ovariectomized smoke-exposed). The smoke-exposed groups were exposed to three cigarettes (one 1R1 and two 2R4F with the filters removed, or two 1R1 and one 2R4F with the filters removed on every other smoking day), for 5days/week for 6 months. All smoke exposures were conducted using our standard nose-only smoke exposure system. All procedures were approved by the University of British Columbia Animal Care Committee (A11-0149).

2.2.2 Morphometric measurements

Histology. The lungs were inflated at 25cmH₂O and fixed under pressure in formalin for 24h. Paraffin-embedded sagittal sections (5µm) were stained with picosirius red for measurement of total airway wall area, haematoxylin & eosin for assessment of mean linear intercept, and Periodic-acid Schiff (PAS) for the detection of glycoprotein from mucus-producing cells.

Analysis of airway walls. Airways were analysed by selecting round airways less than 200 µm in internal diameter. All airway wall measurements were performed on picosirius red-stained sections. The wall area of each airway was calculated by the measuring the difference in area

enclosed by outlining the adventitial border and the basement membrane. The airway wall area was then normalized by the length of the airway outlined at the basement membrane.

Mean linear intercept. Methods were previously described [181]. For measurements of mean linear intercept, 15 random fields were photographed at 10X magnification. Using the ImagePro system, a grid of 130 lines and 250 points with a line length of 1000 μ m was used to count the number of intercepts. The formula for mean linear intercept (L_m) is $2 \cdot (\text{line length}) / N_{\text{intercepts}}$.

Airway epithelial cell count. Total epithelial cell count was based on counting the number of nuclei with normalization to the length of the basement membrane in all distal airways less than 200 μ m in diameter in all groups.

2.2.3 Immunohistochemical staining for neutrophils and macrophages

Methods were previously described in detail [43]. Briefly, immunohistochemistry was carried out on formalin-fixed paraffin-embedded tissues using rat anti-mouse macrophage antibody (sc-101447) and rat anti-mouse neutrophil antibody (sc-71674) (Santa Cruz Biotechnology, Dallas TX), each diluted 1:250 and incubated overnight at room temperature after antigen retrieval with pH 6.0 10 mM sodium citrate and heat. The secondary antibody was biotinylated anti-rat IgG 1:200 (Vector Laboratory Inc. Burlingame CA BA-9401). Reaction product was visualized using streptavidin/HRP (Dako catalog P0397) and Nova Red (Vector Laboratory Inc). Numbers of macrophages and neutrophils were quantitated by counting 5 random high power fields and expressed as numbers of cells/mm² of tissue.

2.2.4 Immunofluorescence staining for Ki67 protein

Frozen left lung sections (5 μ m) were fixed and permeabilized in acetone at -20°C for 10 minutes. Sections were incubated with antibodies against Ki67 protein (ab16667, Abcam) overnight for

4°C and stained with Alex Fluor® 562 anti-rabbit IgG (A-21441, Life Technologies) for 2 h at room temperature. Slides were mounted on VECTASHIELD HardSet Mounting Medium with DAPI and visualized using confocal microscope. Fluorescence intensity in the airways was quantified using Image J software and normalized to the length of the basement membrane.

2.2.5 Statistics

Data were analyzed using non-parametric t-test, two-way ANOVA with Bonferroni's multiple comparisons test using GraphPad Prism version 6 (GraphPad Software Inc, San Diego, CA, USA). All data were expressed as mean \pm SEM. Statistical significance was considered at $P < 0.05$.

2.3 Results

2.3.1 Female mice showed greater morphologic small airway remodelling than male and ovariectomized mice after smoke exposure

After 6 months of air or smoke exposure, paraffin-embedded lung sections from male, female and ovariectomized mice were stained with picosirius red to show small airway wall matrix (Figure 2.1A-F). Smoke exposure significantly increased total airway wall area normalized to the length of basement membrane from $9.2 \pm 0.4 \mu\text{m}$ to $12.7 \pm 1.6 \mu\text{m}$ in female mice (38.0% increase, $p < 0.05$), but not in male mice or ovariectomized mice (Figure 2.1G). In contrast, 6 months of smoke exposure increased mean linear intercept in the parenchyma of male, female, and ovariectomized female mice, but there was no sexual dimorphism that was detectable (Figure 2.2A-G). Similarly, tissue neutrophil and macrophage cell counts were significantly increased in all groups after smoke exposure, but no sexual dimorphism was present (Figure 2.2H-I). Histologic lung sections revealed an absence of PAS-positive cells in the distal airways of all

control and smoke-exposed mice (Figure 2.3A-F). However, the large conducting airways expressed trace amounts of PAS-positive cells in all groups, which were used as positive controls for mucus-producing cells (Figure 2.3G).

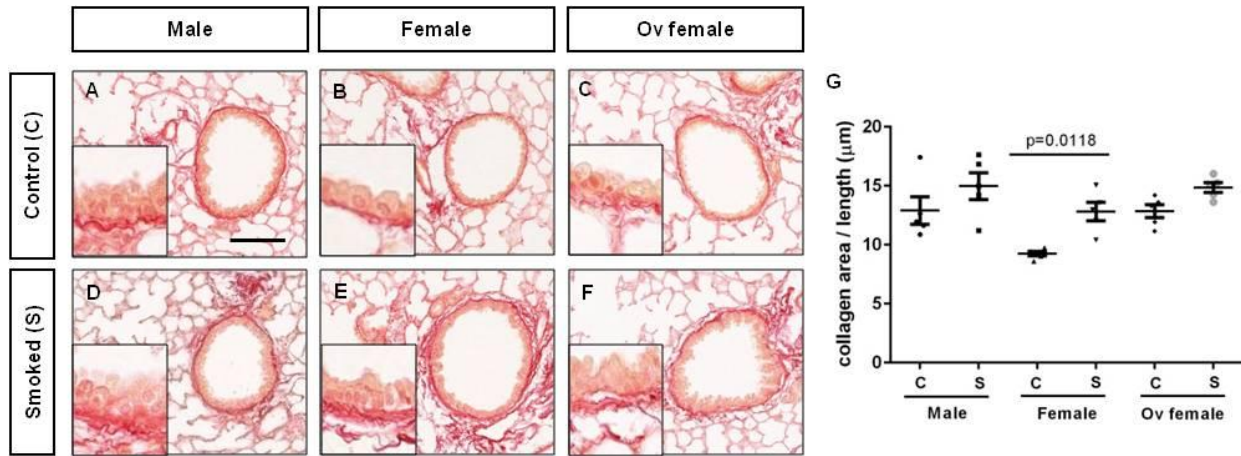


Figure 2.1: Female mice show greater morphologic small airway remodelling (dark red = total collagen) after cigarette smoke (CS) exposure than male mice, and this effect can be prevented by ovariectomy before smoke exposure.

A-F) Representative images of picosirius red-stained mouse lung sections in control (C) and smoke-exposed (S) male, female and ovariectomized mice were shown. (Dark red = total collagen; scale bar = 100µm). G) Total airway collagen area was normalized by the length of basement membrane using airways less than 200µm in diameter. Data were expressed as mean ± SEM with N=5 per group. One-way ANOVA with Bonferroni's multiple comparisons test was used in panel G.

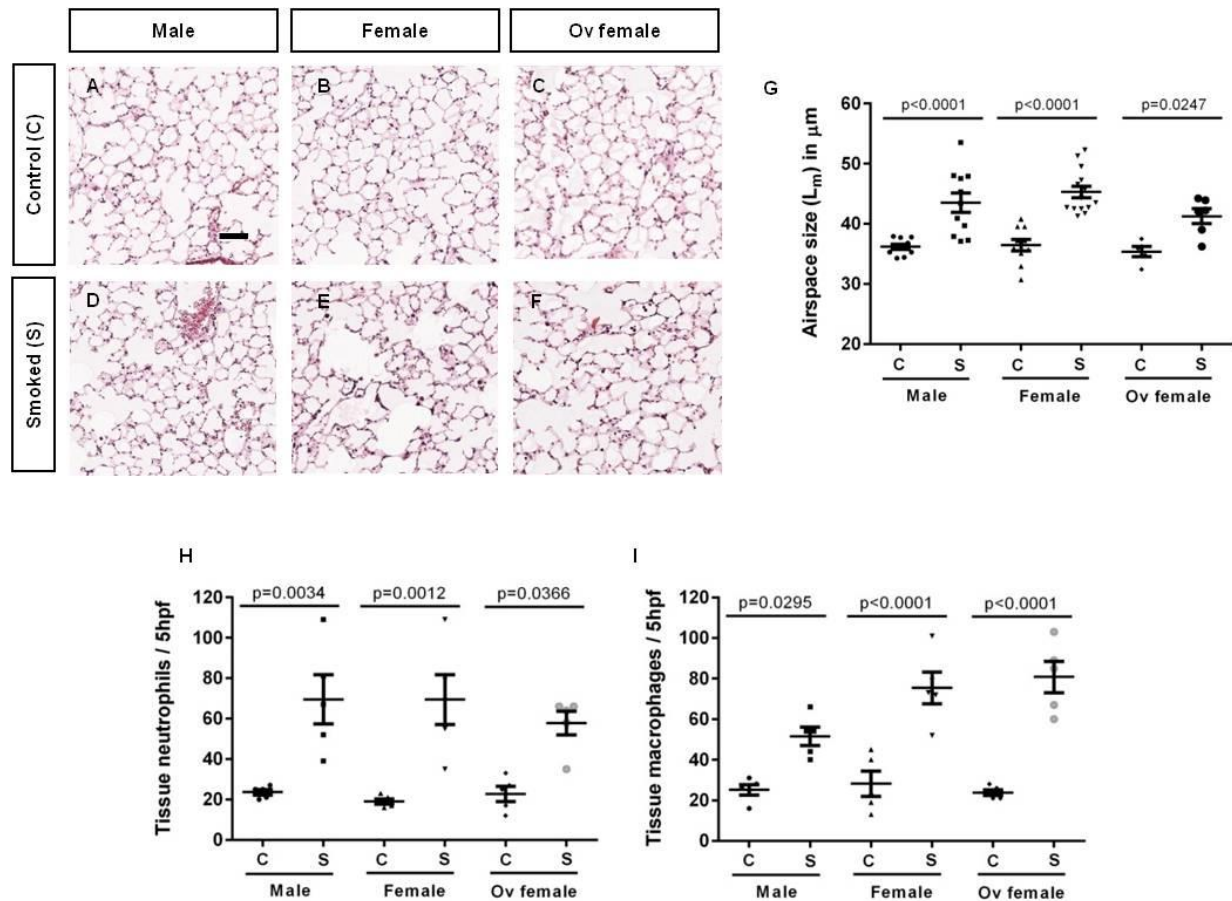


Figure 2.2: 6 months of cigarette exposure increased mean linear intercept, but no sexual dimorphism was present.

Paraffin-embedded mouse lung sections in control A) male, B) female and C) ovariectomized mice, and smoke-exposed D) male, E) female and F) ovariectomized mice were stained with H&E. (Scale bar = 50µm). G) Quantification of mean linear intercept (µm), tissue H) neutrophil and I) macrophage counts per 5 high-power fields were shown. Data were expressed as mean ± SEM with N=5 per group. One-way ANOVA with Bonferroni's multiple comparisons test were used in panels G-I.

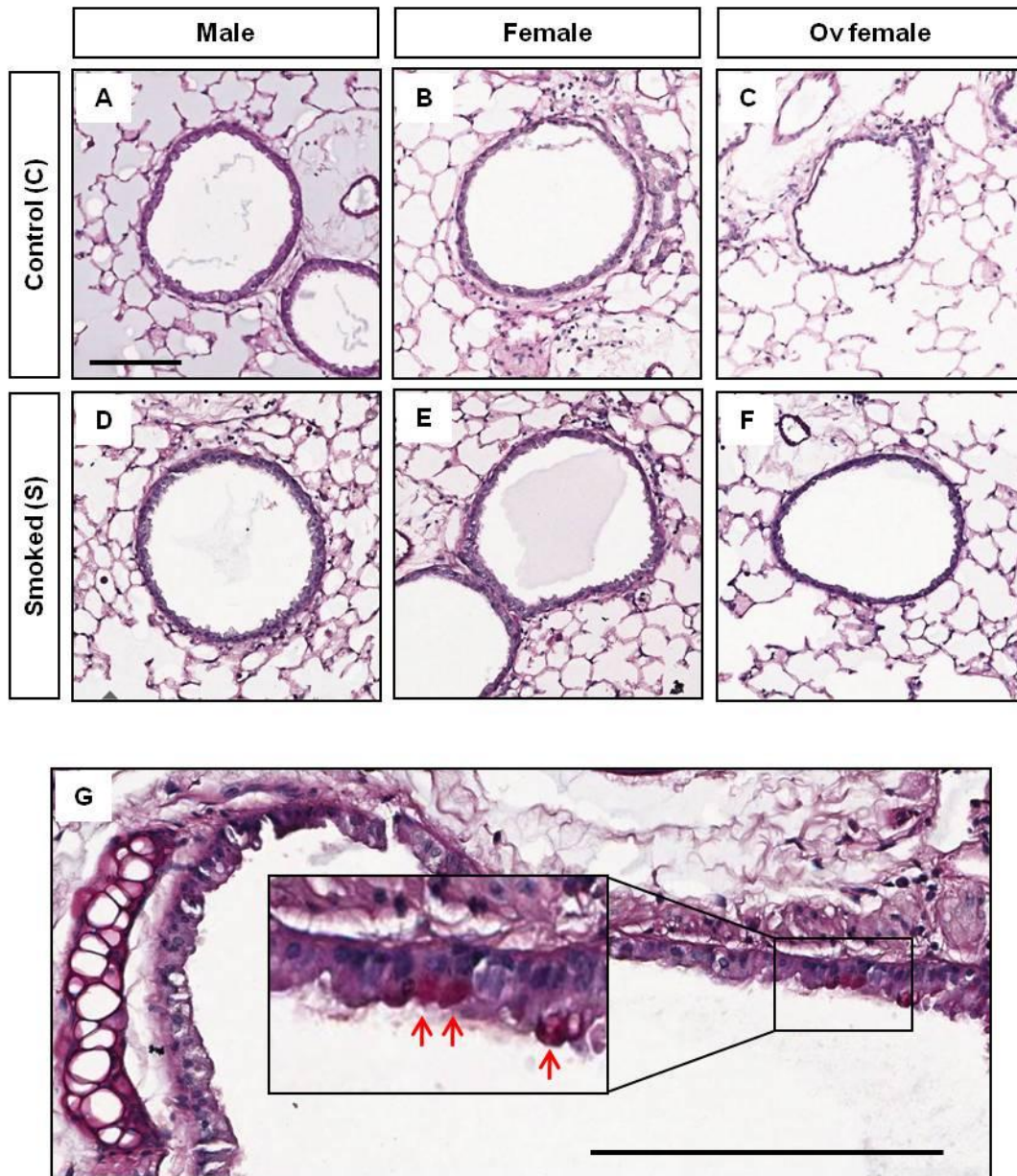


Figure 2.3: Absence of PAS-positive cells in the distal airways of mice after 6 months of cigarette exposure.

Paraffin-embedded mouse lung sections in control A) male, B) female and C) ovariectomized mice, and smoke-exposed D) male, E) female and F) ovariectomized mice were stained with Periodic acid-schiff (PAS), a marker of glycoprotein (i.e. mucus-producing cells). (Scale bar = 100 μ m). G) Large airways from smoke-exposed male mice was used as positive control for PAS staining (red arrows). (Scale bar = 200 μ m). Images were representative of N=5 per group.

2.3.2 Distal airways in female mice have greater epithelial cell count and Ki67-positive cells than male and ovariectomized mice after smoke exposure

Smoke exposure increased total epithelial cell counts/length of basement membrane in the distal airways of female but not in male mice, and this effect was abolished in ovariectomized mice (Figure 2.4A-G). This observation was supported by an increase in proliferating marker, Ki67 protein, in the distal airway epithelium of female but not male mice after smoke exposure, and this effect was attenuated in ovariectomized mice (Figure 2.4H-N). Ki67 protein was minimally detected in the distal airway epithelium and was not significantly different amongst all control mice. The observed biological effects of ovariectomy were confirmed in uterus, which demonstrated reduced gross size and decreased epithelial thickness in ovariectomized female mice compared with those in female mice with intact ovaries (Figure 2.5A-D). Smoke exposure had no effect on airway-specific mRNA expression of estrogen receptors (ER α , ER β) or progesterone receptors (PR-A/B) compared to their respective control groups (Figure 2.5E-G).

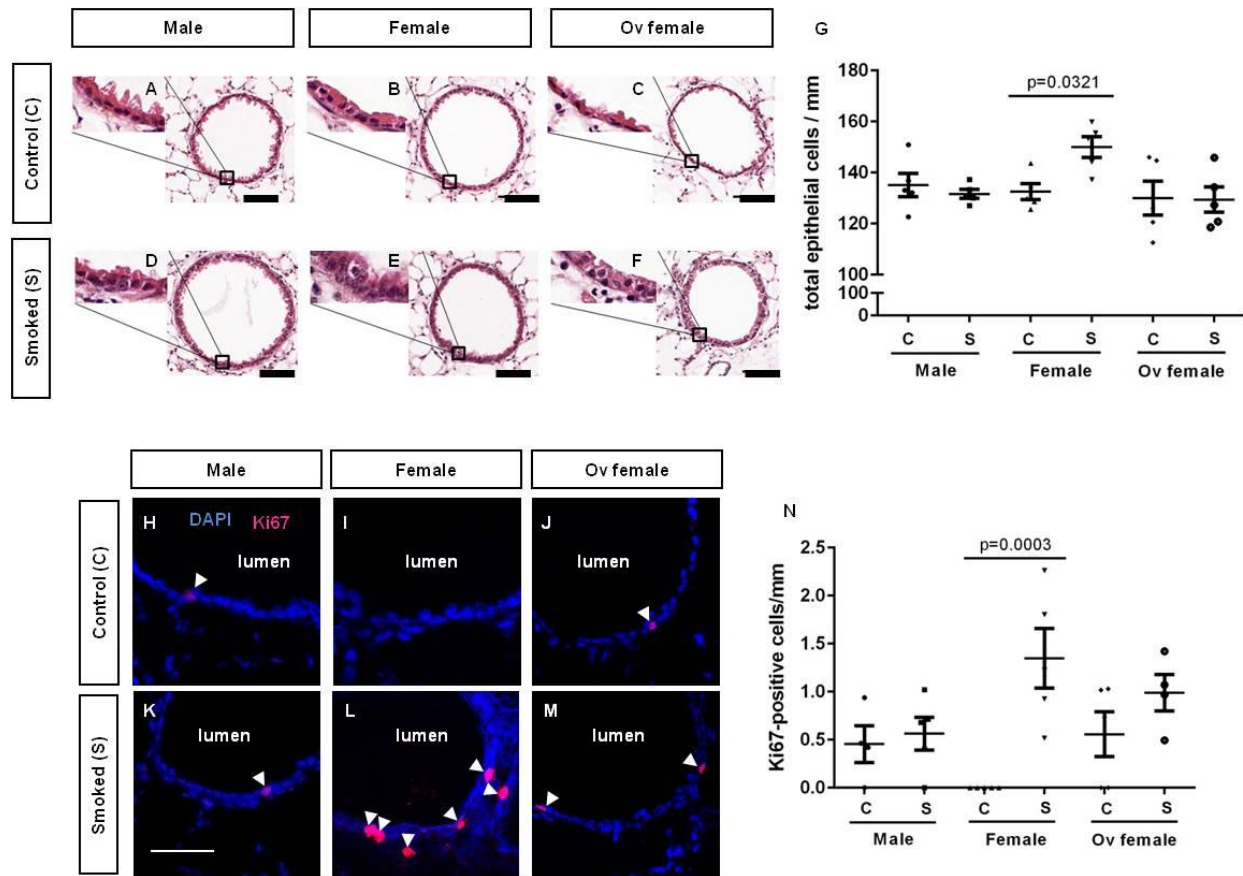


Figure 2.4: 6 months of cigarette exposure increased total airway epithelial cell count and Ki67-positive cells in female but not male mice, and these effects were attenuated in ovariectomized mice.

Paraffin-embedded mouse lung sections in control A) male, B) female and C) ovariectomized mice, and smoke-exposed D) male, E) female and F) ovariectomized mice were stained with H&E. (Scale bar = 50 μ m). G) Total airway epithelial cells were normalized by the length of the basement membrane in millimeters. Frozen mouse lung sections in control H) male, I) female and J) ovariectomized mice, and smoke-exposed K) male, L) female and M) ovariectomized mice were stained for Ki67 protein. (Scale bar = 50 μ m). N) Total Ki67-positive cells were normalized by the length of the basement membrane in millimeters. Data were expressed as mean \pm SEM with N=5 per group. One-way ANOVA with Bonferroni's multiple comparisons test were used in panels G and N.

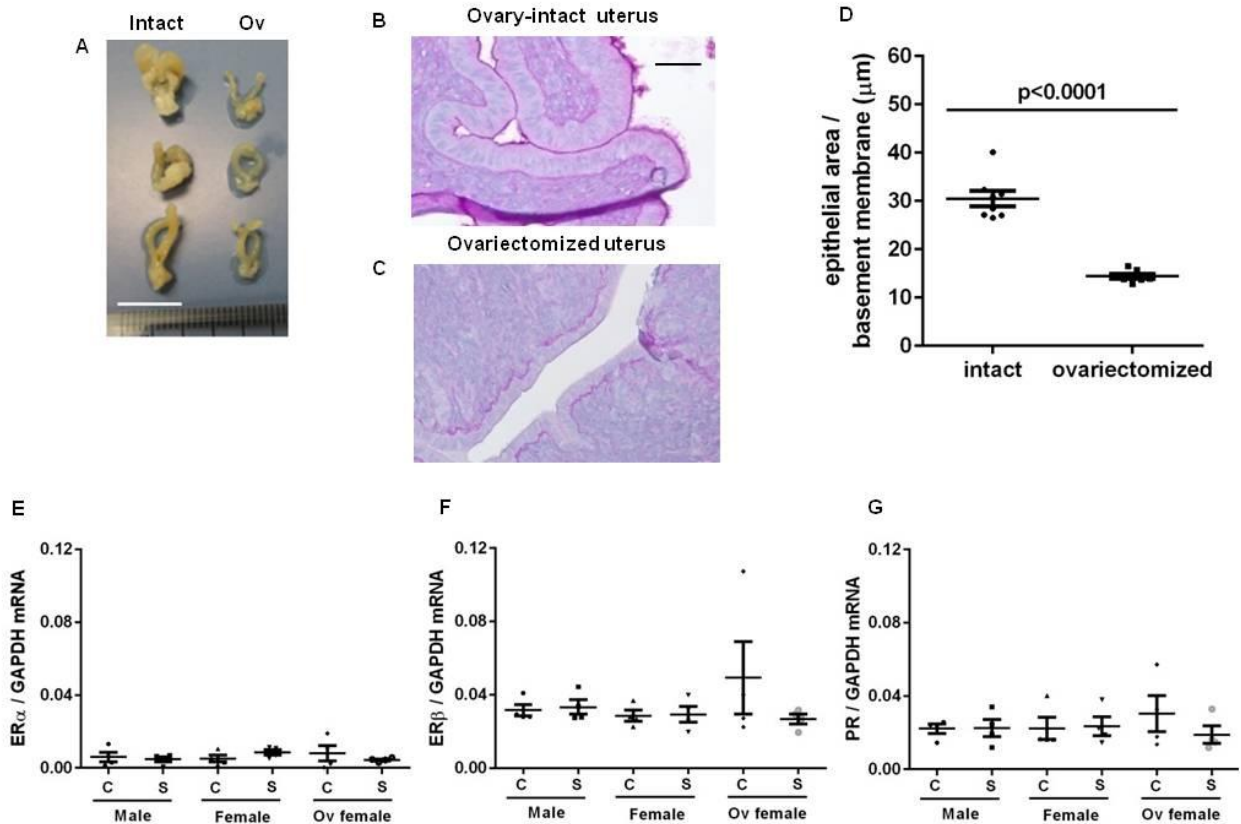


Figure 2.5: Morphologic differentiation between ovary-intact and ovariectomized mice, and airway-specific sex hormone receptor mRNA expression.

A) Gross image of uteri from female mice with intact ovaries (Intact) and uteri that have undergone ovariectomy (Ov) (scale bar = 10mm). 5µm thick histologic sections of formalin-fixed paraffin-embedded uterus in B) ovary-intact and C) ovariectomized mice were stained with Periodic acid-schiff (scale bar = 50µm). D) Uterus epithelial area was normalized to the length of the epithelium measured at the basement membrane (µm) in female and ovariectomized mice. Values were expressed as mean \pm SEM with N=8 per group. Non-parametric t-test was used in panel D. E) Estrogen receptor (ER- α), F) ER- β and G) progesterone receptor (PR) mRNA expression were quantified by real time PCR. Values were expressed as mean \pm SEM with N=4 per group. One-way ANOVA with Bonferroni's multiple comparisons test were used in panels F-H.

2.4 Discussion

Small airway remodelling has been recognized as an important cause of airflow limitation in human smokers [28, 182]. Hogg and colleagues showed a negative correlation between small airway wall thickness and lung function in patients with COPD [28]. Using real time polymerase chain reaction (PCR) of microdissected small airway tissues of COPD patients, Gosselink and colleagues showed that smoke exposure increased the expression of pro-fibrotic mediators including those related to the TGF β 1 signalling pathway and matrix protein, which were associated with thickening of the small airway walls [183]. These data have been complemented with the well-established murine model of COPD, which expressed several important parallel features of COPD such as emphysematous-like destructions and small airway remodelling [41, 42, 184, 185].

We have reproducibly demonstrated small airway remodelling in mice after 6 months of daily cigarette smoke exposure [41-44]. The most striking finding, for the first time, is the presence of a sexual dimorphism in a mouse model of COPD where chronic smoke exposure increased small airway remodelling in female compared with male mice, and that this excess risk was prevented by ovariectomy. Our findings are consistent with Martinez and colleagues, who found that in those with severe-to-very severe COPD, human female patients demonstrated an airway-predominant disease with narrowed airway lumens and thickened airway walls compared to male patients [12]. The increase in small airway remodelling after chronic smoke exposure was associated with an increase in cellular proliferation, as indicated by Ki67, in the distal airway epithelium, and an increase in airway epithelial cell count in female mice.

There are two general schools of thought in the pathogenesis of smoke-induced small airway remodelling in COPD [186]. The first theory suggests that small airway remodelling is

derived by repeated inflammatory insults by smoke-induced immune cell infiltration [1, 170, 187], but there is little direct evidence to support this hypothesis because anti-inflammatory compounds have been generally unsuccessful in preventing or attenuating the process of remodelling [186]. An alternative theory of smoke-induced airway remodelling suggests an excess production of growth factors, which contributes to increased fibrosis of tissues independent of inflammation [41, 186]. Churg and colleagues have shown that pro-collagen, connective tissue growth factor (CTGF) and platelet-derived growth factor-B (PDGF-B) mRNA expression levels were elevated in laser-capture microdissections of airway tissues in C57BL/6 mice female mice exposed to cigarette smoke over time [41]. Furthermore, in the absence of infiltrating immune cells, acute smoke exposure on normal rat tracheal explants increased collagen-1 mRNA expression, suggesting that inflammatory response and increased expression of growth factors on airway remodelling may be independent processes. In the next chapter, we will describe our proposed mechanism to explain why female mice have more airway remodelling than male mice after 6 months of CS exposure.

Clinical evidence showed that women are biologically more susceptible to smoke than men [13, 18-20]. March and colleagues demonstrated that emphysematous-like lesions were first seen after 10 weeks of smoke exposure in female A/J mice, while male mice did not develop emphysema until 16 weeks, and no substantial remodelling of the conducting airways and mucus production was present in both sexes [188]. Although we showed the presence of mild emphysema in all groups of mice exposed to chronic smoke exposure, no sex difference was found. It is important to note that administration of an injurious agent such as cigarette smoke may interfere with alveolarization during prenatal period of lung development and may be falsely interpreted as emphysema [53]. Therefore, all C57BL/6 mice were first exposed to

cigarette smoke after maturity at 12 weeks of age. Furthermore, there is an absence of goblet cells in the distal airways of C57BL/6 mice after 6 months of smoke exposure. Mice expressed trace amount of goblet cells in the trachea but are almost absent in the distal airway epithelium [189]. Collectively, our mouse model of COPD revealed that female mice have greater histologic evidence of small airway remodelling than male mice; however, although chronic smoke exposure resulted in mild emphysema, there were no significant sex differences in the extent of emphysema with smoke exposure.

Chapter 3: Sex-Related Differences in Pulmonary Function Measurements Following 6 Months of Cigarette Exposure: Implications for Sexual Dimorphism in Mild COPD

3.1 Introduction

In the previous chapter, we have reproduced two important phenotypes of COPD in a well-established mouse model of COPD [41-43], and demonstrated attenuation of small airway remodelling in ovariectomized female mice. These findings suggest that women who show signs of COPD prior to menopause may be at greater risk for developing severe disease than those in whom COPD appears only later in life, which would have significant implications for smoking cessation counselling. However, our prior study focused on changes to the lung tissue that are only evident histologically and thus are not easily translated to the screening of at-risk patients because their detection would require lung biopsy.

We performed this investigation in our mouse COPD model because the pathology in this model is well characterized and subtle changes in lung function can be detected with high precision in mice using the flexiVent system via measurements of respiratory system impedance. The outcome of this study may have potential to be translated into clinical practice that might identify patients at risk for developing severe disease. Patients with COPD exhibited increased lung function abnormalities, which may be indicative of a heterogeneous restrictive process in the lung periphery [190]. In this study, we hypothesize that the increase in small airway remodelling in female mice is associated with an increase in distal airway resistance.

3.2 Materials and methods

3.2.1 Animals

Adult male (N=20), female (N=20) and ovariectomized (N=20) C57BL/6 mice (12 weeks old) were obtained from Charles River (Montreal, PQ, Canada). Surgical ovariectomy of female mice was performed at Charles River four weeks prior to cigarette smoke exposure. 1R1 and 2R4F research grade cigarettes were obtained from the University of Kentucky (Lexington, KY). All procedures were approved by the University of British Columbia Animal Care Committee (A11-0149).

3.2.2 Smoke exposure

We studied 6 groups of mice (n = 10 per group): 1) male control, 2) male smoke-exposed, 3) female control, 4) female smoke-exposed, 5) ovariectomized control, and 6) ovariectomized smoke-exposed. The smoke-exposed groups were exposed to three cigarettes (one 1R1 and two 2R4F with the filters removed, or two 1R1 and one 2R4F with the filters removed on every other smoking day) for 5 days per week for 6 months. All smoke exposures were conducted using our standard nose-only smoke exposure system.

3.2.3 Pulmonary function test

Immediately after the last smoke exposure, all 10 mice per group from the 6 month CS study were anesthetized (150mg/kg ketamine and 10mg/kg xylazine), tracheostomized (closed thorax) with an 18-gauge blunted needle advanced 5 tracheal rings and secured with silk ties. An additional dose of a ketamine/xylazine mix (25% of initial dose) was given 30 min from the initial injection. The tracheal cannula was connected to a computer-controlled small animal ventilator (flexiVent; SCIREQ, Montreal, Canada). Mice were mechanically ventilated in a

supine position at a respiratory rate of 150 breaths/min with a tidal volume of 10ml/kg, and pressure limit of 30 cmH₂O coupled to a constant positive expiratory end-pressure (PEEP) level of 3 cmH₂O. Muscle paralysis was achieved using pancuronium (2mg/kg intraperitoneally) to prevent respiratory efforts during the measurement. A 60 W incandescent light bulb was placed 30 cm directly above the mouse to maintain body temperature. Heart rate was monitored with an electrocardiogram (ECG) (SCIREQ, Montreal, Canada) attached to the limbs of the animal to check for proper anesthetic depth. Before each mouse was connected to the flexiVent, we collected calibration signals by applying a volume perturbation initially through a completely closed tracheal cannula and then opened to the atmosphere to estimate the flow resistance of the tracheal cannula and the elastance of air in the ventilator cylinder. To provide a constant volume history, a 6s deep inflation maneuver to 27 cmH₂O was performed twice prior to data collection. A 8 s volume perturbation signal containing frequencies between 1 and 20.5 Hz (primewave-8, SCIREQ, Montreal, Canada) with a peak-peak amplitude of 3 ml/kg was applied to the lungs to measure its mechanical impedance. Fitting the constant-phase model of impedance to the measured impedances provided estimates of airway resistance (R_n), tissue damping (G) and tissue stiffness (H) [56]. Model fits were accepted only if the coefficient of determination of the curve fit was > 0.95 . Three measurements of impedance were obtained under each experimental condition and the resulting values of R_n , G and H were averaged. Pressure-volume loops were generated by applying a series of volume-steps that inflated to lungs to 30 cmH₂O followed by deflation, all in the complete absence of spontaneous breathing efforts. Measurements were made over a series of 10 consecutive days, so to avoid time effects in our data we measured impedance in one mouse from each of the 6 groups on each of the 10 days. Measurements on a control

mouse and its smoke-exposed counterpart (male, female, or ovariectomized groups) were performed immediately one after the other.

3.2.4 Statistics

Data were analyzed using parametric t-test (normally distributed), non-parametric t-test (non-normally distributed), two-way ANOVA with Bonferroni's multiple comparisons test, and linear regression using GraphPad Prism version 6 (GraphPad Software Inc, San Diego, CA, USA). All data were expressed as mean \pm SEM. Statistical significance was considered at $P < 0.05$.

3.3 Results

3.3.1 Female mice have increased tissue damping than male and ovariectomized mice after smoke exposure.

No differences in Rn were observed across any of the groups (Figure 3.1A). However, smoke exposure increased significantly tissue damping (G) in female but not in male mice, and this effect was not present in ovariectomized mice (Figure 3.1B). H was not significantly different between female and ovariectomized mice both at baseline and after smoke exposure, but H increased significantly following smoke exposure in male but not female mice (Figure 3.1C).

3.3.2 Female mice have greater respiratory resistance than male and ovariectomized mice after smoke exposure.

These findings were similar for the respiratory resistance (Zrs) as shown in Figures 3.2A-C. Specifically, Zrs was not different between air-exposed and smoke-exposed male mice at all frequencies investigated, but it increased significantly at the low frequency (1Hz) in female mice but not in male or ovariectomized female mice. Respiratory reactance (Xrs) was unchanged

between control and smoke-exposed male mice at all frequencies (Figure 3.2D), but was significantly more negative in the smoke-exposed female mice at the lowest frequency (1Hz) (Figure 3.2E), an effect that was not present in ovariectomized female mice (Figure 3.2F).

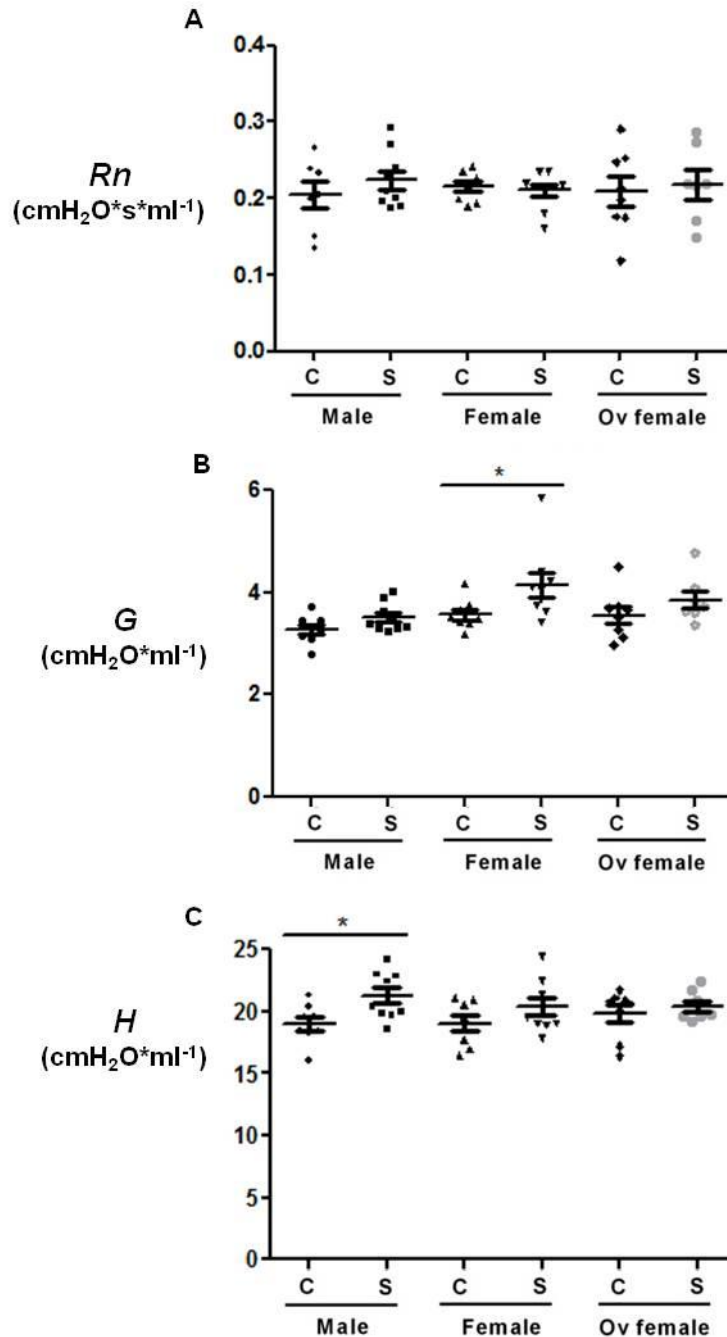


Figure 3.1: Female mice have greater tissue damping than male mice after smoke exposure, and these effects were abolished with ovariectomy.

A) Airway resistance (R_n), B) tissue damping (G) and C) tissue elastance (H) were measured in control (C) and smoke-exposed (S) male, female and ovariectomized mice. Values expressed as mean \pm SEM from N=7-9 per group. * $p < 0.05$ represents statistical significance. Non-parametric t-test was used in panel B. Parametric t-test was used in panel C.

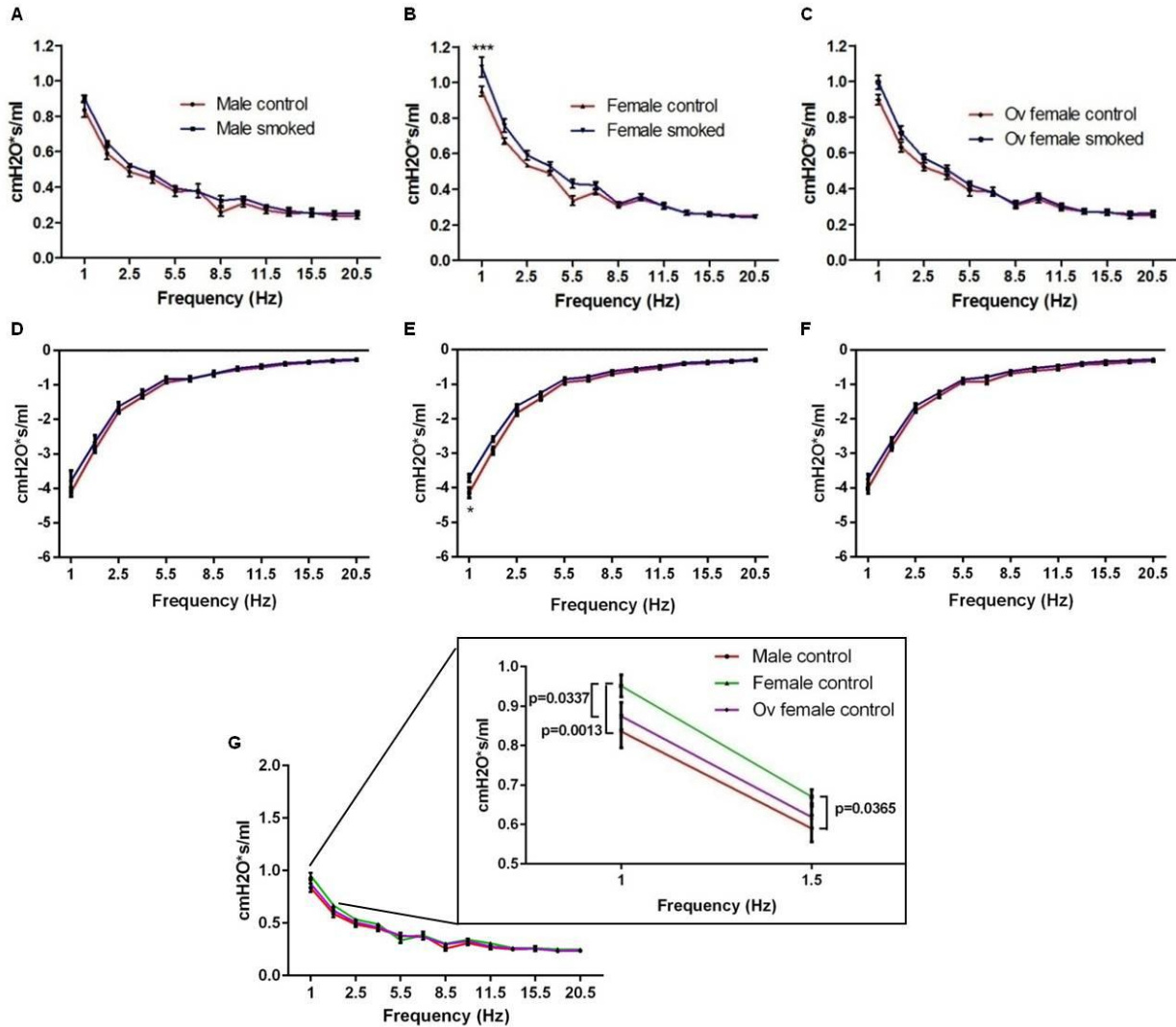


Figure 3.2: Female mice have greater Zrs than male mice after smoke exposure, and this effect was abolished after ovariectomy.

Frequency-dependence of respiratory system resistance (Zrs) and reactance (Xrs) in control and smoke-exposed male (A, D), female (B, E), and ovariectomized mice (C, F) were shown. * $p < 0.05$, ** $p < 0.01$ compared between control and smoke-exposed female mice. G) Zrs in male, female and ovariectomized control mice were shown. Values were expressed as mean \pm SEM with $N = 7-9$ per group. Two-way ANOVA with Bonferroni's multiple comparisons tests were performed in all analyses.

3.3.3 Female mice have lower inspiratory capacity than male and ovariectomized mice after smoke exposure.

Figures 3.3A-C showed that the inspiratory and expiratory pressure-volume curves were not significantly different between control and smoke-exposed male and ovariectomized mice. However, there was a downward shift in the curves at higher lung volumes in female mice after smoke exposure. Correspondingly, the only significant effect of smoking on inspiratory capacity was observed in female mice (Figure 3.3D). Quasi-static lung compliance (C_{st}) was not different between all groups after normalization to the inspiratory capacity within each group (Figure 3.3E). The curvature of the deflating PV-loop (K) was not different between all groups (Figure 3.3F).

3.3.4 Inspiratory capacity does not depend on whole body weight of mice

Body weight increased by 21%, 33% and 29% in control male, female and ovariectomized mice, respectively, from 3 to 9 months of age (Figure 3.4A-C). However, chronic smoke exposure imparted similar effects on weight gain in all groups of mice, reducing body weight by 20-25% in all groups. To determine whether differences in body weight influenced inspiratory capacity we plotted inspiratory capacity versus body weight but found no significant correlations (Figure 3.4D-F).

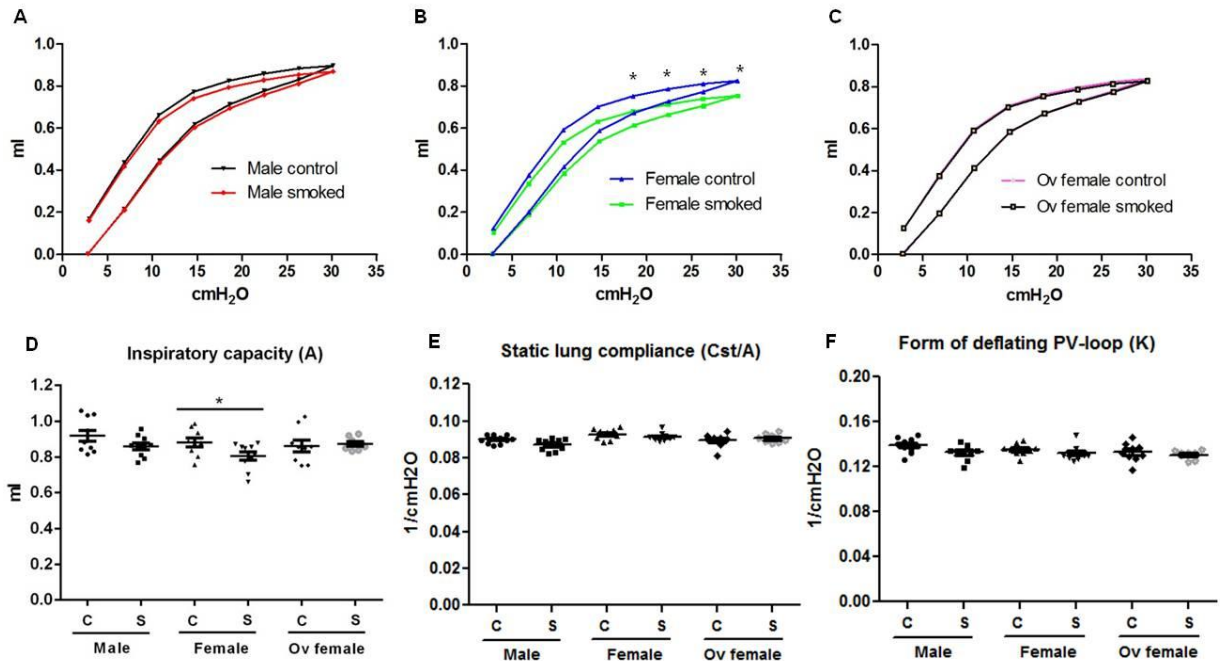


Figure 3.3: Female mice have lower inspiratory capacity than male mice after smoke exposure, and this effect was abolished with ovariectomy.

Pressure-volume (PV) loops were shown in control (C) and smoke-exposed (S) A) male, B) female, and C) ovariectomized mice. D) Inspiratory capacity (A), E) quasi-static lung compliance with normalization to A, and F) the form of the deflating PV-loop (K) were shown. Values were expressed as mean \pm SEM with N=8-10 per group. Two-way ANOVA with Bonferroni's multiple comparisons tests were used in panels A-C. Parametric t-tests were used in panels D-F.

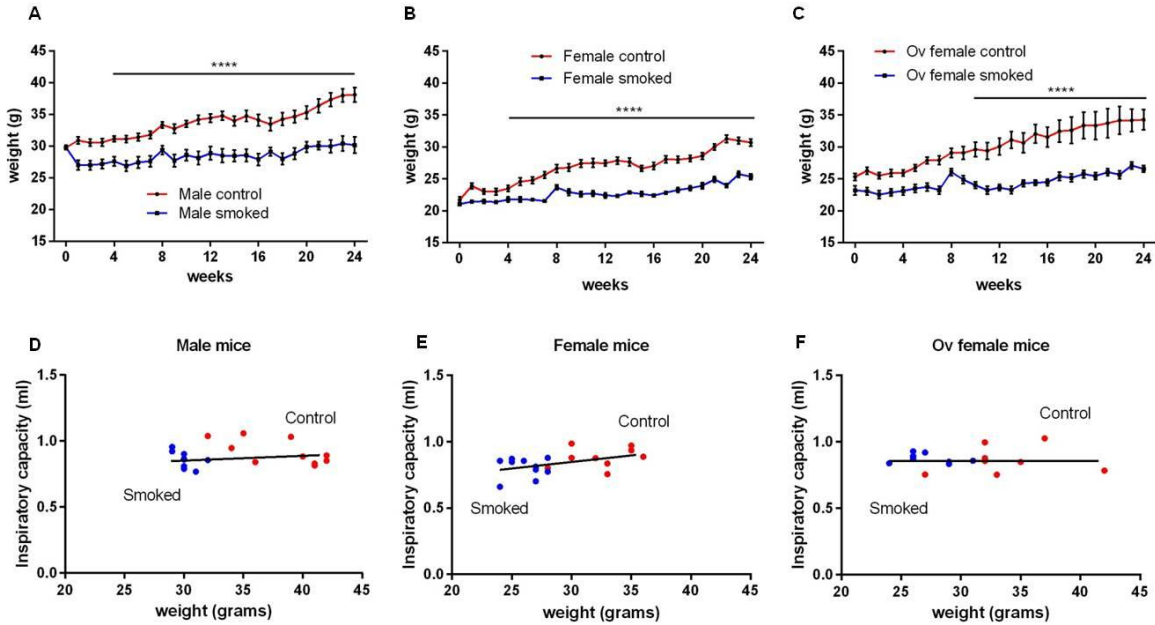


Figure 3.4: Inspiratory capacity does not depend on whole body weight of mice.

Whole body weight of control and smoke-exposed A) male, B) female, and C) ovariectomized mice were measured weekly over 24 weeks of smoke exposure. Values were expressed as mean \pm SEM. **** $p < 0.0001$ compared between control vs. smoke-exposed mice at each time point with $N = 8-10$ per group. Two-way ANOVA with Bonferroni's multiple comparisons tests were used in panels A-C. The relationship between inspiratory capacity and whole body weight of control and smoke-exposed D) male, E) female and F) ovariectomized mice were shown. Linear regression analyses were used in panel D-F.

3.4 Discussion

In patients with severe COPD, female smokers are at increased risk of small airways disease compared with male smokers [12]. In mild to moderate COPD, female smokers have accelerated decline in lung function compared with male smokers with similar pack-years of smoking exposure [13]. However, because there are significant differences in the amount and the way in which men and women smoke [191], the influence of confounding factors cannot be fully resolved in these observational studies. To our knowledge, the present study is the first of its kind to evaluate sex-related differences in lung function following 6 months of cigarette exposure in mice with and without intact ovaries. We found that 6 months of cigarette exposure in these mice, which produced mild histologic changes of emphysema and small airway remodelling, resulted in significant perturbations in lung function reflective of disease in the “small airways” of female mice in particular (Figure 3.1B and 3.2B), consistent with GOLD 1 or 2 COPD severity in humans.

We found the greatest impact on lung function to be manifested in the impedance parameters G and H . In a perfectly homogeneous lung, G is a measure of the degree to which energy is dissipated in the respiratory tissue as lung volume increases and decreases. Similarly, H is a measure of the elastic stiffness of the tissues that opposes expansion as lung volume increases. The fact that G and H are both non-zero attests to the viscoelastic nature of the tissues. However, G and H may also be increased by derecruitment of airspaces, by an increase in the regional heterogeneity of lung mechanics, or by a reduction in lung size. Smoking did not seem to significantly affect lung size (Figure 3.4), but we did find that smoking increased G in the female group (Figure 3.1B) and H in the male group (Figure 3.1C). The increased G is explicable as the functional consequence of increased airway remodelling in the females relative to the males and

ovariectomized female mice that showed no changes in G . That is, the females with intact ovaries experienced either an increase in the intrinsic resistive properties of their lung tissues and/or increased regional lung heterogeneity as a result of their smoke exposure compared to the other two groups, which is consistent with an increase in collagen deposition in the very small airways as previously described [192].

It was only in the females that smoking elevated both resistance and reactance at the lowest frequency we measured (Figures 3.2B and E); the other two groups showed no effects of smoking on impedance. Resistance and reactance at low frequencies determine G and H , respectively, via the fits provided by the constant-phase model [56]. However, although these model fits are generally extremely good, they are never perfect because the constant-phase model does not perfectly describe the actual impedance. These errors in fit may thus explain our otherwise curious observation of an increase in H only in the male mice (Figure 3.1C). That is, because the effects of smoking on impedance were so subtle, a small amount of model fitting error could lead to spurious results in terms of the best-fit model parameter. Patients with COPD typically show much greater effects on lung mechanics due to smoking than we have observed in our mice in the present study. Patients with COPD have also been shown to exhibit increased G , H , and hysteresivity which are indicative of a heterogeneous restrictive process in the lung periphery [190] similar to but more significantly more extreme than in our mice.

Interestingly, COPD caused by cigarette smoking is often associated with dynamic hyperinflation and increased lung compliance, which would be expected to lead to a decrease in H and an increase in inspiratory capacity [193]. We found smoke exposure to produce comparable (and mild) degrees of emphysematous-like lesions in the parenchyma of male, female, and ovariectomized female mice (Figure 2.2G), but inspiratory capacity was decreased

only in the smoke-exposed female mice while remaining unchanged in the other two groups (Figure 3.3). One possibility is that residual volume may have increased in the female mice, corresponding to dynamic hyperinflation in patients with emphysema, which may reflect an increased tendency for remodeled peripheral airways to collapse at low lung volumes. On the other hand, it is by no means certain that the pathology of smoking exposure in mice will precisely recapitulate that seen in humans. Mice have much larger airways relative to lung size as well as fewer airway generations compared with humans [194], so airway remodelling may affect overall lung mechanics differently. However, we must also acknowledge the limitations imposed on our ability to draw conclusions by the subtle changes we found; the consequence airway remodelling (Figure 2.1) and the degree of emphysema produced by the smoke exposure (Figure 2.2) in our mice were mild, and the resulting functional changes in the lung were correspondingly small (Figures 3.1-3.3). These minor yet detectable changes may simply reflect the realities of trying to recapitulate a pathology that takes a lifetime to develop in a human by treating a mouse over a necessarily much shorter time span.

In summary, we have found evidence of sex-linked decrements in lung mechanics in smoke-exposed mice that were abolished by ovariectomy, implicating a key role for sex hormones. These results shed mechanistic light on the predilection for pre-menopausal women to develop more severe COPD than men, and offer the possibility that measurements of *Zrs* in patients might have a role in identifying individuals at particular risk for developing severe disease.

In the next chapter, we will demonstrate a plausible biological mechanism why female mice have more severe small airway remodelling than male mice after chronic smoke exposure.

Chapter 4: Female Mice Have Increased Oxidative Stress and Airway Remodelling After Chronic Smoke Exposure: Implication for Sexual Dimorphism in Mild COPD

4.1 Introduction

In chapter 2 and 3, we have demonstrated that female mice have increased airway remodelling than male mice, and this was associated with increased distal airway resistance after chronic smoke exposure. Oxidative stress has been shown to be important in the pathogenesis of COPD, but the precise mechanism by which this occurs is not clearly known [148]. Cigarette smoke (CS) exists as a gaseous and a particulate phase, producing more than 10^{14} reactive oxygen species per puff, and an important exogenous source of superoxide anion [195]. Smokers smoking an average of 10.7 cigarettes/day has a saliva cotinine level of 113ng/ml, and for the same number of cigarettes smoked per day, saliva cotinine level is greater in men than in women [146], suggesting that women have an accelerated metabolism of cotinine. Clinical data showed that female smokers have increased CYP enzymes compared to male smokers, and this may be related to estrogen levels because stimulation of estrogen receptor increases CYP1A1 protein expression [196]. Recent evidence revealed a direct activation of TGF- β protein in air-exposed control rat tracheal explants, and recombinant TGF- β latency-associated peptide *in vitro* by cigarette smoke via an oxidative mechanism [150]. In support for the role of oxidative stress on airway remodelling *in vivo*, Rubio and colleagues demonstrated a 25% increase in wall area of small bronchi in rats after 10 weeks of cigarette smoke exposure, and this effect was prevented by the administration of N-acetyl cysteine [151]. Furthermore, Hecker and colleagues showed that intratracheal instillation of Nox4 siRNA, an important producer of superoxide, in mice attenuated bleomycin-induced increase in hydrogen peroxide release, α -SMA and fibronectin expression [167]. Similarly, they found that treatment of Nox4 siRNA on human fetal lung

mesenchymal cells attenuated TGF β -induced increase in these markers, suggesting a strong potential link between oxidative stress and TGF β -mediated activation of a fibrotic phenotype. In this study, we determined whether the increase in airway remodelling in female mice demonstrated in chapter 2 and 3 is associated with increased oxidative stress in the airways.

4.2 Materials and methods

4.2.1 Animal smoke exposure

Male, female and ovariectomized C57BL/6 mice were exposed to research grade cigarettes (University of Kentucky, Lexington, KY) 5 days/week, for 6 months. For the intervention study, female mice were implanted with one 75mg Tamoxifen free base pellet released at steady state over 60 days (E361, Innovative Research of America, Sarasota, FL) and pre-treated for three weeks prior to smoke exposure, followed by smoke exposure 5 days/weeks for 1 month. Refer to methods in chapter 2 for more details.

4.2.2 Laser-capture micro-dissection and real time PCR

Whole left lungs were inflated with 50% embedding medium for frozen tissues (OCT) in DEPC-treated water and snap frozen. Frozen lungs were cut into 5 μ m-thick sections using a cryostat (Leica Biosystems, Concord, ONT) and laser capture microdissection was performed using the Leica LMD6500 Laser Microdissection System (Leica Microsystems, Concord, ONT). Small airways (<200 μ m in diameter) and parenchyma from six histologic sections per mouse were collected separately in an RNeasy lysis buffer-containing Eppendorf 500- μ l tube (Mississauga, ON, Canada) and stored at -80°C until the RNA extraction procedure. Total RNA (50ng) was reverse transcribed into cDNA using the iScript cDNA synthesis kit according to the manufacturer's protocol (Biorad, Mississauga, ON). Real time PCR was performed on an

Applied Biosystems platform (Applied Biosystems-ABI, Carlsbad, CA). TaqMan PCR probes for *Nrf-2* (Mm00477784_m1), *Nqo1* (Mm01253561_m1), *Hmox1* (Mm00516005_m1), *Cyp1a1* (Mm00487218_m1), *Cyp1b1* (Mm00487229_m1), *Aldh9a1* (Mm00480240_m1), *Adh5* (Mm00475804_g1), *Sdha* (Mm01352363_m1), *Aldh3a1* (Mm00839312_m1), *Gsr1* (Mm00439154_m1), *Cyp2f2* (Mm00484087_m1) were obtained from Applied Biosystems. RNA quality in all samples were confirmed (RNA Integrity Number 5-6) using an Agilent BioAnalyzer. Gene expression quantification was based on the Δ CT method of relative quantification with normalization to beta-2 macroglobulin (β 2m).

Nox4 (ID: 146134358c3), *asma* (ID: 31982518c1) primer sequences were obtained from PrimerBank (<http://pga.mgh.harvard.edu/primerbank/>), and were synthesized by Invitrogen. Gene expression quantification was based on the Δ ^{CT} method of relative quantification using SYBR green assay. All mRNA expression were normalization to *Gapdh*.

4.2.3 Trolox-equivalent antioxidant capacity

Whole right lungs were homogenized in extraction buffer (100mg tissue/0.5mL buffer; A3605, Sigma-Aldrich) supplemented with protease inhibitor (5871, Cell Signalling) and phosphatase inhibitor (P5726, Sigma-Aldrich) using a TissueLyser LT (Qiagen) for 1.5 minutes at 50 oscillations per second. Lung homogenates were centrifuged at 13,000rpm for 15 minutes at 4°C and stored at -80°C. Total antioxidant capacity was assessed in whole lung homogenate by using a colorimetric assay. The principle is based on the formation of a ferryl myoglobin radical from metmyoglobin and hydrogen peroxide, which oxidizes ABTS (2,2'-azino-bis(3-ethylbenzthiazoline-6-sulfonic acid) to produce a radical cation, ABTS^{•+}, a soluble chromogen that is green in color and can be determined spectrophotometrically at 405nm. Trolox, a water-soluble vitamin E analog, was used as a standard antioxidant for the suppression of radical cation

generation in a concentration dependent manner with an inverse relationship between total antioxidant capacity and color intensity (CS0790, Sigma-Aldrich, St. Louis, MO). Data were normalized to total protein in milligram per reaction.

4.2.4 Dihydroethidium labelling

Briefly, to measure reactive oxygen species (ROS) production *in-situ*, left lungs were inflated with 50% OCT. 10 μ m frozen lung issues were sectioned and stained with 10 μ M dihydroethidium (DHE) (D11347, Life Technologies), a specific marker of superoxide, for 30 minutes at room temperature and imaged using fluorescent microscopy. Un-oxidized DHE exhibits blue fluorescence in the cytosol, whereas oxidized DHE gets intercalated into the nucleus and stains the nucleus red. The excitation/emission wavelength of DHE is 518/606nm. Slides were mounted on VECTASHIELD HardSet Mounting Medium with DAPI and visualized using a conventional fluorescence microscope. Fluorescence intensity was quantified using Image J software and normalized to the length of the basement membrane of airways less than 200 μ m.

4.2.5 ELISA assays for 3-nitrotyrosine and active TGF β 1

The range of detection of the 3-nitrotyrosine ELISA was 8-1000ng/ml. Lung homogenates were also used to measure active TGF β 1 by ELISA (MB100B, R&D Systems). This ELISA specifically recognizes the active form of TGF β 1. The range of detection of this ELISA was 5-2000pg/ml. Data were expressed as mean \pm SEM with normalization to total protein in milligrams per reaction.

4.2.6 Immunofluorescence staining for active TGFβ1

5µm OCT-inflated frozen left lung sections were fixed/permeabilized in acetone at -20°C for 10 minutes. Sections were incubated with antibodies against active TGFβ1 (MAB1835; R&D systems) overnight for 4°C and stained with Alex Fluor® 488 Chicken anti-rabbit IgG (A-21441, Life Technologies) for 2 h at room temperature. Slides were mounted on VECTASHIELD HardSet Mounting Medium with DAPI and visualized using confocal microscopy. Fluorescence intensity in the airways was quantified using Image J software and normalized to the length of the basement membrane.

4.2.7 Isolation of primary fibroblasts and bronchial epithelial cell culture

The whole length of the mice trachea (N=3 female C57BL/6 mice at 12 weeks old) was dissected free from surrounding tissues and diced into fine pieces of approximately 1X1 mm² pieces. After washing in ice cold sterile PBS 3 times, tissue explants were placed in 6 well plate (BD Bioscience, Mississauga, ON, Canada) containing Dulbecco's modified Eagle's Medium with L-glutamine (GIBCO/Invitrogen, Burlington, ON, Canada) supplemented with 10% Fetal Bovine Serum (GIBCO) and 1% PSF (penicillin, streptomycin and fungizone solution) (GIBCO). Tissue explants were cultured at 37°C at 5%CO₂ for 14 days with a change of medium everyday for the first week and three time a week thereafter. After reaching 90% confluence, cells were split into 75-cm² flasks (BD Bioscience) and referred as passage 1. Primary cells were seeded on 6-well plates with fresh media 3 times a week or until 90% confluence. Cells were grown for an additional 48h with or without 10ng/ml of recombinant human TGFβ1 (R&D Systems, Minneapolis, MN, USA). Cells between passage 2–4 were used for all experiments.

4.2.8 Uteri epithelial thickness

The uterus of female mice with or without the ovaries removed were dissected and fixed in formalin for 24h. Uterine wet weight was measured, and paraffin-embedded sections (5µm) were stained with periodic acid-Schiff (PAS) for measurement of epithelial thickness (area of epithelium/length of basement membrane) as a physiologic index of the effect of ovariectomy.

4.2.9 Statistics

Data were analyzed using non-parametric t-test, and one-way ANOVA with Bonferroni's multiple comparisons tests using GraphPad Prism version 6 (GraphPad Software Inc, San Diego, CA, USA). All data were expressed as mean \pm SEM. Statistical significance was considered at $P < 0.05$.

4.3 Results

4.3.1 Increased small airway remodelling was associated with impaired antioxidant gene expression in response to cigarette exposure in female mice, and this effect was attenuated by ovariectomy.

To determine the sexual dimorphism in cigarette smoke-induced small airway remodelling in our mouse model of COPD, we examined a select set of antioxidant genes including those regulated by NRF2 protein in all groups. Overall antioxidant mRNA expression was constitutively lower in female than male control airway tissues (Figure 4.1A). In general, antioxidant gene expression in airway tissues of male mice was increased after chronic CS exposure but the increases were blunted in female mice.

Smoke exposure increased *Cyp1a1*, *Cyp1b1* and *Nrf2* mRNA expression in the airways of male but not female mice, and this effect was partially restored with ovariectomy (Figure 4.1B-D). One of the genes regulated by *Nrf2* is NADPH:quinone oxidoreductase 1 (*Nqo1*). The *Nrf2* mRNA expression pattern was reflected in the NRF2-regulated *Nqo1* mRNA expression in response to smoke exposure (Figure 4.1E). Although smoke exposure did not affect *Nqo1* mRNA expression in male and female mice, female airway tissues had lower *Nqo1* mRNA expression than male mice ($p < 0.001$). Collectively, these mRNA expression data showed sex differences in phase I and II detoxifying enzyme mRNA expression levels in airway tissues of male and female mice.

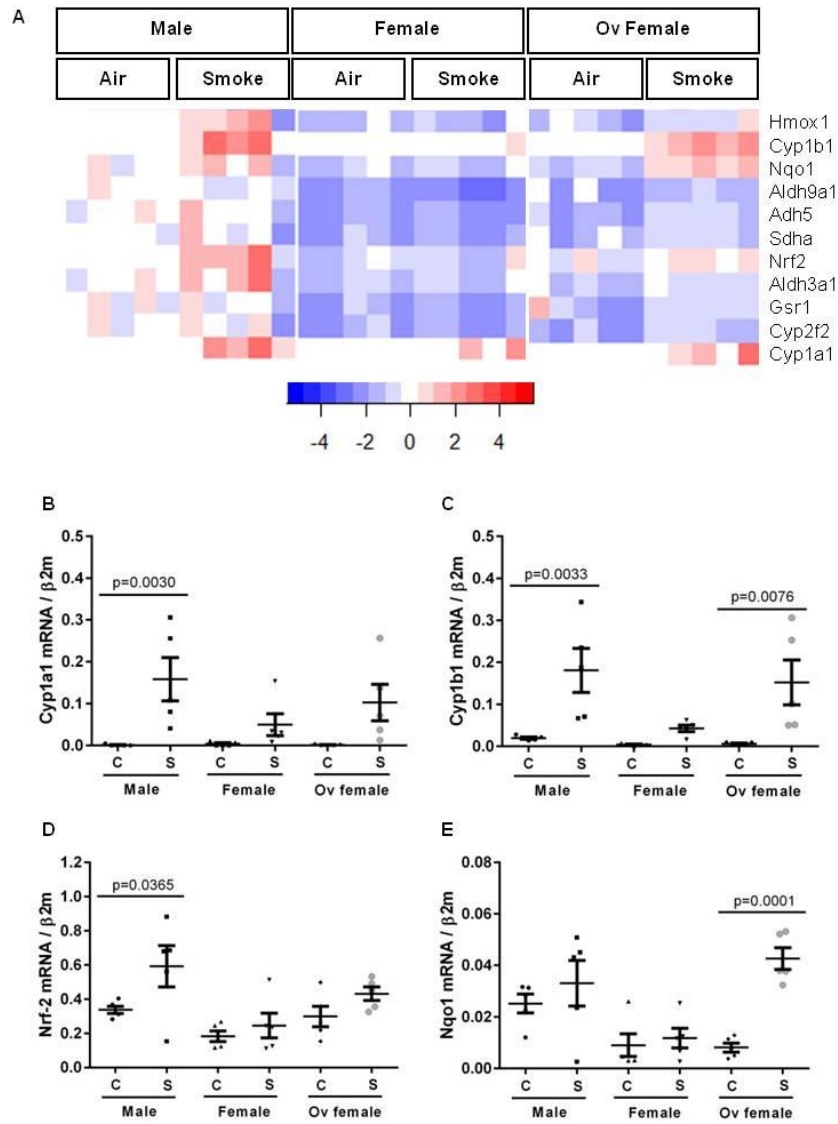


Figure 4.1: Female mice have an impaired antioxidant gene response to cigarette smoke compared to male mice or ovariectomized mice.

A) Heat map of antioxidant gene expression in laser-capture airway tissues of control (C) or smoke-exposed (S) male, female and ovariectomized mice at 6 months. Color intensities were normalized to the average gene expression in male control mice within each gene. Blue=lower than male control values, red=higher than male control values. B) *Cyp1a1*, C) *Cyp1b1*, D) *Nrf2*, and E) *Nqo1* mRNA expression normalized to $\beta 2m$ in airway tissues. Values expressed as mean \pm SEM with N=5 per group. One-way ANOVA with Bonferroni's multiple comparisons tests were used in all groups. (beta-2 macroglobulin- $\beta 2m$, Heme oxygenase-*Hmox1*, cytochrome p450-*Cyp1a1/1b1/2f2*, NADPH: quinone oxidoreductase1-*Nqo1*, aldehyde dehydrogenase-*Aldh9a1/3a1*, alcohol dehydrogenase-*Adh5*, Succinate dehydrogenase complex-*Sdha*, nuclear factor erythroid-related factor-*Nrf2*, glutathione reductase-*Gsr1*).

4.3.2 Female mice showed greater pulmonary oxidative stress than male mice, and this effect was attenuated by ovariectomy.

To determine the downstream effects of antioxidant gene expression changes in the lung, we measured 3-nitrotyrosine (3NTyr) levels in whole lung homogenates as a marker of oxidative stress. 3NTyr per milligram of total protein in whole lung homogenates was increased in female but not male mice after smoke exposure, and this effect was abolished with ovariectomy (Figure 4.2A). Smoke exposure decreased total antioxidant capacity in whole lung homogenates of female but not in male mice, and this effect was rescued with ovariectomy (Figure 4.2B).

To determine whether a decrease in total antioxidant capacity associates with an accumulation of reactive oxygen species in the lungs of smoke-exposed mice, we measured oxidative stress in the small airways using dihydroethidium (DHE), which is a fluorescent marker of superoxide anion [197]. Smoke exposure increased total intracellular superoxide anion level in the small airways of female mice by 50% ($p < 0.05$) compared to air-exposed female mice, but this effect was abolished in ovariectomized mice (Figure 4.2C). No significant difference in superoxide level was observed between air-exposed and smoke-exposed male mice. To determine whether the accumulation of oxidants in the airways of smoke-exposed female mice leads to the release of active TGF β 1, we showed that smoke exposure increased the release of active TGF β 1 in female but not male mice, and this effect was attenuated with ovariectomy (Figure 4.2D).

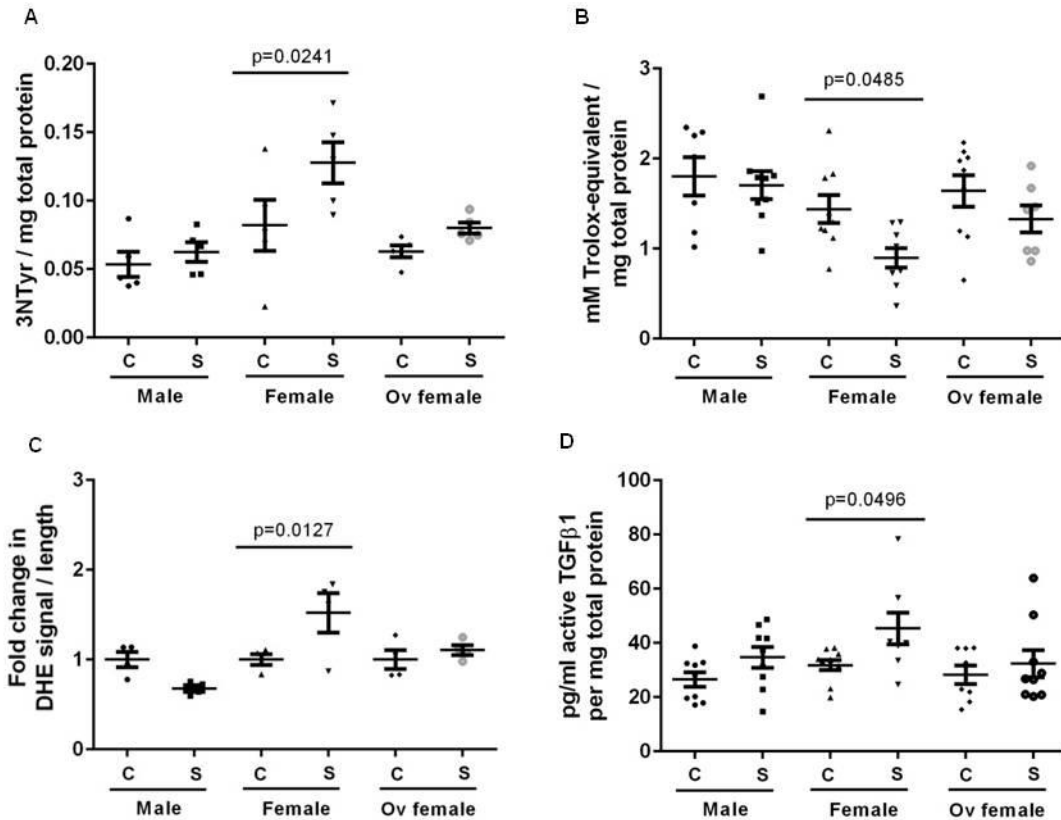


Figure 4.2: Female mice have increased nitrosative and oxidative stress, and increased active TGFβ1 protein expression.

A) 3-nitrotyrosine and B) Trolox-equivalent total antioxidant capacity were measured from whole lung homogenate and normalized to total protein loaded per reaction. * $p < 0.05$ compared between control (C) and smoke-exposed (S) groups after 6 months of air or smoke exposure. # $p < 0.05$ compared between two different (S) groups. Values expressed as mean \pm SEM with $N=5$ per group in panel A, and $N=8-10$ per group in panel B. C) Fluorescence intensity of dihydroethidium (DHE) in airway tissues was normalized to the length of the basement membrane. Values were expressed as fold change in DHE signal \pm SEM relative to control mice in each animal group with $N=4$ per group in panel C. D) Active TGFβ1 protein in whole right lung homogenate was normalized to total protein loaded per reaction. Values expressed as mean \pm SEM with $N=8-10$ per group in panel D. One-way ANOVA with Bonferroni's multiple comparisons tests were used in all analyses.

4.3.3 Female mice showed greater airway-specific active TGFβ1 protein and downstream signalling compared to male or ovariectomized mice

Using immunofluorescence staining and imaging by confocal microscopy, we showed an increase in active TGFβ1 protein in the airways of female mice after smoke exposure ($p < 0.05$), whereas ovariectomy abolished this effect (Figure 4.3A-G). Smoke exposure did not affect the amount of active TGFβ1 protein in the airways of male mice compared to air-exposed male control mice. To determine whether the increased expression of active TGFβ1 in the airways of female mice associated with an increase in total collagen expression in the airway walls of smoke-exposed female mice, we confirmed the activation of the TGFβ1 signalling cascade at the transcriptional level. As a potent downstream transcript of TGFβ1 activation and an important producer of superoxide, *Nox4* mRNA expression was increased in the airways of female but not male mice after smoke exposure, and this effect was attenuated with ovariectomy (Figure 4.3H). To confirm the specificity of TGFβ1 activation on the transcription of *Nox4* mRNA, stimulation of normal female mouse tracheal fibroblasts with TGFβ1 for 48h increased *Nox4* mRNA expression (Figure 4.3I). *αsma* mRNA expression was increased in the airways of female mice ($p < 0.05$) after chronic smoke exposure, but were attenuated with ovariectomy (Figure 4.3J). Collectively, these data showed that a build-up of oxidants in the lungs of female mice after smoke exposure was associated with an increased release of active TGFβ1 protein and downstream signalling response.

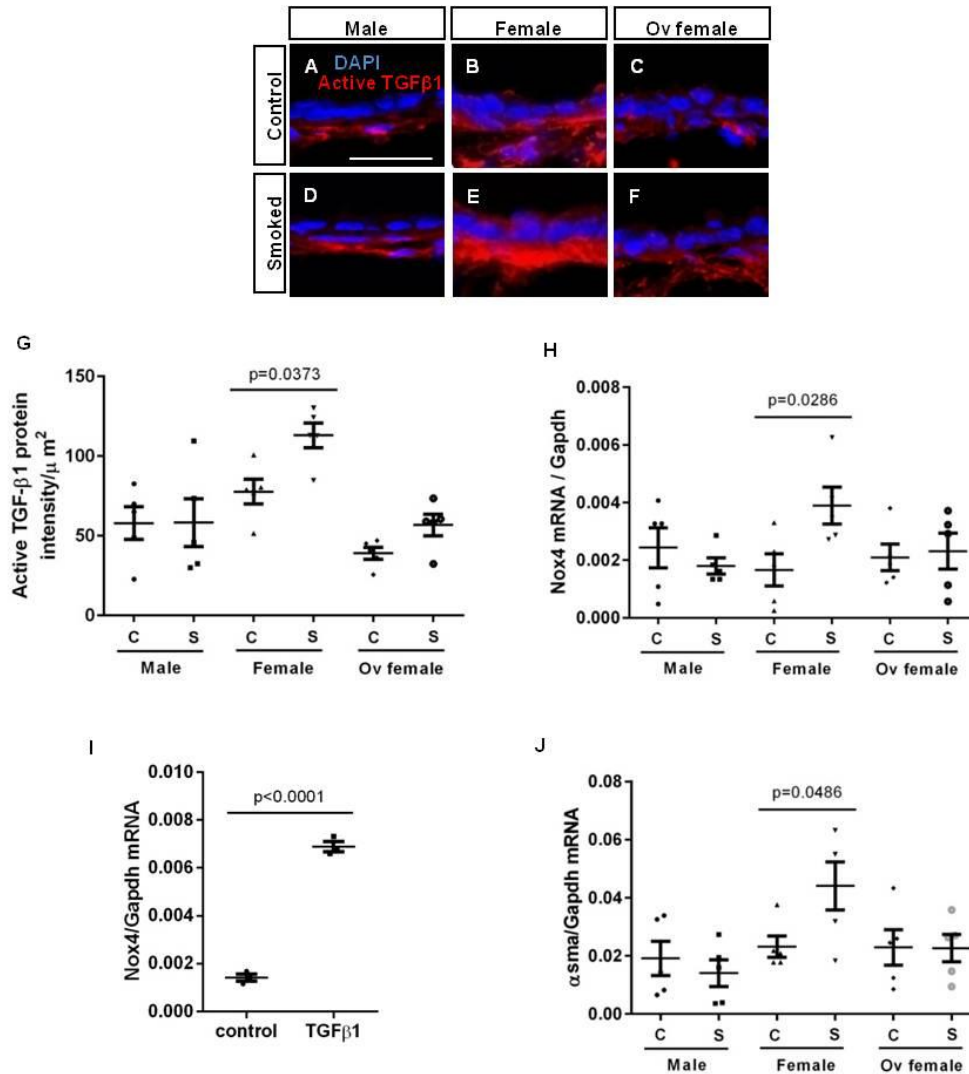


Figure 4.3: Female mice have increased expression of active TGFβ1 protein and TGFβ1-responsive genes in airway tissues.

Immunofluorescence image of control (C) and smoke-exposed (S) male (A,D), female (B,E) and ovariectomized (C,F) mouse lung sections were stained for active TGFβ1 protein in the airway wall. G) Fluorescence intensity of active TGFβ1 protein was normalized to the area of airway tissues. Nuclei were counterstained with DAPI. Scale bar=20μm. Values were expressed as mean intensity / μm² ± SEM with N=5 per group. H) *Nox4* mRNA expression were normalized to *Gapdh* in airway tissues from all groups. Values were expressed as mean ± SEM with N=5 per group. I) *Nox4* mRNA expression in normal mouse tracheal fibroblasts stimulated with 10ng/ml of TGFβ protein for 48h were normalized to *Gapdh*. Values were expressed as mean ± SEM with N=3 per group. Non-parametric t-test was used in panel I. J) *asma* mRNA expression was normalized to *Gapdh* in airway tissues of all groups. Values expressed as mean ± SEM with N=5 per group. One-way ANOVA with Bonferroni's multiple comparisons tests were used in panels G, H and J.

4.3.4 Tamoxifen attenuated smoke-induced increase in *Cyp1a1* mRNA expression in the airways of female mice after 1 month of smoke exposure

Since *Cyp1a1*, *Cyp1b1*, *Nrf2*, and *Nqo1* genes contain estrogen response elements in the promoter region [198], it is plausible that estrogen and estrogen receptor activation may affect expression of these oxidant-related genes and the production of excess reactive oxygen species if phase I and II xenobiotic enzymes were disproportionately expressed. We selectively blocked estrogen receptors by subcutaneously implanting tamoxifen (TAM) pellets in female mice with intact ovaries to determine whether estrogen plays a role in CS-induced oxidative stress. 1 month of smoke exposure significantly increased *Cyp1a1*, *Cyp1b1*, *Nrf2*, and *Nqo1* mRNA expression in airway tissues of female mice compared to air-exposed female control, whereas tamoxifen treatment differentially attenuated *Cyp1a1* but not *Cyp1b1*, *Nrf2*, and *Nqo1* mRNA expression (Figure 4.4A-D). Smoke exposure, however, increased *Cyp1b1* but not *Cyp1a1*, *Nrf2* or *Nqo1* mRNA expression in airway tissues of male mice. Female mice have greater *Cyp1a1* mRNA expression than male mice after smoke exposure and this excess increase appeared to be driven by estrogen.

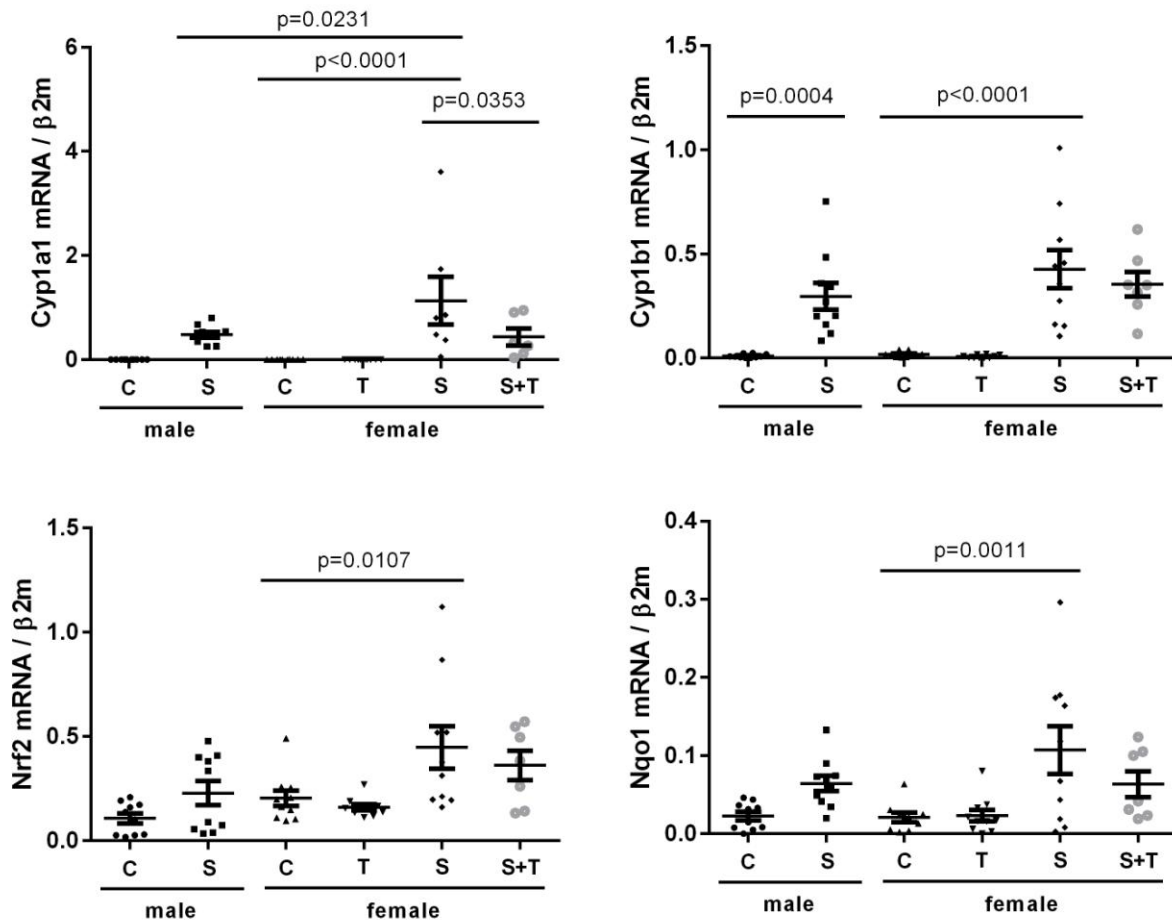


Figure 4.4: Tamoxifen attenuated smoke-induced increase in *Cyp1a1* mRNA expression in the airways of female mice.

A) *Cyp1a1*, B) *Cyp1b1*, C) *Nrf2* and D) *Nqo1* mRNA expression were normalized to $\beta 2m$ in airway tissues of male and female control (C), smoke-exposed only (S), 75mg tamoxifen (T) only, and (S+T) mice after 1 month of smoke exposure. Values were expressed as mean \pm SEM with N=7-10. One-way ANOVA with Bonferroni's multiple comparisons tests were used in all analyses.

4.3.5 Tamoxifen attenuated smoke-induced increase in *Nox4* mRNA expression in the airways of female mice after 1 month of smoke exposure

We have previously showed that 6 months of smoke exposure increased *Nox4* mRNA expression in the airways of female mice and this effect was attenuated by ovariectomy. To determine whether this effect was driven by estrogen, we showed that tamoxifen attenuated smoke-induced increase in *Nox4* mRNA expression compared to ovary-intact air-exposed mice (Figure 4.5A). To confirm whether tamoxifen exerted a biological effect on female mice, we showed that tamoxifen treatment for three weeks increased uterus epithelial thickness compared to ovary-intact control mice (Figure 4.5B-D). Collectively, these data demonstrated that smoke-induced increase in *Nox4* mRNA expression were influenced by estrogen and also may be indicative of increased TGF β 1 signalling in airway tissues of female mice.

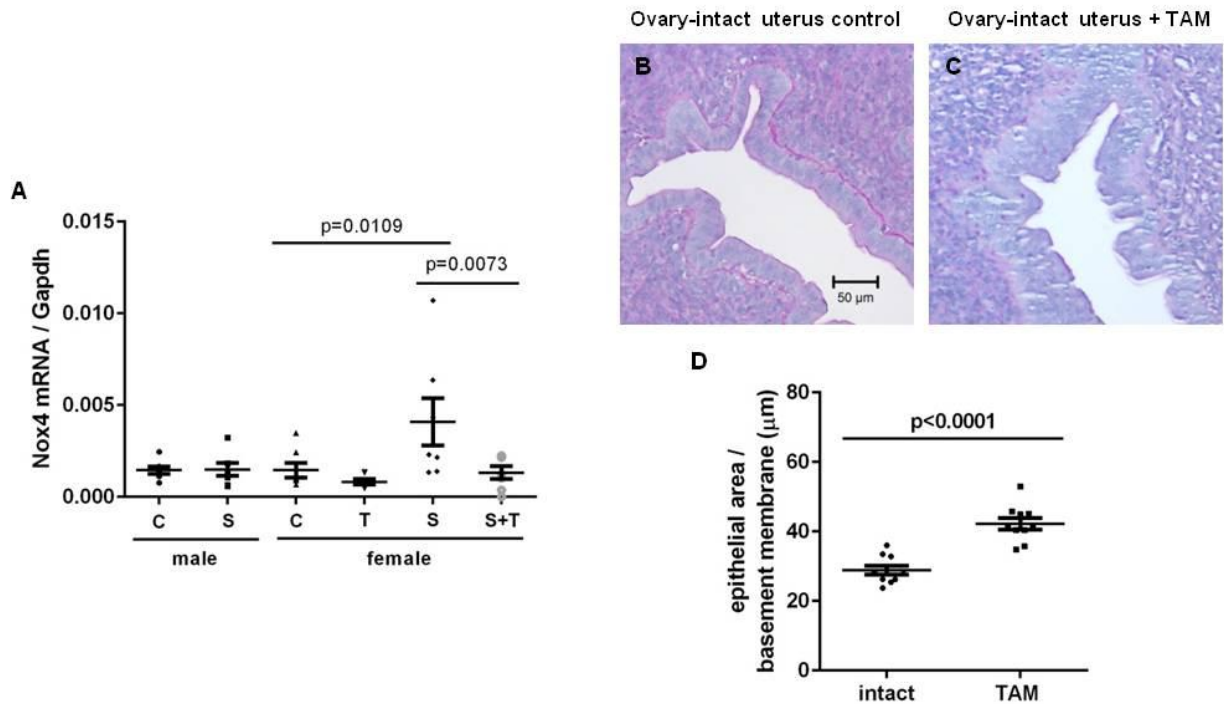


Figure 4.5: Tamoxifen attenuated smoke-induced increase in Nox3 and Nox4 mRNA expression in the distal airways of female mice.

A) *Nox4* mRNA expression were normalized to *Gapdh* in airway tissues of male and female control (C), smoke-exposed only (S), 75mg tamoxifen (T) only, and (S+T) mice after 1 month of smoke exposure. Data were expressed as mean \pm SEM with N=7 per group. One-way ANOVA with Bonferroni's multiple comparisons test was used in panel A. 5 μ m thick histologic sections of formalin-fixed paraffin-embedded uterus in B) ovary-intact control and C) ovary-intact mice implanted with Tamoxifen were stained with Periodic acid-schiff (scale bar = 50 μ m). D) Uterus epithelial area was normalized to the length of the epithelium measured at the basement membrane (μ m) in female mice. Values were expressed as mean \pm SEM with N=10 per group. Non-parametric t-test was used in panel D.

4.3.6 Estrogen differentially enhanced smoke-induced increase in *Cyp1a1* but not *Cyp1b1* and *Nqo1* mRNA expression in normal human bronchial epithelial cells.

To demonstrate a biological relevance of estrogen in the modulation of smoke-induced changes in antioxidant genes from our mouse model to human bronchial epithelial (NHBE) cells cultured in air liquid interface, we showed that smoke exposure increased *Cyp1a1*, *Cyp1b1* and *Nqo1* but not *Nrf2* mRNA expression in female NHBE cells compared to air-exposed controls (Figure 4.6A-D). Estradiol differentially enhanced smoke-induced increase in *Cyp1a1* but not *Cyp1b1*, *Nqo1* and *Nrf2* mRNA expression. In the absence of cigarette smoke, estradiol differentially increased *Cyp1a1* and *Nqo1* but not *Cyp1b1* and *Nrf2* mRNA expression at baseline (Figure 4.6E-H). Primer specificities for *Cyp1a1*, *Cyp1b1*, *Nrf2* and *Nqo1* were confirmed by the presence of a single DNA product in 1.1% agarose gel at an annealing temperature of 60°C (Figure 4.6I-L).

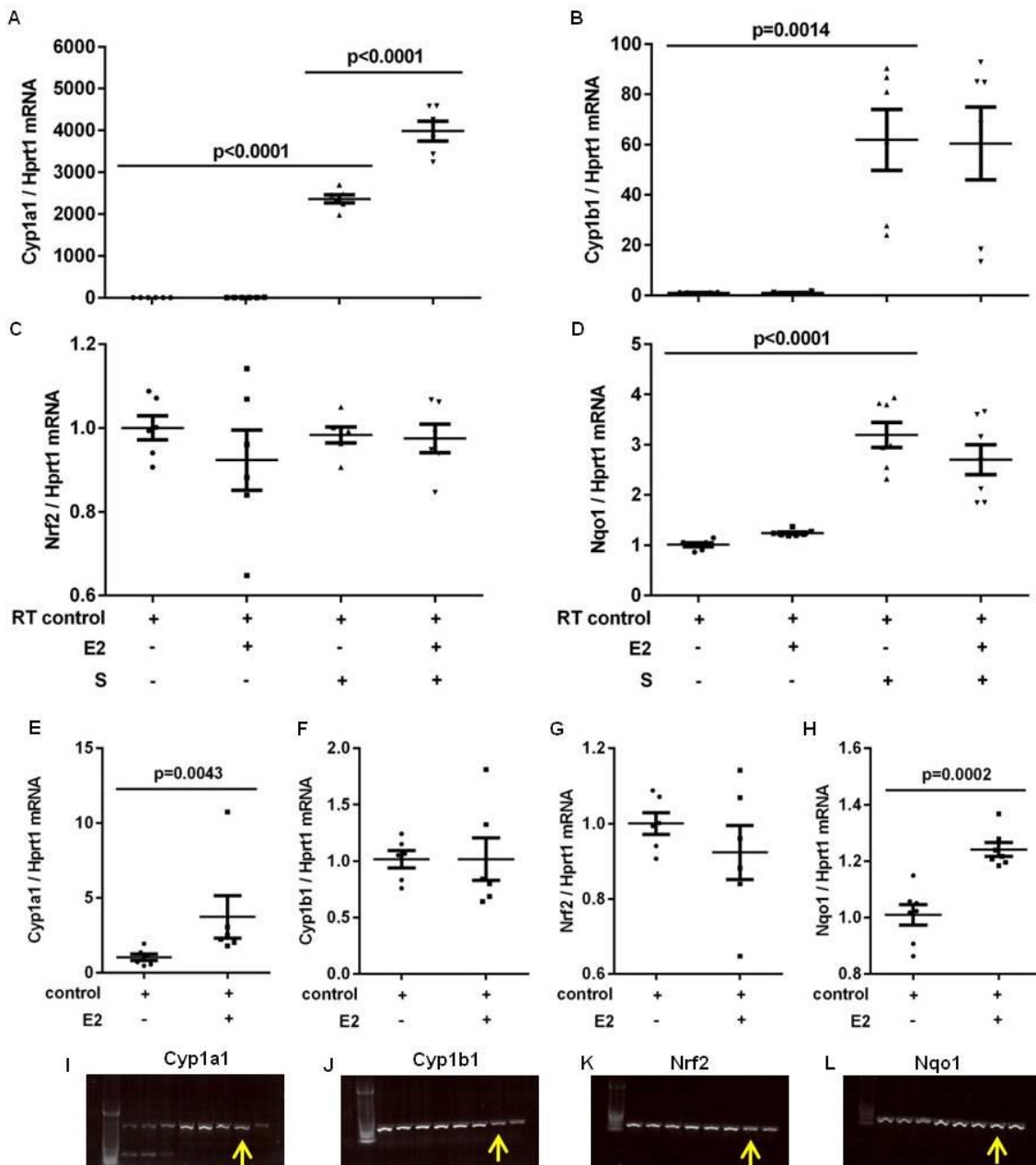


Figure 4.6: Estradiol differentially enhanced smoke-induced increase in Cyp1a1 but not Cyp1b1 and Nqo1 mRNA expression in normal human bronchial epithelial (NHBE) cells.

A) *Cyp1a1*, B) *Cyp1b1*, C) *Nrf2* and D) *Nqo1* mRNA expression were normalized to *Hprt1* in air-exposed control, estradiol only (E2), smoke-exposed only (S), and E2 + S exposed female NHBE cells for one week. Values were expressed as mean \pm SEM with N=2 female NHBE cell donors. Primer specificities for I) *Cyp1a1*, J) *Cyp1b1*, K) *Nrf2* and L) *Nqo1* were confirmed on DNA gels with single product at an annealing temperature of 60°C (yellow arrow). A 100bp DNA ladder was indicated. One-way ANOVA with Bonferroni's multiple comparisons tests were used in panels A-D. Non-parametric t-tests were used in panels E-H.

4.4 Discussion

Although oxidative stress has been suggested to be important in the pathogenesis of COPD, the precise mechanisms by which this occur remain largely elusive [148]. The findings of the present study indicate that female sex hormones blunt the airways' ability to mount an effective anti-oxidant response to chemical irritants such as cigarette smoke, leading to a build-up of oxidant stress, dysregulated TGF β 1 signalling and fibrosis in the small airways of mice. An important mediator of this process is NRF2. NRF2 protein is a redox sensor and a master-switch regulator of antioxidant genes [199]. Deficiency in *Nrf2* gene has been shown to increase susceptibility to smoke-induced emphysema, bronchoalveolar inflammation and oxidative stress in mice [185].

All of the selected antioxidant genes in our study (Figure 4.1) are transcriptionally regulated by NRF2 [200] and contain estrogen response elements [198]. Using a mouse liver cell line, Kharat and colleagues showed that estrogen interfered with the binding of TCDD-activated AhR onto the xenobiotic response element in the promoter of the *Cyp1a1* gene [201]. Furthermore, 17 β -estradiol has been shown to inhibit NRF2-mediated enzyme activities by estrogen receptor-alpha (ERA) and NRF2 protein interaction [202, 203]. Estrogen has also been demonstrated to suppress NQO1, a Phase 2 xenobiotic enzyme, via an ER-dependent mechanism. Anti-estrogens (tamoxifen and ICI-182,780), on the other hand, up-regulate *Nqo1* expression in ER-positive breast cancer cells [204]. This gene reduces quinones to hydroquinones, thus preventing the accumulation of reactive semiquinone that generates superoxide [205]. NQO1, which is transcriptionally regulated by NRF2, has been shown to protect cells from oxidative stress [206-208] and is highly expressed in the cytoplasm of normal airway epithelium [209]. Similarly, deficiency in *Hmox1* has been reported to cause

susceptibility to oxidant-mediated lung injury in mice [210]. Consistent with these observations, we showed reduced total antioxidant capacity and increased levels of 3-nitrotyrosine in whole lung homogenates of female but not male mice or ovariectomized female mice following smoke exposure. We also showed increased superoxide generation in the small airways of female but not male mice or ovariectomized mice. Collectively, these data suggest that female mice have a dampened ability to metabolize cigarette smoke in the airways, leading to the accumulation of reactive oxygen species in the airways.

Although the central role of TGF β 1 signalling on airway fibrosis is known [211], the upstream mechanisms by which cigarette smoke activates TGF β 1 have not been fully elucidated. In the present study, we showed that female mice when exposed to cigarette smoke demonstrate increased activation of TGF β 1 protein in small airways. Ovariectomy, on the other hand, suppressed the smoke-related increases in oxidative stress and reduced TGF β 1 activation in airway tissues of female mice. We previously showed that cigarette smoke exposure directly oxidizes the latency-associated peptide (LAP) of TGF β 1 by oxidizing cysteine or methionine residues, causing the active form of TGF β 1 protein to be released into tissues [149, 212]. Treatment of mice with tetramethylthiourea (TMTU), a scavenger of reactive oxygen species, on the other hand, prevents the release of active TGF β 1 protein into tissues in response to cigarette smoke, and suppresses pro-collagen mRNA expression [212]. Once liberated into the tissue, active TGF β 1 binds to TGF β R1/R2 and induces the phosphorylation of SMAD2 and SMAD3 (pSMAD2/3), which are key protein mediators in the TGF β -signalling cascade. Direct binding of pSMAD2/3 to its response element up-regulates *Nox4*, *α -sma*, *Col1* and *Col3* mRNA expression [163-165]. Consistent with histologic findings of increased airway remodelling, we showed that *Nox4* and *α -sma* mRNA expression were increased in airway tissues of smoke-exposed female

but not in male or ovariectomized female mice. Since Nox enzymes are major contributors in many oxidative damage-related diseases including COPD, twenty-four compounds have been shown to inhibit Nox4 activity with micromolar IC(50) values of which three were selected for drug testing and development [213].

To demonstrate whether an increase in estrogen can explain the excess risk for the chronic smoke-induced airway remodelling in our mouse model, tamoxifen, a selective estrogen receptor modulator, was delivered subcutaneously as a therapeutic intervention in addition to one month of smoke exposure. Unlike the blunted effects of phase I and II xenobiotic gene expression after 6 month of smoke exposure, airways tissues from female mice were still responsive to the induction of *Cyp1a1*, *Cyp1b1* and *Nqo1* mRNA expression after sub-chronic (1month) smoke exposure. Female mice have disproportionately greater level of *Cyp1a1* mRNA expression than male mice, and tamoxifen treatment attenuated this excess increase to those of male levels after 1 month of smoke exposure. The interaction between estrogen and smoke-induced changes in antioxidant appears to be dynamic, and may depend on the duration of smoke exposure. However, our data provided some evidence that disrupting the estrogen receptor by tamoxifen affects the transcriptional response of certain estrogen-sensitive antioxidant genes. Further study is required to understand the kinetics of all phase I and II xenobiotic enzyme expression with acute, sub-chronic and chronic smoke exposure.

To translate the impact of estradiol on smoke-induced changes in antioxidant genes from our in vivo model onto human bronchial epithelial cell culture model, we showed that estradiol differentially enhanced sub-chronic smoke-induced increase in *Cyp1a1* but not *Cyp1b1* and *Nqo1* mRNA expression, suggesting that phase I and II xenobiotic enzymes may be disproportionately regulated at the transcriptional level. Our data has recapitulated clinical

findings that female smokers have increased *Cyp1a1* mRNA and protein expression than male smokers [196], suggesting the contribution of estrogen on the excess increase in *Cyp1a1* mRNA expression.

Collectively, our data indicate that female mice are more susceptible to airway remodelling after chronic smoke exposure and this effect appears to be largely affected estrogen receptor-mediated disruption of the phase I and II xenobiotic expression, antioxidant capacity to release the oxidants and the TGF β activation response, thus raising the possibility that targeting the estrogen receptor and its associated downstream pathways may be important in reducing the risk of small airway remodelling in female smokers with COPD.

Chapter 5: Estrogen Increases Mucus Synthesis in Bronchial Epithelial Cells

5.1 Introduction

In most chronic inflammatory diseases of the airway (e.g, asthma, COPD, CF), female patients generally have more symptoms, worse quality of life and poorer prognosis than male patients [111, 112]. One pathological link that is common to these conditions is mucus hypersecretion with plugging of airways [25]. Mucins are large, oligomeric, O-linked glycoprotein with high molecular weight (2-40MDa) and size (0.5-10 μ m) [214]. As the predominant mucins in the human airway, MUC5AC is produced mostly by goblet cells, while MUC5B is produced mainly in submucosal glands [76, 215]. MUC5AC is thought to be an acute phase product that responds rapidly to direct contact with environmental insults, whereas MUC5B may be involved in the chronic inflammatory response to infections [77]. Mucin expression has been shown to be regulated by a variety of inflammatory mediators including lipopolysaccharide (LPS) [216], tumor necrosis factor (TNF)- α [217], interleukin (IL)-1 [217], IL-17 [218], IL-13 [219] β neutrophil elastase [220], and growth factors such as EGF [221], and environmental insults including cigarette smoke [222] and bacteria [223]. Even in genetically determined diseases such as CF, in which abnormal mucus secretion is a prominent feature of disease, lung function is the lowest at ovulation when estrogen levels are elevated [112], raising the possibility that estrogens may play an active role in this condition. Estrogen receptors alpha and beta exist in normal human bronchial epithelial (NHBE) cells with ER- β in predominance [224]. However, little is known whether estradiol plays any role in the regulation of mucus in the airways.

MUC5AC gene expression has been shown to be regulated by a variety of transcription factors including Forkhead box protein A2 (FOXA2), (NF κ B), activating protein 1 (AP1), specificity

protein (SP1) and cyclic AMP response element binding (CREB) protein [60]. In this study, we used an *in-vitro* model of the human airway epithelium and showed that nuclear factor of activated T-cell c1 (NFATc1) is a novel regulator of estradiol-mediated mucus synthesis.

5.2 Materials and methods

17- β estradiol was purchased from Sigma (St. Louis, MO). MPP [1,3-Bis(4-hydroxyphenyl)-4-methyl-5-[4-(2-piperidinyloxy)phenol]-1H-pyrazole dihydrochloride] (ER- α antagonist), and PHTPP [4-[2-Phenyl-5,7-bis(trifluoromethyl)pyrazolo[1,5-*a*]pyrimidin-3-yl]phenol] (ER- β antagonist) were obtained from Tocris (Ellisville, MO). Antibodies against ER- α (ab2746), ER- β (ab3577), and MUC5AC (ab24071) were obtained from Abcam (Cambridge, MA). Anti-IgG (sc-2343), HRP-conjugated anti- β -actin (sc-47778), superoxide dismutase –SOD (sc-11407), histone H3 (sc-8655) and NFATc1 antibody (sc-7294) were obtained from Santa Cruz Biotechnology. Heat shock protein -HSP90 (610418) antibody was obtained from BD Biosciences (Mississauga, ON). Goat HRP-conjugated anti-mouse IgG was from BD Pharmingen (Franklin Lakes, NJ) and goat HRP-conjugated anti-rabbit IgG from Millipore (Billerica, MA).

5.2.1 Cell cultures

This study was approved by the University of British Columbia/Providence Health Care Research Ethics Board (Number H11-02151 and A13-0207). Written informed consent was obtained from subjects where appropriate. NHBE cells were purchased from Lonza (Walkersville, MD) and the International Institute for the Advancement of Medicine (IIAM, Jessup, PA) (N=4 females, age: 16-45yr). Initially, cells were seeded at passage 0 into T25 flasks in Bronchial Epithelial Growth Media (BEGM, Lonza) and sub-cultured when 90% confluent. Cells were seeded in an air liquid interface at passage 4 on a 0.4 μ m semi-permeable membrane insert (BD Biosciences) in PneumaCult-ALI medium (StemCell Technologies, Vancouver,

Canada). Apical media was removed when cells reached 100% confluence while media in the basal compartment was replaced 3 times per week. At 21 days post-seeding, cells became fully differentiated, followed by treatment of physiological concentrations of estradiol (E2) (10^{-9} M to 10^{-7} M) for 2 weeks. Mucus overlying the epithelium in each well was washed with 500 μ L warmed PBS and collected every 7 days. ALI cultures were pre-treated with hormone receptor antagonists 24h prior to the beginning of experiment. 10^{-6} M MPP and 10^{-6} M PHTPP were added to the basal media and replaced 3 times per week. 0.01% final concentration of ethanol was used as a vehicle control. Human airway epithelial cell line (1HAE₀) was obtained from Dr Dieter Gruenert University of California, San Francisco [225] and cultured in DMEM (Gibco BRL; Invitrogen, Carlsbad, CA) with 10% fetal bovine serum (FBS). Estradiol concentration in media containing 10% FBS was less than 0.2pg/ml and was negligible compared to the estradiol concentrations added in culture.

5.2.2 Histological staining

5 μ m sections of paraffin-embedded human lung tissue from N=4 pre-menopausal female subjects (age: 16-45yr) with normal lung function and ALI cultures were stained for ER- α , ER- β , MUC5AC and Ki67 using the high sensitivity universal detection system-MACH kit (Biocare Medical, Concord, CA) (red). Sections were stained with Periodic Acid Schiff (PAS) for polysaccharides; nuclei were counterstained with Mayer's hematoxylin, dried overnight at room temperature and coverslipped in Cytoseal mounting solution. We used a point counting method to quantify the percentage of cells stained positively for the protein of interest by dividing the total number of epithelial cells counterstained with hematoxylin in three random fields at 200X final magnification from 4 different female subjects. PAS-positive cell count was based on counting nucleus to the nearest apical surface immediately beneath the PAS stain; whereas

ciliated cells were determined by counting nucleus nearest to the apical surface in cells with cilia but without PAS staining. Both of these measurements were normalized to the length of the epithelium in millimeters. To ensure that we accurately quantify the amount of PAS staining, we also measured the area of the PAS stain and expressed this value as a percentage of the total epithelial cross sectional area using color segmentation (ImagePro Plus 4.0, Media Cybernetics, L.P). These experiments were performed in N=4 female donors. The data are shown as mean \pm SEM.

5.2.3 Transcription factor activation protein array

A transcription factor (TF) activation profiling plate array from Signosis (FA-1001; Sunnyvale, CA) was used to screen for activated TFs in nuclear protein extract from female primary NHBE cells (N=2) stimulated with 10^{-7} M estradiol for 24h. A mixture of biotin-labelled probes based on the consensus sequences of TF DNA-binding sites was incubated with nuclear protein extract for 30 min at room temperature and allowed to form TF/probe complexes. The TF/probe complexes were separated from free probes through a simple spin column purification step. The bound probes eluded from the column were denatured at 98°C for 5min and allowed to hybridize with the biotin-conjugated consensus sequence initially bound on the bottom of each well in a 96-well plate. The captured DNA probe was detected with streptavidin-HRP. Luminescence was reported as relative light units on a microplate luminometer. Data were generated from 2 female donors.

5.2.4 Real time PCR

RNA from ALI cultures and 1HAE₀ cells was isolated using an RNeasy mini extraction kit from (Qiagen, Germantown, USA). High RNA quality in all samples was confirmed (RNA Integrity Number greater than 8) using an Agilent BioAnalyzer at The Centre for Applied Genomics

(TCAG) in Toronto (data not shown). 200ng of RNA was converted to cDNA with random hexamers using SuperScript III reverse transcriptase (Invitrogen, Life Technologies). TaqMan PCR probe-primers sets for FUT-1 (Hs00382532_m1), FUT-2 (Hs00704693_m1), FUT-3 (Hs01868572_m1), FUT-4 (Hs01106466_s1), FUT-5 (Hs00704908_s1), FUT-6 (Hs00173404_m1), FUT-7 (Hs00237083_m1), FUT-8 (Hs00189535_m1), FUT-9 (Hs00276003_m1) (Applied Biosystem-ABI, Carlsbad, CA), and NFATc1, NFATc2, NFATc3, NFATc4, MUC5AC and HPRT1 (sequences obtained from primerbank <http://pga.mgh.harvard.edu/primerbank/> and synthesized by Invitrogen) were used to create and quantify PCR products with iTaq™ Universal SYBR® Green Supermix (172-5850; Biorad) using an ABI 7900HT real-time qPCR machine using the Δ^{CT} method of relative quantification with HPRT1 as the housekeeping gene. mRNA expression were plotted as mean \pm SEM. Data were generated from N=4 female donors.

5.2.5 Western blot analysis

For western blot analysis, ALI cultures were mechanically detached in ice-cold phosphate-buffered saline (PBS) using rubber cell scrapers, and pelleted by centrifugation at 17,000x gravity for 8 minutes. Cells were lysed in cytoplasmic extraction buffer (Thermo scientific, Ontario, CAN) for 30 minutes at 4°C on a rotating apparatus and the supernatant was collected and stored at -80°C. Nuclear protein was subsequently extracted in nuclear extraction buffer from the pellet after centrifugation according to the manufacturer. 15µg of cellular protein lysates from ALI cultures were resolved by 10% SDS-PAGE and transferred to a nitrocellulose membrane (Millipore, Bedford, MA). Membranes were incubated with a final concentration at 1µg/ml of primary antibodies against ER- α , ER- β , NFATc1, MUC5AC, HSP90 (housekeeping protein) or (LTA-lotus tetragonolobus asparagus pea: H1601-1, AAA-anguilla anguilla lectin

from fresh water eel: H4901-1, and UEA-1-ulex europaeus lectin from gorse: H2201-1) lectins (EY Laboratories Inc., San Mateo, CA) followed by incubation of secondary HRP-conjugated anti-rabbit, anti-mouse and beta-actin antibodies for 1h at room temperature, and visualized using an enhanced chemiluminescence substrate (Thermo Scientific, Ontario, CAN) and a Chemigenius imaging system (Syngene, Cambridge, UK). Data were generated from N=4 female donors.

5.2.6 Small interfering RNA treatment

The role of NFATc1 in mediating the effect of estrogen in the transcription of MUC5AC was examined using small interfering (si)RNA siNFATc1 to silence NFATc1 mRNA. siNFATc1 (sc-156125) was purchased from Santa Cruz Biotechnology. The siRNA Universal Negative Control (SIC001) was used. 100nM of siNFATc1, and siRNA negative control were used for transfection using Nanoparticle siRNA Transfection System (N2913) from Sigma according to the manufacturer's procedures. 1HAE₀ cells were transfected for 48h prior to estradiol stimulation at 10⁻⁷M for 24h, followed by harvesting for RNA and protein. Data were generated from 3 independent experiments.

5.2.7 DNA gel

1.1% w/v UltraPure Agarose (16500-500; Life Technologies) was dissolved in Tris-acetate-EDTA buffer (B49; Life Technologies) for the electrophoresis of nucleic acids. 200ng of RNA was converted to cDNA using iScript cDNA synthesis kit (170-8891; Biorad). NFATc1, NFATc2, NFATc3, NFATc4 DNA products were generated using forward/reverse primers, and Platinum Taq DNA polymerase (10966-018; Life Technologies) as per the instruction of the manufacturer. DNA products were mixed with (6X) DNA gel loading dye (R0611; Life

Technologies), and 10ul was loaded onto each lane and subjected to electrophoresis at 80V for 2h. 0.5ug of 100bp DNA ladder per lane was loaded as internal size control for products of interest. Bands on the DNA gel were visualized using standard ultraviolet (UV) radiation.

5.2.8 Cytotoxicity

An *In Situ* Apoptosis Detection Kit was used to detect apoptotic cells in paraffin-embedded ALI culture sections (Trevigen; Gaithersburg, MD). We used a TACS•XL®-DAB *In Situ* Apoptosis Detection Kit to detect nuclear DNA fragmentation as an indicator of cell apoptosis. This is performed *in situ* by incorporating labeled nucleotides (BrdU) onto the free 3'-OH ends of DNA fragments using a terminal deoxynucleotidyl transferase enzyme (TdT). Biotinylated anti-BrdU antibody and streptavidin-HRP were used for visualization of DNA fragmentation. Apoptotic cells were stained in brown and nuclei were counterstained with methyl green. Data were generated from N=4 female donors.

5.2.9 Statistical analyses

For statistical analysis of histochemical staining, immunohistochemistry and western blotting, non-parametric t-test was used to compare between two groups. One-way ANOVA with Bonferroni's test was used to account for multiple comparisons where appropriate. Statistical significance for all analyses was considered at $P < 0.05$ using GraphPad Prism version 6 (GraphPad Software Inc, San Diego, CA, USA). All data values are expressed as mean \pm SEM.

5.3 Results

5.3.1 Estrogen receptor beta is the predominant form in the human airway epithelium

To confirm the expression of estrogen receptors in the human airway epithelium in human tissues and cells in culture, human breast tumour sections and breast cancer cell line (MCF-7) were used as positive controls for the detection of ER- α and ER- β by immunostaining and western blot, respectively (Figure 5.1A-D). Intact human female airway tissue was used as a positive control for MUC5AC protein expression, an indicator for goblet cells (Figure 5.1E), and PAS-staining for total glycoprotein (Figure 5.1F).

Next, we evaluated the expression of the two estrogen receptors ER- α (68kDa) and ER- β (55kDa) in the large airways of female subjects in the pre-menopausal age group (15-45 years) with normal lung function (Figure 5.2 A-C) and in ALI cultures (Figure 5.2 D-F) by immunohistochemistry. To further confirm the specificity of the ER- α and ER- β antibodies, we have also performed western blot using cytoplasmic and nuclear protein fractions from control ALI cultures. Beta-actin, superoxide dismutase (SOD) and histone 3 were used as house-keeping protein, cytoplasmic and nuclear-specific markers, respectively (Figure 5.2G). Western blot data showed that ER- β protein was the predominant form of estrogen receptor in both cytoplasmic and nuclear compartment of control ALI cultures, with greater expression in the cytoplasm. This observation was reflected in the quantification of estrogen receptors by immunohistochemistry where ER- β was the predominant form of estrogen receptor with $38.2\pm 9.9\%$ and $31.6\pm 4.3\%$ of epithelial cell population resided in the nuclear compartment by cell counting in intact tissues and ALI cultures, respectively (Figure 5.2H).

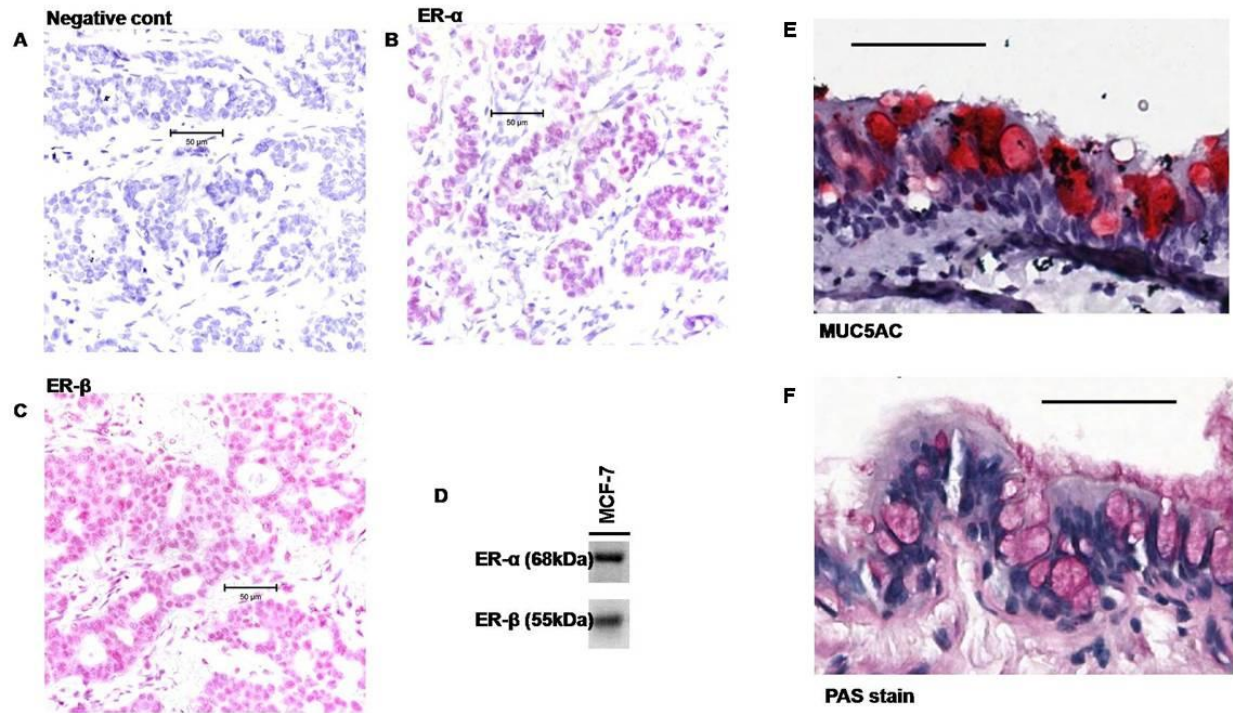


Figure 5.1: Determining the specificities for estrogen receptors and goblet cell expression

A) Negative control, B) ER- α and C) ER- β immunostaining in human breast tissue sections as positive control were shown. D) ER- α and ER- β protein expression in breast cancer cells (MCF-7) as positive control were shown by Western blot. E) MUC5AC immunostaining in human lung tissues as positive control for MUC5AC staining (red). F) PAS-staining in human lung tissues as positive control for PAS-staining (purple). Scale bar=50 μ m. All sections were counterstained by hematoxylin.

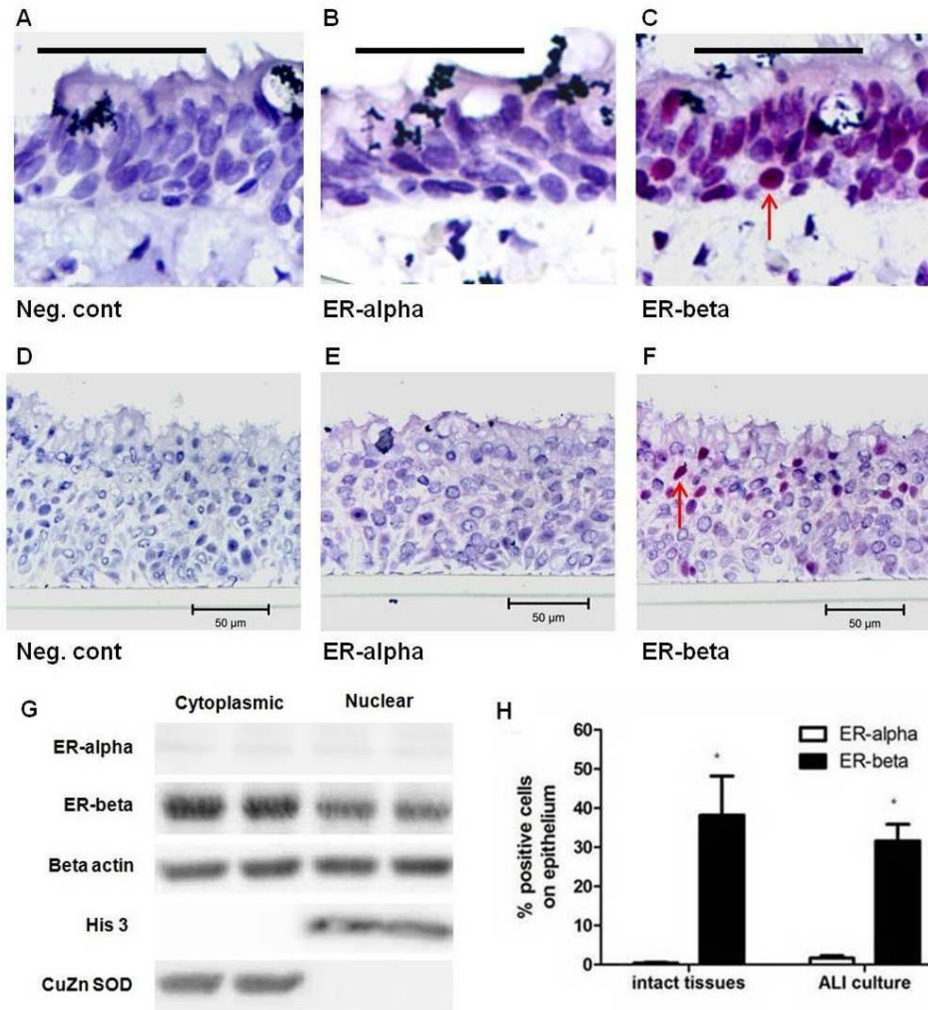


Figure 5.2: Estrogen receptor expression in human female airway tissues and NHBE cells in air liquid interface.

Negative control (A,D), estrogen receptor (ER)- α (B,E) and ER- β (C,F) in excised human large airways of control lungs and in air liquid interface (ALI) cultures by immunohistochemistry were shown respectively. G) ER- α and ER- β protein expression in cytoplasmic and nuclear fraction of control ALI cultures were shown by western blot (WB). β -actin, superoxide dismutase (SOD) and histone 3 were used as house-keeping protein, cytoplasmic, and nuclear-specific markers, respectively. Representative WB images of N=4 in duplicate lanes is shown. H) Quantification of positive cell staining of nuclei in red is expressed as a percentage of total cells on the epithelium of intact human airways and in control ALI cultures. Images are representative of N=4 female excised airways and N=4 ALI cultures. Sections were counterstained with hematoxylin for nuclei (blue) and positive stains were indicated by red arrows. (5 μ m sections; scale bars=50 μ m). Non-parametric t-test was used in panel H. *P<0.05 represents statistical significance.

5.3.2 Estradiol increases PAS-positive cell count in ALI cultures.

Incubation of mucociliated NHBE cells in ALI with estradiol (in physiologic concentrations) for 2 weeks resulted in a concentration-dependent increase in the total % PAS-stained area, and PAS-positive cell count, which was normalized to the total length of the epithelium in millimeters (Figure 5.3A; purple color stain indicates PAS-positive cells; scale bar = 50 μ m). The total cell count, as measured by the number of nuclei, did not change with all treatment groups (Figure 5.3B). The % area of PAS staining increased from a baseline control value of 5.5 \pm 0.5 to 11.4 \pm 0.8 with 10⁻⁷ M estradiol treatment and reduced to 7.7 \pm 1.0 with PHTPP, but not with MPP, at a concentration of 10⁻⁶ M (Figure 5.3C). All PAS-positive cells were localized to the apical compartment of the epithelium. Total number of PAS-positive cells on the apical surface was increased from a baseline control value of 43 \pm 3 to 92 \pm 10 and 118 \pm 6 per mm epithelium in the presence of 10⁻⁸ M and 10⁻⁷ M estradiol, respectively, and was attenuated with 10⁻⁶ M PHTPP, but not with 10⁻⁶ M MPP (Figure 5.3D; black bar = PAS-positive cells). ALI cultures treated with 10⁻⁷ M estradiol resulted in a decrease in total ciliated cell count from 150 \pm 9 to 63 \pm 4 per mm epithelium, and was restored to baseline control values with 10⁻⁶ M PHTPP, but not with MPP antagonist (Figure 5.3D; white bars = ciliated cells).

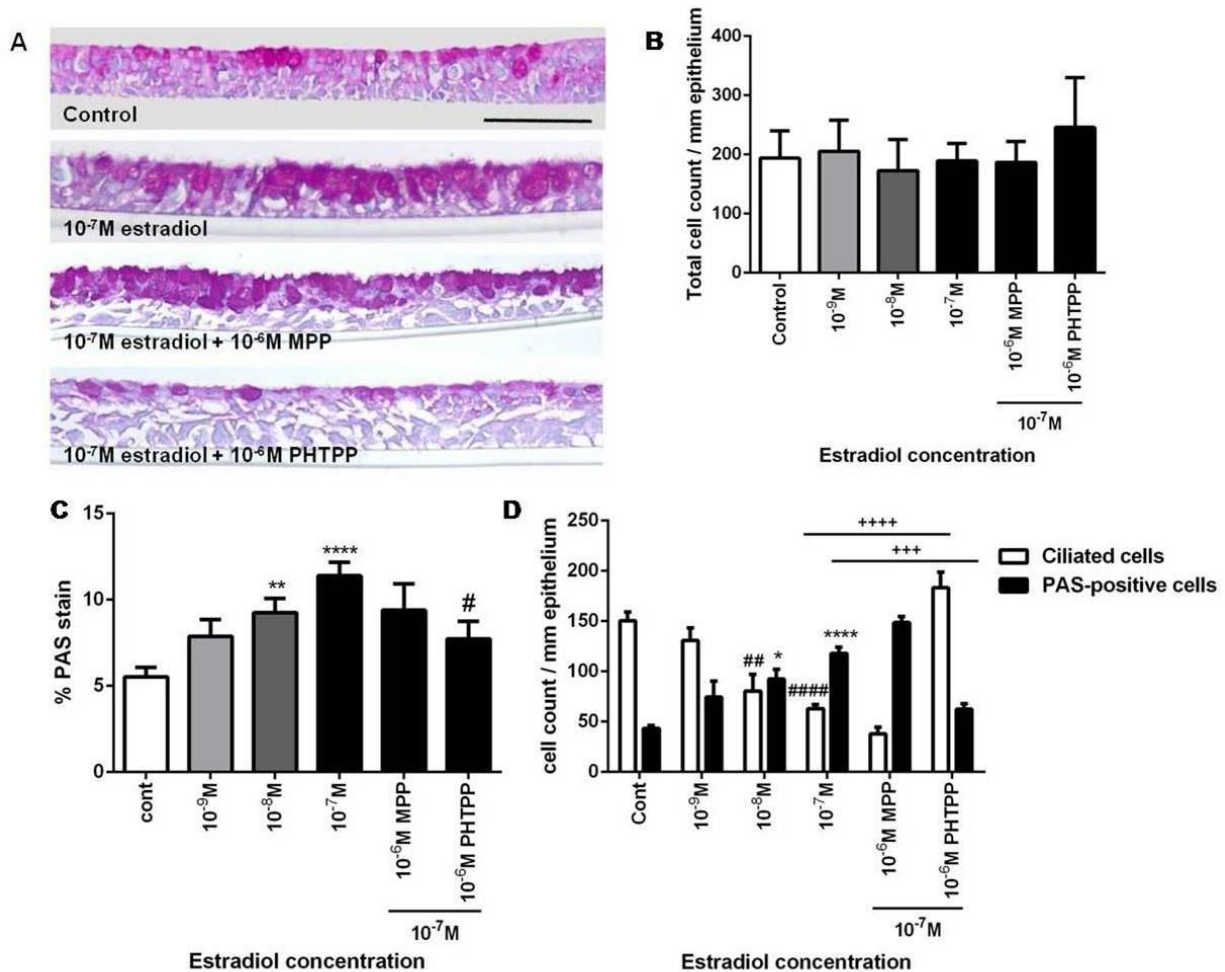


Figure 5.3: Effect of estradiol on periodic acid schiff (PAS)-positive cell staining in air liquid interface (ALI) cultures.

A) ALI cultures (N=4) were treated with estradiol (vehicle control, 10^{-9} , 10^{-8} , 10^{-7} M) and ER- α (10^{-6} M MPP) or ER- β (10^{-6} M PHTPP) antagonists for 2 weeks. Images are representative of 4 female donors (5 μ m sections; scale bars=50 μ m). B) Total cell count normalized to millimeters of epithelium by manual counting of nuclei counterstained with hematoxylin (N=4). C) Quantification of the percentage of PAS stain of the entire cross section of the epithelium (**P<0.01, ****P<0.0001 against control, #P<0.05 against 10^{-7} M estradiol-treated group). D) Quantification of cell count for PAS-positive cells and ciliated cells in the apical compartment of the epithelium with increasing estradiol concentration, and in the presence of 10^{-6} M PHTPP or MPP with a single fixed concentration of estradiol at 10^{-7} M (N=4). * P<0.05, ## P<0.01 and ****/##### P<0.0001 compared against vehicle control, +++ P<0.001 and ++++ P<0.0001 compared against 10^{-7} M estradiol. One-way ANOVA with Bonferroni's multiple comparisons tests were used in all analyses.

5.3.3 Estradiol increases MUC5AC expression in ALI cultures

To further determine the increase in PAS-positive cells correlated in mucin protein expression, MUC5AC immunostaining was performed in control and 10^{-7} M estradiol-treated ALI cultures (Figure 5.4A; red arrow indicates goblet cells; scale bar = 50 μ m). In baseline vehicle control cultures, ciliated cells were the predominant cell type and accounted for $93.6\pm 1.1\%$ of epithelial cells, while goblet cells accounted for $6.3\pm 1.1\%$ (Figure 5.4B). The percentage of goblet cells increased from $6.3\pm 1.1\%$ in vehicle control to $39.9\pm 4.7\%$ in 10^{-7} M estradiol. Treatment with 10^{-7} M estradiol for two weeks decrease the percentage of ciliated cells from $93.6\pm 1.1\%$ in vehicle control to $60.1\pm 4.7\%$. Quantification of mRNA transcripts by quantitative real-time PCR showed that 10^{-7} M estradiol increased MUC5AC mRNA expression from 1.0 ± 0.3 to 2.1 ± 0.4 compared to vehicle control (Figure 5.4C). Estradiol increased MUC5AC protein by 1.8 ± 0.2 fold above vehicle control in apical ALI culture secretion after normalizing by the volume of apical wash per well (Figure 5.4D, red arrow indicates MUC5AC protein; figure 5.4E is the densitometry of 5.4D).

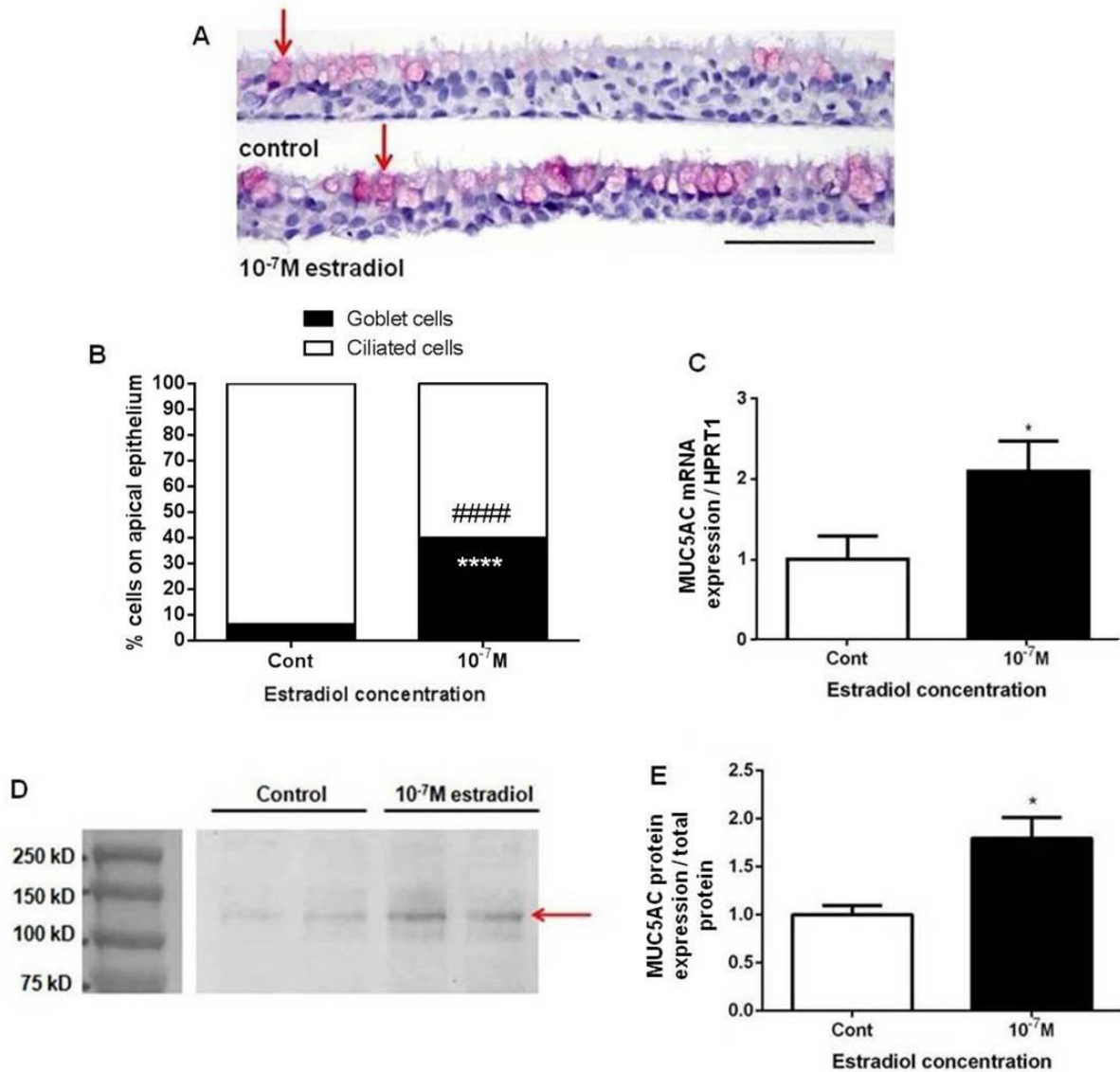


Figure 5.4: Effects of estradiol on MUC5AC mRNA and protein expression in ALI cultures.

A) MUC5AC immunostaining in ALI cultures treated with 10⁻⁷M estradiol for 2 weeks (goblet cells indicated by red arrows and counterstained with hematoxylin of nuclei). B) Quantification of the number of goblet cells and ciliated cells in the apical compartment of estradiol-treated ALI cultures expressed as a percentage of all cells in the apical compartment. ##### P<0.0001 and **** P<0.0001 compared between treatment group vs. vehicle control. C) MUC5AC mRNA expression normalized to HPRT1 housekeeping using real time PCR. D) MUC5AC protein present in ALI culture secretion was analysed by western blot, normalized by the total volume of apical washes per well and quantified by densitometry in panel E. All values shown are mean ± SEM from N=4 female donors. Non-parametric t-tests were used in all analyses.

5.3.4 Estradiol increases nuclear factor of activated protein c1 (NFATc1)

A transcription factor (TF) activation profiling plate array was used to screen for activated TFs in the nuclear protein extract from primary NHBE cells in monolayer that were treated with 10^{-7} M estradiol for 24h (Figure 5.5A-B). The dotted line in figure 5.5B indicated a threshold of a 2-fold increase in luminescence (estradiol-treated cells over vehicle controls). Estradiol increased the expression of total NFAT protein by 10 fold in the nuclear fraction of NHBE cells after 24h of incubation. We further investigated the presence of NFAT and its role in regulating MUC5AC mRNA and protein expression with estradiol stimulation in ALI cultures. We showed that ALI cultures expressed all four isoforms of NFAT mRNA: NFATc1, NFATc2, NFATc3 and NFATc4 at baseline levels in vehicle controls with values expressed as absolute change in C_t values and normalized to HPRT1 (Figure 5.6A). Estradiol increased NFATc1 mRNA by 3.8 ± 1.0 fold (Figure 5.6B), and protein expression by 2.2 ± 0.3 fold over control after two weeks (Figure 5.6C-D). No changes were observed in NFATc2 and NFATc4 mRNA expression with estradiol treatment; however NFATc3 mRNA was attenuated from 1.0 ± 0.2 to 0.7 ± 0.06 fold below vehicle control level.

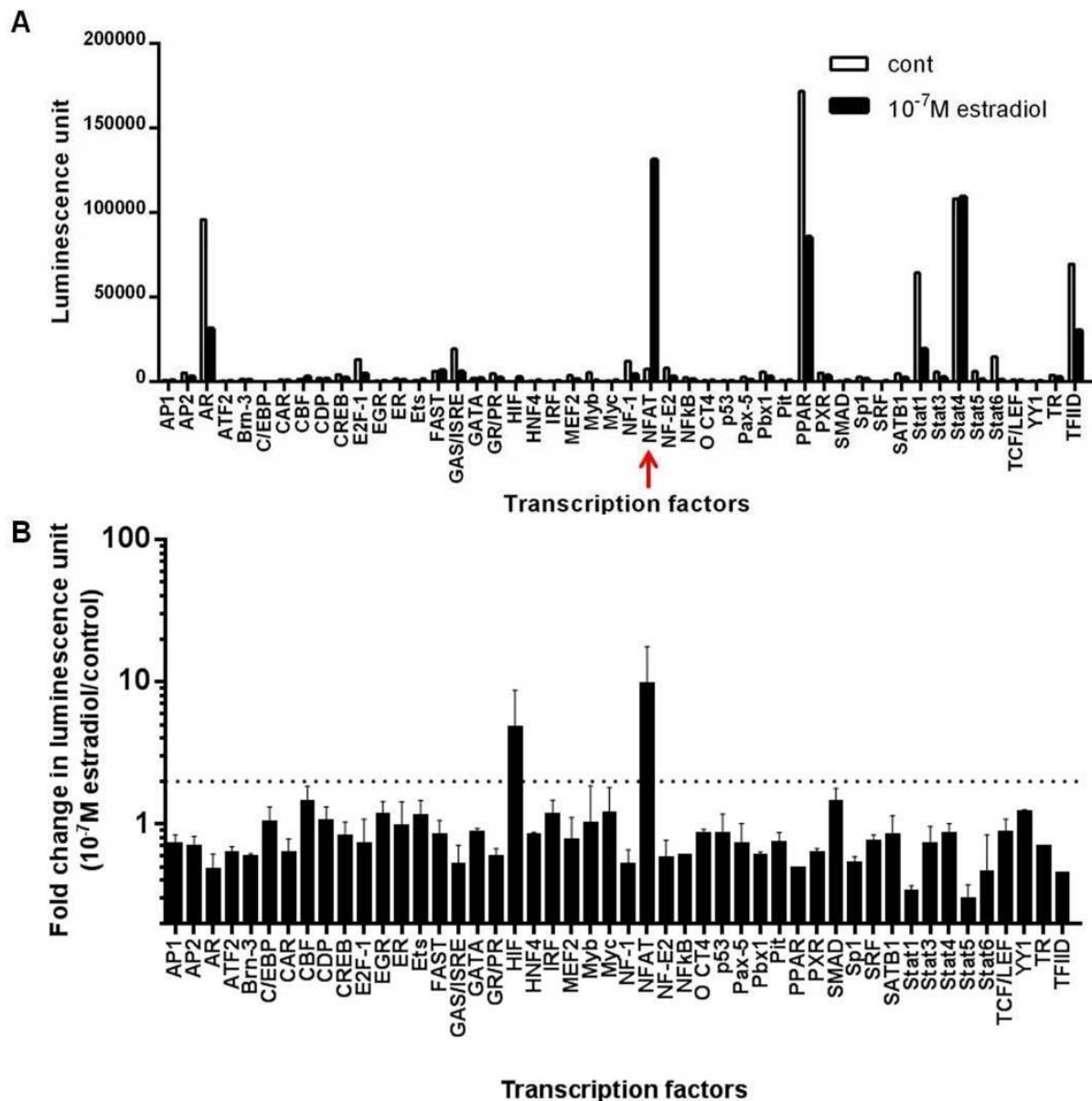


Figure 5.5: Transcription factor expression panel demonstrates increased total nuclear factor of activated T-cell (NFAT) protein in the nuclear fraction of primary female NHBE cells after 10⁻⁷M estradiol treatment for 24h.

Data are expressed as (A) relative fold increase in luminescence unit over vehicle controls. The dotted line indicates a threshold of a 2-fold increase in protein expression in estradiol-treated cells compared to vehicle controls. NFAT protein is indicated by red arrow. Values shown are mean ± SEM from N=2 female NHBE cell donors.

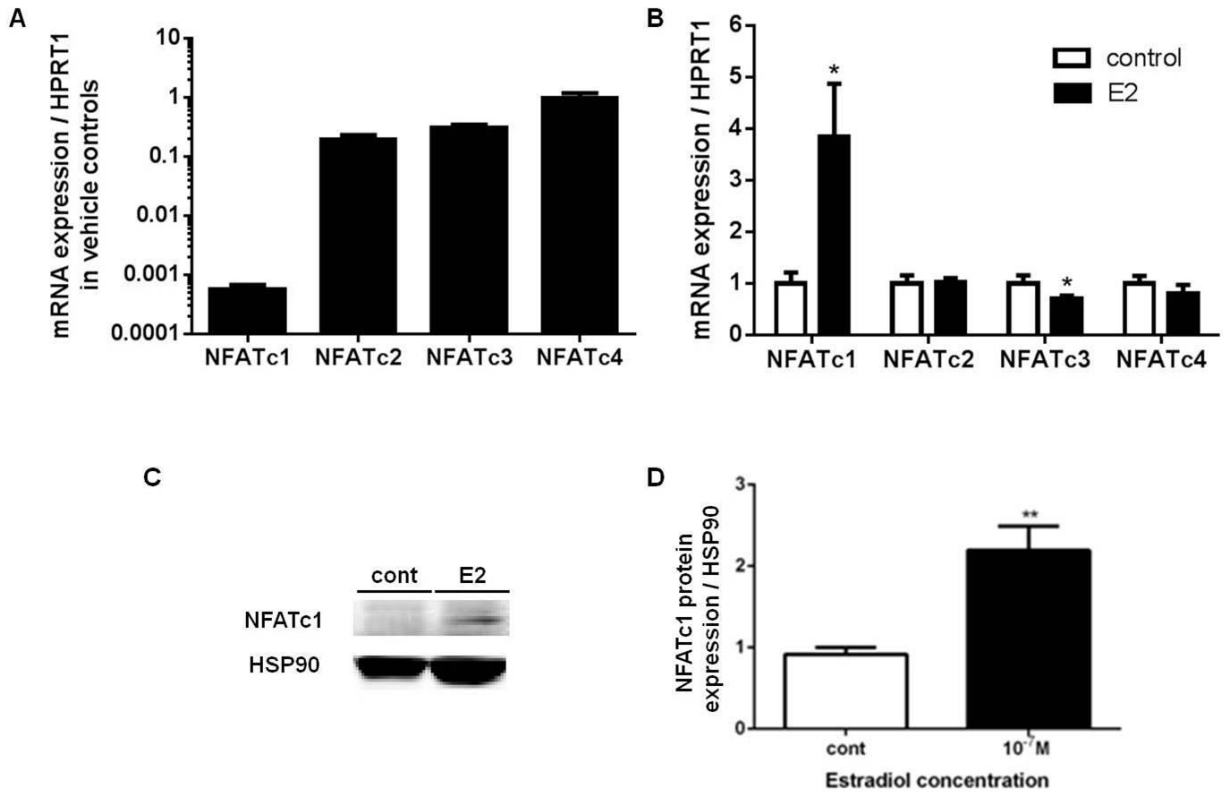


Figure 5.6: NFAT mRNA and protein expression in ALI cultures after 2 weeks of estradiol treatment.

A) Quantitative real-time PCR demonstrates baseline vehicle control mRNA expression of NFAT (c1-c4) expressed as absolute C_t value normalized to HPRT1. B) NFATc1-c4 mRNA expression normalized to HPRT1 in vehicle vs. 10^{-7} M estradiol-treated cultures for 2 weeks. C) Western blot showed total NFATc1 protein expression with HSP90 housekeeping protein in vehicle vs. 10^{-7} M estradiol-treated ALI cultures and quantified by densitometry in panel D. * $P < 0.05$ and ** $P < 0.01$ compared between treatment group vs vehicle control using non-parametric t-test and expressed as fold increase over control in panel B and D.

5.3.5 NFATc1 siRNA attenuated estradiol-induced increase in MUC5AC expression

In order to demonstrate whether NFATc1 plays any role in regulating MUC5AC mRNA expression, we used 1HAE₀ cells as a model. Baseline mRNA expression levels of NFATc1-c4 in control 1HAE₀ cells are shown in Figure 5.7A. 10⁻⁷M estradiol treatment increased NFATc1, but not NFATc2-c4, mRNA expression by ~2.5 fold after 24h (Figure 5.7B). We further showed a time-dependent increase in NFATc1 mRNA with 10⁻⁷M estradiol, which peaked at 4h with a 5.9±0.9 fold increase and declined to 2.5±0.3 fold above control at 24h (Figure 5.8A). A time-dependent increase in MUC5AC mRNA was also observed with estradiol stimulation, which peaked at 24h with a 2.2±0.3 fold increase above control (Figure 5.8B). We silenced NFATc1 with siNFATc1 for 48h prior to the addition of 10⁻⁷M estradiol for 24h and observed changes in MUC5AC mRNA expression. 10⁻⁷M estradiol (E2) and siCon+E2 increased NFATc1 mRNA by 1.7±0.2 and 1.6±0.2 fold over control, respectively (Figure 5.8C). The use of siNFATc1 in the presence of estradiol attenuated NFATc1 mRNA to 0.7±0.2 fold below the control group with statistical comparison with the siCon+E2 treated group. 10⁻⁷M estradiol (E2) and siCon+E2 increased MUC5AC mRNA by 2.3±0.4 and 2.0±0.1 fold over control, respectively (Figure 5.8D). MUC5AC mRNA levels were attenuated by siNFATc1 in the presence of estradiol to 1.2±0.2 fold above the control group with statistical comparison with siCon+E2 treated group. NFATc1 siRNA alone reduced NFATc1 mRNA expression by ~50%, while NFATc2-c4 mRNA expression was unchanged after 48h of siNFATc1 treatment (Figure 5.8E). 100nM NFATc1 siRNA treatment in 1HAE₀ cells for 48h significantly reduced NFATc1 protein expression by ~70% (control: 1.0±0.03 and siNFATc1: 0.3±0.05) after normalization to HSP90 (Figure 5.8F-G). Furthermore, we showed that 10⁻⁷M estradiol (E2) and siCon+E2 increased total cellular NFATc1 protein by 6.0±0.8 and 6.0±0.8 fold over control (Figure 5.9A-B). The use of

siNFATc1 attenuated estradiol-stimulated NFATc1 protein to 4.1 ± 0.4 fold over control. Similarly, 10^{-7} M estradiol (E2) and siCon+E2 increased total MUC5AC protein levels by 8.5 ± 2.2 and 7.8 ± 0.9 fold over control. This was attenuated to 4.6 ± 0.6 fold over control with siNFATc1 treatment (Figure 5.9C-D). Primer specificities were confirmed by the presence of a single DNA product in 1.1% agarose gel (Figure 5.9E). Collectively, these data suggest that NFATc1 is a novel regulator of estradiol-mediated increase in MUC5AC expression.

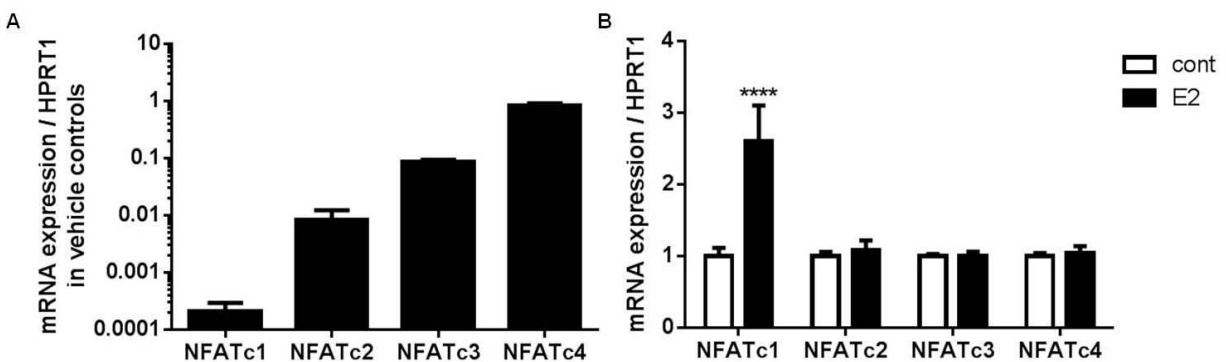


Figure 5.7: Characterization of NFATc1-4 mRNA expression and effect of estradiol in 1HAE₀ cells.

A) Baseline mRNA expression of NFAT (c1-c4) in 1HAE₀ cells quantified by real-time PCR expressed as absolute change in C_t value normalized to HPRT1. B) NFATc1-c4 mRNA expression normalized to HPRT1 in cells treated with 10^{-7} M estradiol for 24h. Data are expressed as fold increase over vehicle controls. Values shown are mean \pm SEM of experiments performed in 3 independent experiments. **** $P < 0.0001$ compared against vehicle control in each gene using non-parametric t-test in B-C.

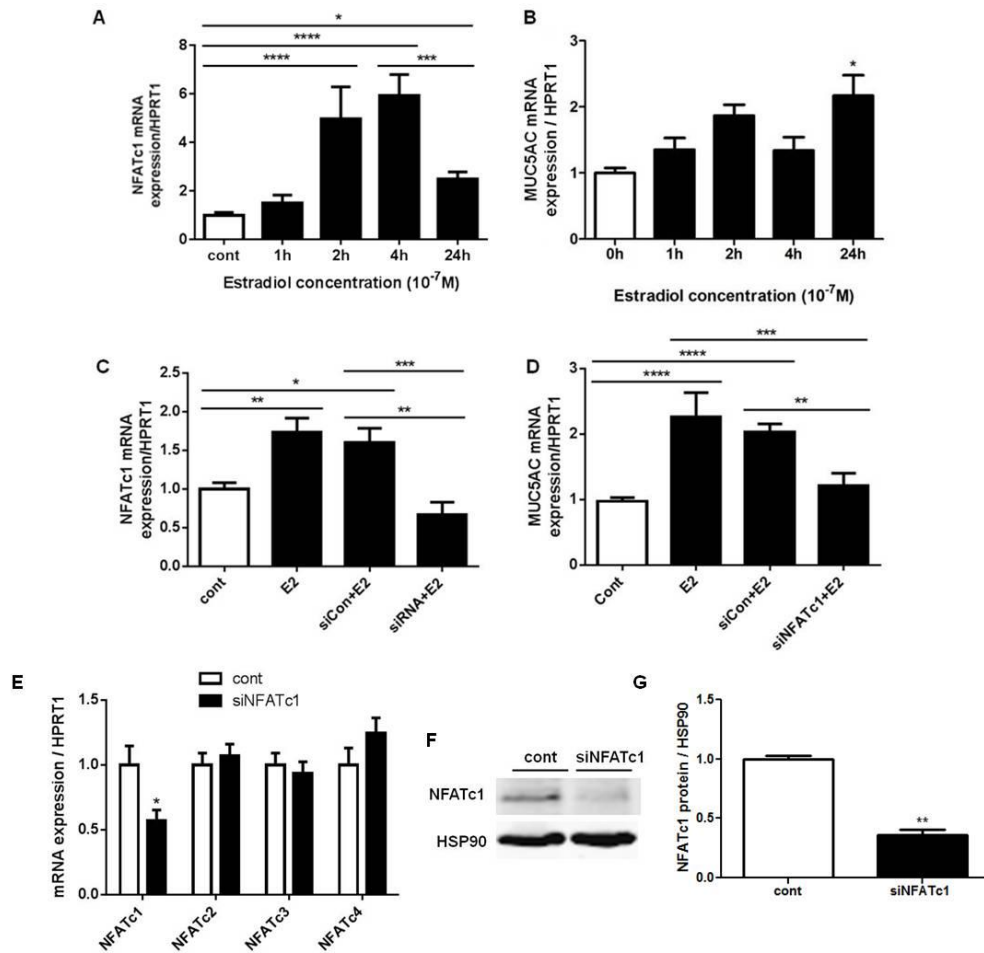


Figure 5.8: Effects of estradiol and NFATc1-specific siRNA on NFATc1 and MUC5AC mRNA expression in 1HAE₀ cells.

A) Quantitative real-time PCR demonstrates 10^{-7} M estradiol stimulates a time-dependent increase in NFATc1 mRNA/HPRT1 expression with maximal increase at 4h. B) 10^{-7} M estradiol stimulates a time-dependent increase in MUC5AC mRNA/HPRT1 expression with maximal increase at 24h. C) 10^{-7} M estradiol treatment increases NFATc1 mRNA/HPRT1 expression in cells 48h post-transfection with scrambled control siRNA (siCon+E2) and this effect is reduced by transfection with NFATc1 siRNA (siNFATc1+E2). D) MUC5AC mRNA/HPRT1 expression was increased by 24h treatment with 10^{-7} M estradiol (E2) with scrambled siRNA transfection (siCon+E2), but was attenuated by transfection with NFATc1 siRNA (siNFATc1+E2). E) NFATc1-c4 mRNA expression in cells treated with 100nM NFATc1 siRNA for 48h. F) A representative western blot of NFATc1 protein knockdown expression with 100nM NFATc1 siRNA treatment for 48h and quantified by densitometry in G) with N=3. Values shown are mean \pm SEM of experiments performed in 3 independent experiments. *P<0.05, **P<0.01, ***P<0.001 and ****P<0.0001 using one-way ANOVA with Bonferroni's test in A-D and non-parametric t-test was used in E and G.

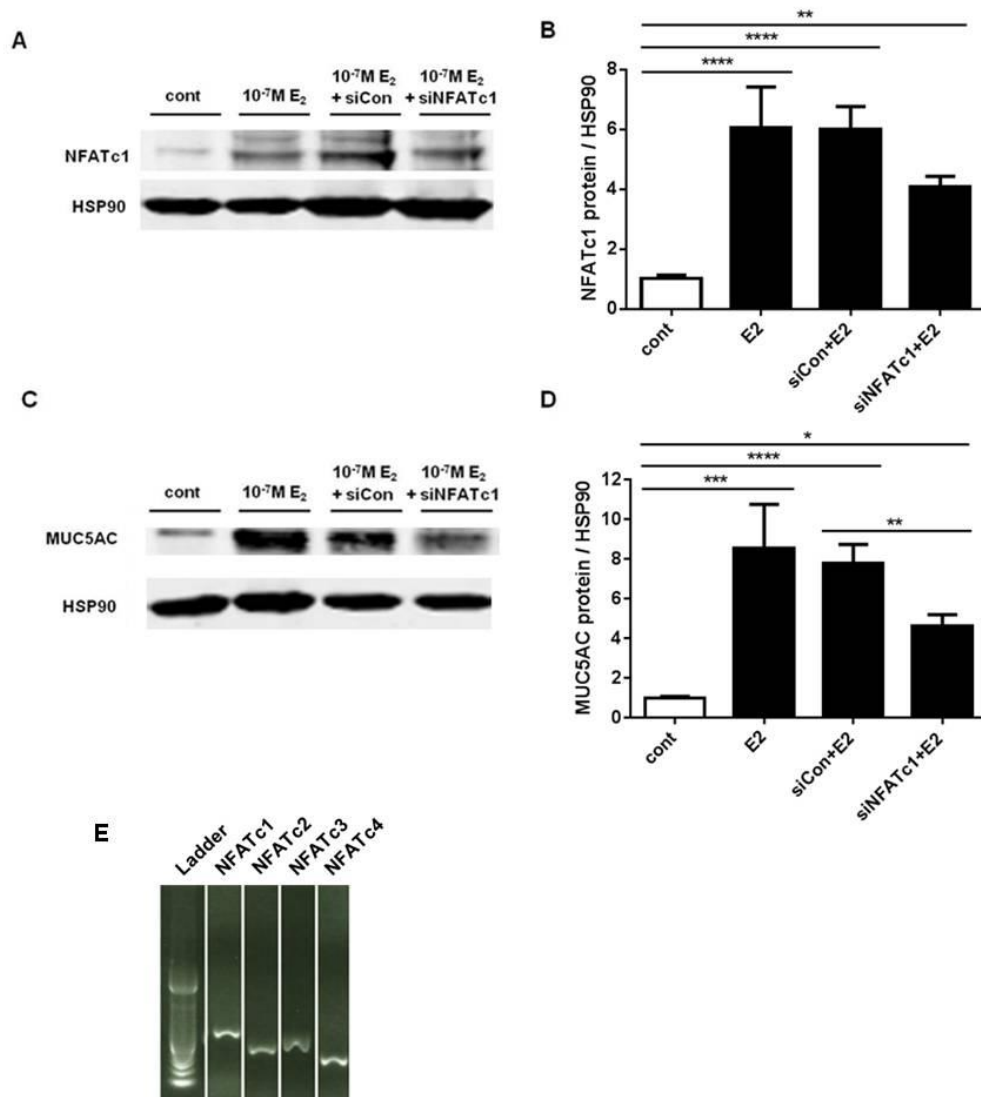


Figure 5.9: NFATc1 siRNA attenuated estradiol-induced increase in NFATc1 and MUC5AC protein expression in 1HAE₀ cells.

A-B) 24h 10⁻⁷M estradiol treatment alone (E2) and 48h post-transfection with scrambled siRNA (siCon+E2) increases total cellular NFATc1 protein expression (normalised to HSP90). The effect of E2 is attenuated in cells transfected with siRNA against NFATc1 (siNFATc1+E2). C-D) Total cellular MUC5AC protein/HSP90 expression was increased by 10⁻⁷M estradiol alone (E2) and in scrambled siRNA controls (siCon+E2), but was attenuated by transfection with NFATc1 siRNA (siNFATc1+E2) treatment. Values shown are mean \pm SEM of experiments performed in 3 independent experiments. *P<0.05, **P<0.01, ***P<0.001 and ****P<0.0001 using one-way ANOVA with Bonferroni's test in all analyses. E) NFATc1-c4 primer specificities were confirmed in a DNA gel with single product. A 100bp DNA ladder was indicated.

5.4 Discussion

Mucus hypersecretion with plugging of airways is one pathological finding that is common to most chronic inflammatory airway disease [25]. As the predominant form of mucin in the human airway, MUC5AC is produced mainly in goblet cells in the surface epithelium [215]. In this study, we used a fully differentiated airway epithelial cell culture model with pseudostratified phenotype grown in an air liquid interface and showed that estradiol increases both mRNA and protein expression of MUC5AC and modifies glycosylation of mucins in human airways. Additionally, we found that this effect is largely mediated by estrogen receptor beta. Inhibition of estrogen receptor beta by 10^{-6} M PHTPP attenuated estradiol-related increase in the number of goblet cells in the bronchial epithelium.

To further characterize the mechanism by which estradiol regulates mucin, we performed protein microarray analysis consisting of a panel of transcription factors. Total activated nuclear factor of activated T-cell (NFAT) was increased in the nuclear fraction of NHBE cells after estradiol stimulation for 24h. Although NFAT protein was originally discovered in T-cells, studies have shown that they are expressed in the human airway epithelium and possess some interesting functional properties. For instance, Dave et al. showed that NFATc3 is a direct activator of surfactant protein A, B, and C, and Forkhead box protein A1 and A2 genes in the airway epithelium during lung maturation [226]. NFATc3 has also been shown to directly interact with thyroid transcription factor-1 in lung epithelial cells to regulate surfactant protein D gene [227]. In our study, NFATc1, NFATc2, NFATc3 and NFATc4 mRNA were confirmed to be expressed in both primary cells in ALI culture and in 1HAE₀ cells. We showed that NFATc1 and MUC5AC mRNA and protein expression were increased with estradiol in both primary cells in ALI culture and 1HAE₀ cells. To determine whether NFATc1 plays a role in regulating

MUC5AC mRNA expression, we silenced NFATc1 in 1HAE_o cells with siNFATc1. siNFATc1 blunted estradiol-related increases in NFATc1 and MUC5AC mRNA and protein expression. Collectively, these data demonstrate that NFATc1 regulates estradiol-mediated mucus production in human bronchial epithelium. Additional studies will be needed to pinpoint the precise mechanisms by which NFATc1 modifies MUC5AC in the presence of estradiol.

In addition to the regulation of MUC5AC mRNA and protein synthesis, our findings indicate that estrogens affect post-translational modification of mucin. In our ALI model, we observed an increase in the mRNA expression of fucosyltransferase as well as total fucose residues in the cytoplasmic fraction of ALI using three different lectins (UEA-1, AAA and LTA) that specifically bind to the same α -1,2 fucose residues present on all protein (Appendix 1A-H). How estrogens modify fucosylation is uncertain. Estradiol may directly increase the expression of fucosyltransferase or indirectly by increasing the number of goblet cells containing these enzymes. Additional studies will be needed to unravel the underlying mechanisms for this observation.

The clinical relevance of increased protein glycosylation of mucin is uncertain. It is now well known that post-translational modification of glycoprotein with fucose, for instance, is essential for normal embryonic growth and development, fertility, and immune function [228]. Alterations in the expression of fucosylated glycans and their cognate fucosyltransferases have been observed in multiple pathologic processes involving inflammation, cancer, and numerous oncogenic events involving signaling events by the Notch receptor family [229]. Moreover, opportunistic bacteria often use lectins (which are protein receptors with high specificity for glycoconjugates) to recognize and adhere to human tissues [223]. Fucosylated glycoconjugates are present in high quantity in CF lungs and may be a target of lectins from pathogenic bacteria

such as *Pseudomonas aeruginosa* [223]. This may increase the risk of infection by *Pseudomonas aeruginosa* in the context of CF.

It is important to note several limitations in our current study. First, the ALI culture in our model was not exposed to the fluctuating concentrations of estradiol over a period of 28 days that resembled the female menstrual cycle. In our current model, we used fixed concentrations of estradiol to examine the regulation of MUC5AC mRNA and protein expression. Second, for clinical relevance, we only used female NHBE cells to model the increased level of estrogen in pre-menopausal period but we do not know if NHBE cells from males would behave differently. Third, although the hormone receptor antagonists we employed have high levels of specificity [230, 231], there may be minor off-target effects that could not be fully accounted for in our analysis. Fourth, it is possible that estradiol may fundamentally alter cellular proliferation of the entire epithelial layer. To determine whether estradiol altered cell proliferation, we stained the ALI cultures with Ki67 (Appendix 2A-C). It was reassuring that estradiol treatment did not change the total cell numbers and did not induce cellular apoptosis. It only slightly increased Ki67 cell positivity, suggesting a slight prolongation of cell cycle. Finally, while we measured total mucus expression, we did not evaluate other aspect of mucus homeostasis in airways including viscoelastic properties of mucus, mucus clearance, and the effect of mucus on airway resistance.

Notwithstanding these limitations, our data maybe relevant to chronic airway diseases such as asthma because an increase in goblet cells is associated with mucus plugging in the small airways, which has been shown to be the single most important pathologic predictor of increased mortality in severe COPD [25]. Our study demonstrates that estradiol may play an important role

in modulating mucus expression in the human airway epithelium, which may impact on disease expression in women who are susceptible to chronic airway diseases.

Chapter 6: Silencing NFATc2 by siRNA Blunted Progesterone-Induced Increase in MUC5AC Synthesis in Human Bronchial Epithelial Cells

6.1 Introduction

Large epidemiologic studies have revealed that female patients with asthma, chronic obstructive pulmonary disease (COPD), and cystic fibrosis (CF) generally have more symptoms and poorer prognosis than male patients [12, 111, 112]. For many years, female sex hormones have been studied in sexual development but their effects in non-reproductive tissues are increasingly being recognized [11]. One important pathologic link that is common to these conditions is airway mucus hypersecretion (particularly mucin-MUC5AC and MUC5B), which contributes to increased morbidity and mortality [25]. However, the exact biological mechanisms for the sexual dimorphism in airways disease need to be clearly defined.

The nuclear factor of activated T-cells (NFAT) family of transcription factors consists of four unique proteins (NFATc1, NFATc2, NFATc3 and NFATc4) that are expressed in a variety of cell types including T cells, B cells, mast cells, natural killer cells and eosinophils, which are regulated by calcium/calcineurin-dependent signaling mechanism [232, 233]. Although NFAT protein was initially discovered in T-cells, studies have showed that they are expressed in the human airway epithelium with functional relevance. For example, Dave and colleagues showed that NFATc3 is a direct activator of surfactant protein A, B, and C, and Forkhead box protein A1 and A2 genes in the airway epithelium during lung maturation [226]. In an *in-vitro* model using mouse tracheal epithelial cells cultured in air liquid interface (ALI), interleukin (IL)-13 induced MUC5AC expression via calcineurin-dependent NFATc4 signaling [234]. In a mouse model of asthma, Takeda showed that ovalbumin-sensitized female mice have greater mucus-producing

cells in the airway epithelium than those in male mice [235]. Female mice deficient in nuclear factor of activated T-cell (NFAT)-c2 was partially protected from ovalbumin-induced increase in mucus-producing cells in the airways compared to wild type mice [236]. However, whether female sex hormones have any direct impact on the airway epithelium is largely unexplored [9, 10]. We have previously showed that estrogen increases mucus production by up-regulating MUC5AC expression potentially through NFATc1 [237]. In this study, we postulate that progesterone regulates MUC5AC expression in NHBE cells cultured in ALI.

6.2 Methods

6.2.1 Cell cultures

This method was previously described with modification [237]. Normal human bronchial epithelial (NHBE) cells were obtained from Lonza (Walkersville, MD) or cells were isolated using pronase digestion from lungs donated for research through the International Institute for the Advancement of Medicine (IIAM, Jessup, PA) (N=4 females, age: 16-45yr) [238]. Airway epithelial cells (AECs) were initially cultured in Bronchial Epithelial Growth Media (BEGM, Lonza) and sub-cultured at 90% confluence. At passage 2, cells were trypsinized and seeded on 12 well, 0.4 μ m semi-permeable inserts (BD Biosciences) and allowed to expand to confluency in PneumaCultTM-ALI media (StemCell Technologies, Vancouver, Canada). At 100% confluence, the apical media was removed and the air liquid interface (ALI) culture was allowed to differentiate for 21 days. ALI cultures were pre-treated with 10⁻⁸M progesterone receptor antagonist, mifepristone (1479, Tocris; Ellisville, MO) or 0.01% final concentration of ethanol was used as a vehicle control, for 24h prior to stimulation with physiological concentrations (10⁻⁹ to 10⁻⁷M) of progesterone (P3972, Sigma; St. Louis, MO) three times per week with fresh basal

media for 2 weeks. Mucus overlying the epithelium in each well was washed with 500 μ L of warm phosphate-buffered saline (PBS) and was collected every 7 days.

Human airway epithelial cell line (1HAE₀) was obtained from Dr. Dieter Gruenert (University of California, San Francisco) [225] and used as a model for gene silencing. 1HAE₀ cells were cultured in DMEM (Gibco BRL; Invitrogen, Carlsbad, CA) with 10% fetal bovine serum (FBS) and reduced to 1% FBS 24h prior to progesterone treatment.

6.2.2 Histological staining

Breast tumor tissues were used to confirm the specificity of the progesterone receptor (PR)-A/B antibody (ab2764, Abcam; Cambridge, MA) using the high-sensitivity universal detection system-MACH kit (Biocare Medical, Concord, CA) (red). Human male (N=5) and female (N=5) lung tissues (age 16-50), obtained from donor lungs through the IIAM, were formalin-fixed, paraffin-embedded and 5 μ m thick sections were taken for staining with (PR)-A/B antibody and nuclear factor of activated T-cell (NFAT)c2 antibody (sc13034, Santa Cruz; Dallas, Texas, USA) using the DAKO Liquid DAB+ Substrate Chromagen System (DAKO, Burlington, ON). Mouse anti-IgG (sc-2343) was used as negative control. To quantify PR-A/B and NFATc2 protein expression, we measured the area of positive staining (brown) and expressed as a percentage of the total epithelial cross-sectional area using color segmentation (ImagePro Plus 4.0, Media Cybernetics, L.P.).

Paraffin-embedded human ALI culture sections were stained with Periodic Acid Schiff (PAS) for the detection of polysaccharide-rich mucus-producing cells, and MUC5AC (ab24071, Abcam; Cambridge, MA) antibody using the high-sensitivity universal detection system-MACH kit (Biocare Medical, Concord, CA) (red), dried overnight at room temperature and cover-slipped in Cytoseal mounting solution. Total PAS-positive cells were normalized to the length of the

basement membrane in millimeters. Total MUC5AC-positive cells were expressed as a percentage of the total number of nuclei stained by hematoxylin on the apical epithelium. Data were expressed as mean \pm SEM of experiments from N=4 female donors.

6.2.3 Transcription factor activation protein array

The transcription factor (TF) activation profiling plate array from Signosis (FA-1001; Sunnyvale, CA) was used to screen for activated TFs in nuclear protein extract from female primary AECs monolayers stimulated with 10^{-7} M progesterone or ethanol vehicle control for 24h. Data are expressed as absolute and fold change in luminescence units relative to vehicle controls from N=2 female donors.

6.2.4 Real time PCR

RNA from ALI cultures and 1HAE₀ cells were isolated using an RNeasy mini extraction kit (Qiagen, Germantown, USA). Total RNA was reverse transcribed into cDNA using the iScript cDNA synthesis kit according to the manufacturer's protocol (Biorad, Mississauga, ON). NFATc1, NFATc2, NFATc3, NFATc4, MUC5AC, MUC5B and HPRT1 primers (sequences obtained from primerbank <http://pga.mgh.harvard.edu/primerbank/> and synthesized by Invitrogen) were used to create PCR products using the Biorad CFX384 real-time qPCR machine (Ontario, Canada) and using the Δ^{CT} method of relative quantification with HPRT1 as housekeeping gene. mRNA expression were plotted as mean \pm SEM from N=4 female donors.

6.2.5 Western blot analysis

15 μ g of cellular protein lysate from breast cancer cell line (MCF-7) was resolved using a 10% SDS-PAGE with reducing conditions and transferred on nitrocellulose membrane (Millipore, Bedford, MA). Membranes were incubated with primary mouse antibody against PR-A/B

(ab2764, Abcam; Cambridge, MA) overnight at 4°C, followed by incubation with secondary HRP-conjugated anti-mouse IgG (553391, BD Pharmingen; Franklin Lakes, NJ) at room temperature, and visualized using an enhanced chemiluminescence substrate (Thermo Scientific, Ontario, CAN) and a Chemigenius imaging system (Syngene, Cambridge, UK).

6.2.6 Small interfering RNA treatment

siNFATc2 (sc-36055) was purchased from Santa Cruz Biotechnology and siRNA Universal Negative Control (SIC001) from Sigma-Aldrich. 100nM of siNFATc2, and negative control siRNA were transfected into human airway epithelial (1HAE₀) cell line using Lipofectamine® LTX Reagent with PLUS™ Reagent (15338100, Life Technologies) according to the manufacturer's procedures. For the kinetic study, 1HAE₀ cells were transfected for 48h prior to progesterone stimulation at 10⁻⁷M for 0h, 1h, 2h, 4h and 24h, followed by RNA extraction for NFATc1-c4 mRNA expression analyses. For gene silencing study, 1HAE₀ cells were transfected for 48h prior to progesterone stimulation, followed by RNA extraction for NFATc1-c4 and MUC5AC mRNA expression analyses.

6.2.7 DNA gel

1.1% w/v UltraPure Agarose (16500-500; Life Technologies) was dissolved in Tris-acetate-EDTA buffer (B49; Life Technologies) for the electrophoresis of nucleic acids. 200ng of RNA was converted to cDNA using iScript cDNA synthesis kit (170-8891; Biorad). NFATc1, NFATc2, NFATc3, NFATc4 DNA products were generated using forward/reverse primers, and Platinum Taq DNA polymerase (10966-018; Life Technologies) as per the instruction of the manufacturer. DNA products were mixed with (6X) DNA gel loading dye (R0611; Life Technologies), and 10ul was loaded onto each lane and subjected to electrophoresis at 80V for

2h. 0.5ug of 100bp DNA ladder per lane was loaded as internal size control for products of interest. Bands on the DNA gel were visualized using standard ultraviolet (UV) radiation.

6.2.8 Statistical analysis

One-way ANOVA followed by Dunnett's multiple comparisons test was used to determine statistical significance of multiple treatment conditions versus control (Prism version 6; GraphPad Software, San Diego, CA). Two-way ANOVA with Bonferroni's multiple comparisons test was used to compare the kinetic response between treatment conditions versus controls. Two-tailed, unpaired t test was used for two category comparisons. Statistical significance for all analyses was considered at $p < 0.05$.

6.3 Results

6.3.1 Progesterone receptor expression in human airway tissues and ALI cultures

We first evaluated the specificity of the progesterone receptor antibody in human breast tumor tissue as positive control by immunohistochemistry (Figure 6.1A-B), and protein lysates from the breast cancer cell line (MCF-7) by Western blot, which detected both isoforms of progesterone receptors: PR-A (84kDa) and PR-B (120kDa) (Figure 6.1C). Using this antibody, we showed no sex differences in PR-A/B expression in normal human airway epithelium of male and female donor lung tissues (Figure 6.1D-F). Therefore, all subsequent *in-vitro* experiments were focused on airway epithelial cells derived from female donor lungs. Histologic analysis revealed that PR-A/B expression was localized in the apical compartment of the airway epithelium in lung tissues and ALI cultures (Figure 6.1D, E, G).

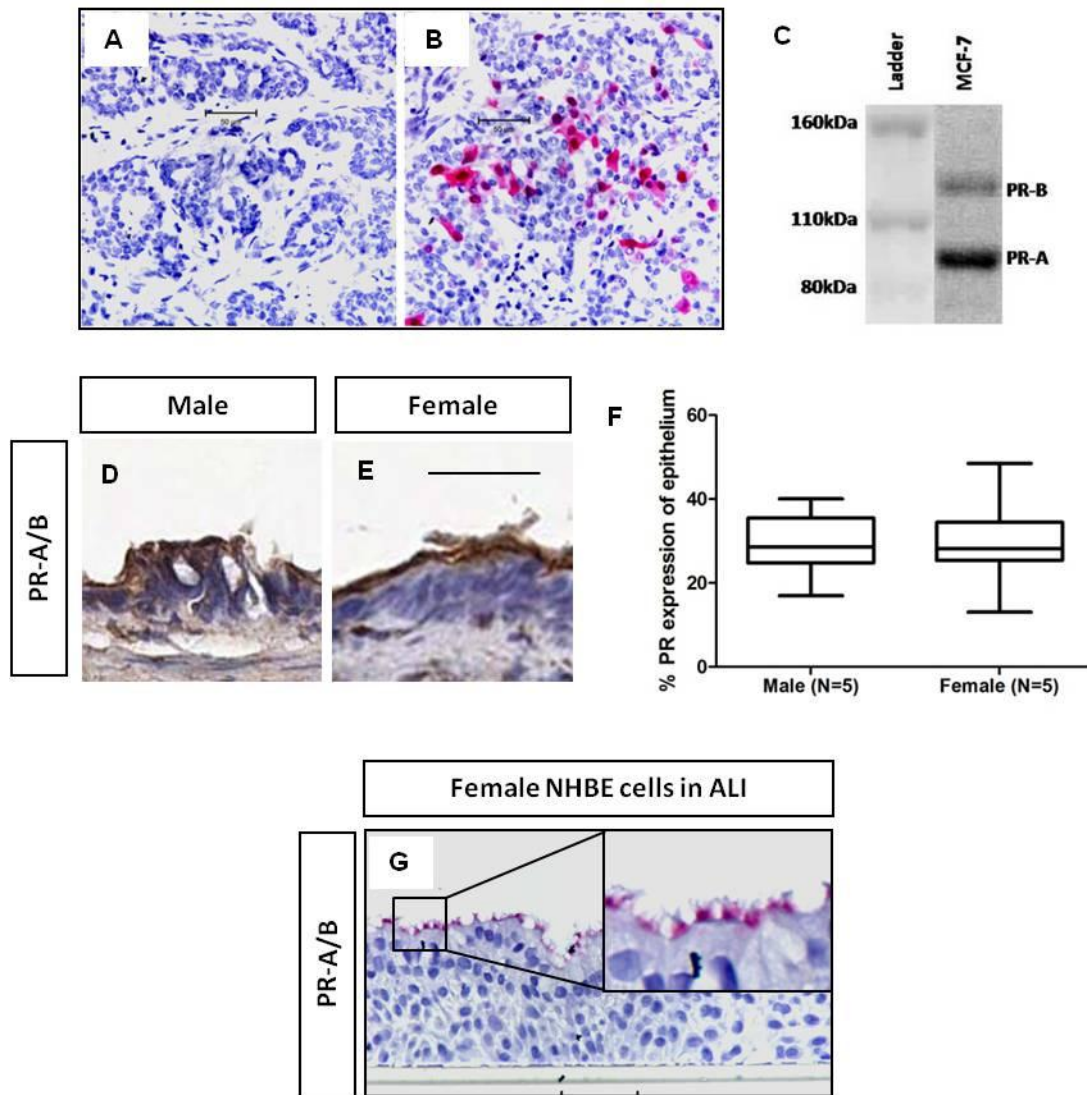


Figure 6.1: Progesterone receptor antibody specificity and protein expression in human airway epithelium.

A-B) Human breast tissue sections were used as positive controls for the binding specificity of progesterone receptor (PR-A/B) antibody. Negative control=replacement of primary antibody with IgG. C) This antibody resolved two isoforms of progesterone receptors: PR-A (90kDa) and PR-B (120kDa) in breast cancer cell line (MCF-7). Representative image of total PR positivity in the apical compartments of human D) male and E) female airway tissues with quantification of total PR expressed as percentage of the cross-sectional area of the epithelium in panel F. G) Female ALI cultures expressed PR in the apical compartment of the airway epithelium. Tissues were counterstained with hematoxylin. Scale bars=50 μ m.

6.3.2 Mifepristone attenuated progesterone-stimulated increase in PAS-positive cell staining in ALI cultures

To characterize the effects of progesterone on mucus production, paraffin-embedded ALI culture sections were stained with periodic acid-Schiff (PAS) for the detection of glycoprotein in mucus-producing cells (Figure 6.2A; scale bar = 50 μ m). Incubation of normal human bronchial epithelial (NHBE) cells cultured in ALI with physiologically relevant concentrations of progesterone for 2 weeks resulted in a concentration-dependent increase in PAS-positive cells and a decrease in PAS-negative cells, and these effects were restored to control levels by mifepristone (Figure 6.2B). The increases in PAS-positive cells by progesterone were reflected by increases in MUC5AC but not MUC5B mRNA expression when assessed by quantitative PCR (Figure 6.2C). The significant increase in MUC5AC mRNA expression was confirmed by an increase in MUC5AC-positive cells by immunohistochemical staining (Figure 6.2D-E).

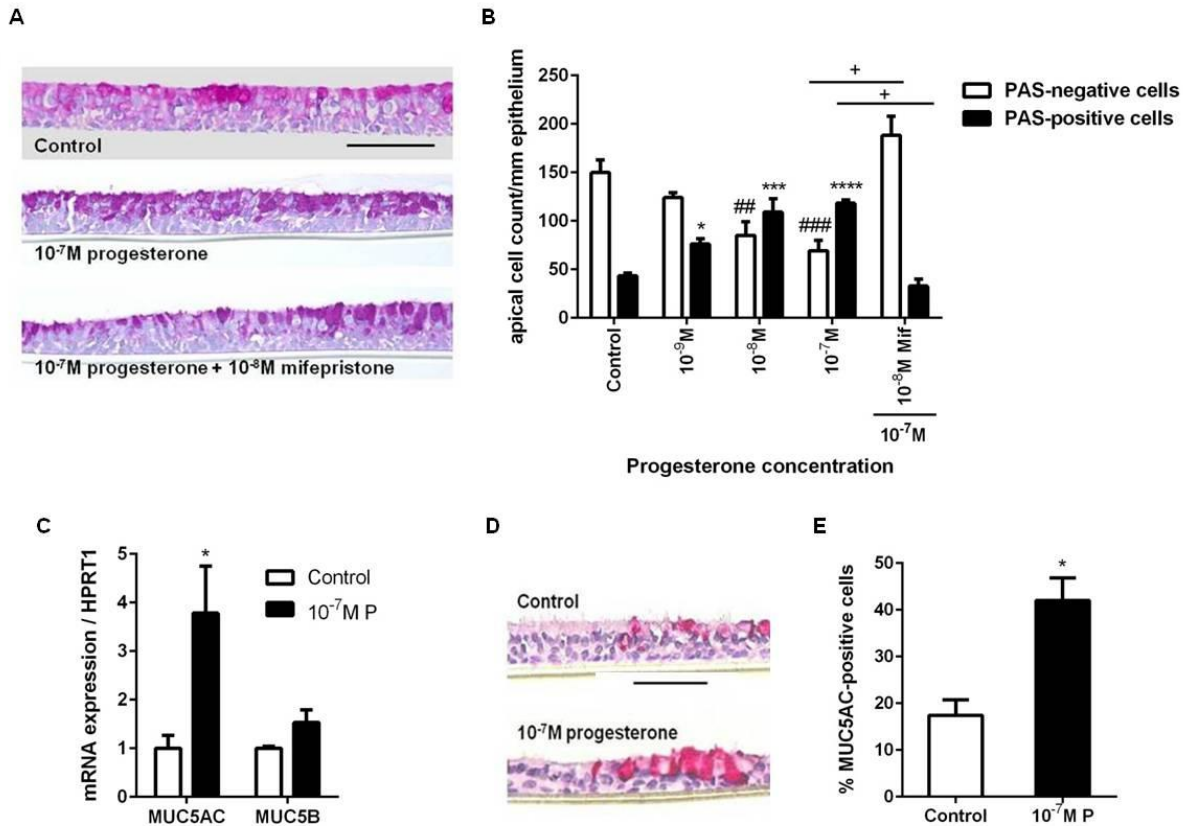


Figure 6.2: Mifepristone attenuated progesterone-stimulated increase in PAS-positive cell count in ALI cultures.

A) ALI cultures treated with ethanol vehicle (control), 10⁻⁷M progesterone and 10⁻⁷M progesterone + 10⁻⁸M mifepristone were stained with periodic acid-schiff (PAS) in detecting glycoprotein from mucus-producing cells. Sections were counterstained with H&E. Scale bars=50µm. B) Total apical cell count (white bar), PAS-negative (black bar) and PAS-positive (hatchet bar) cells were normalized to the length of the epithelium in millimeters. Data were representative of N=4 female donors. *p<0.05, ***p<0.001 compared between progesterone treatments and vehicle control in PAS-negative cell count. ###p<0.001, ####p<0.0001 compared between progesterone treatments and vehicle control in PAS-positive cell count. +++p<0.001 compared between 10⁻⁷M progesterone only and (10⁻⁷M progesterone + 10⁻⁸M mifepristone). C) ALI cultures treated with ethanol vehicle (control) and 10⁻⁷M progesterone were stained for MUC5AC protein in detecting goblet cells by immunohistochemistry. Sections were counterstained with H&E. Images were representative of N=4 female donors. Scale bars=50µm. D) MUC5AC-positive cell counts were expressed as a percentage of the total apical cell count on the epithelium. E) MUC5AC mRNA expression was normalized with HPRT1 using real time PCR. Data were expressed as mean ± SEM from N=4 female donors with 3 biological replicates. One-way ANOVA with Bonferroni's multiple comparisons test was used in panel B. Non-parametric t-test was used in panel D and E.

6.3.3 Progesterone increases nuclear factor of activated T- cell protein (NFAT)

To determine which transcription factor may be activated by progesterone in the regulation of MUC5AC expression, a protein transcription factor (TF) activation profiling array was used to screen for activated TFs in nuclear protein extract of primary NHBE cells in monolayer that were treated with 10^{-7} M progesterone or vehicle control for 24h. Absolute and fold change in luminescence of TF activation were showed in figure 6.3A-B. The dotted line represented a threshold of a 2-fold increase in luminescence unit in TF activation after progesterone stimulation with normalization to vehicle controls. Progesterone increased total NFAT protein in the nuclear fraction of NHBE cells after 24h (Figure 6.3A-B). Following stimulation of ALI cultures with 10^{-7} M progesterone for 2 weeks, we observed an increase in NFATc2 mRNA, a decrease in NFATc4 mRNA, and no changes in NFATc1 and NFATc3 mRNA expression compared to vehicle controls (Figure 6.4A). Immunohistochemical staining for NFATc2 protein revealed no significant sex difference but were localized in the apical compartment of the airway epithelium from both non-diseased male (n=5) and female (n=5) lung donors (Figure 6.4B-D).

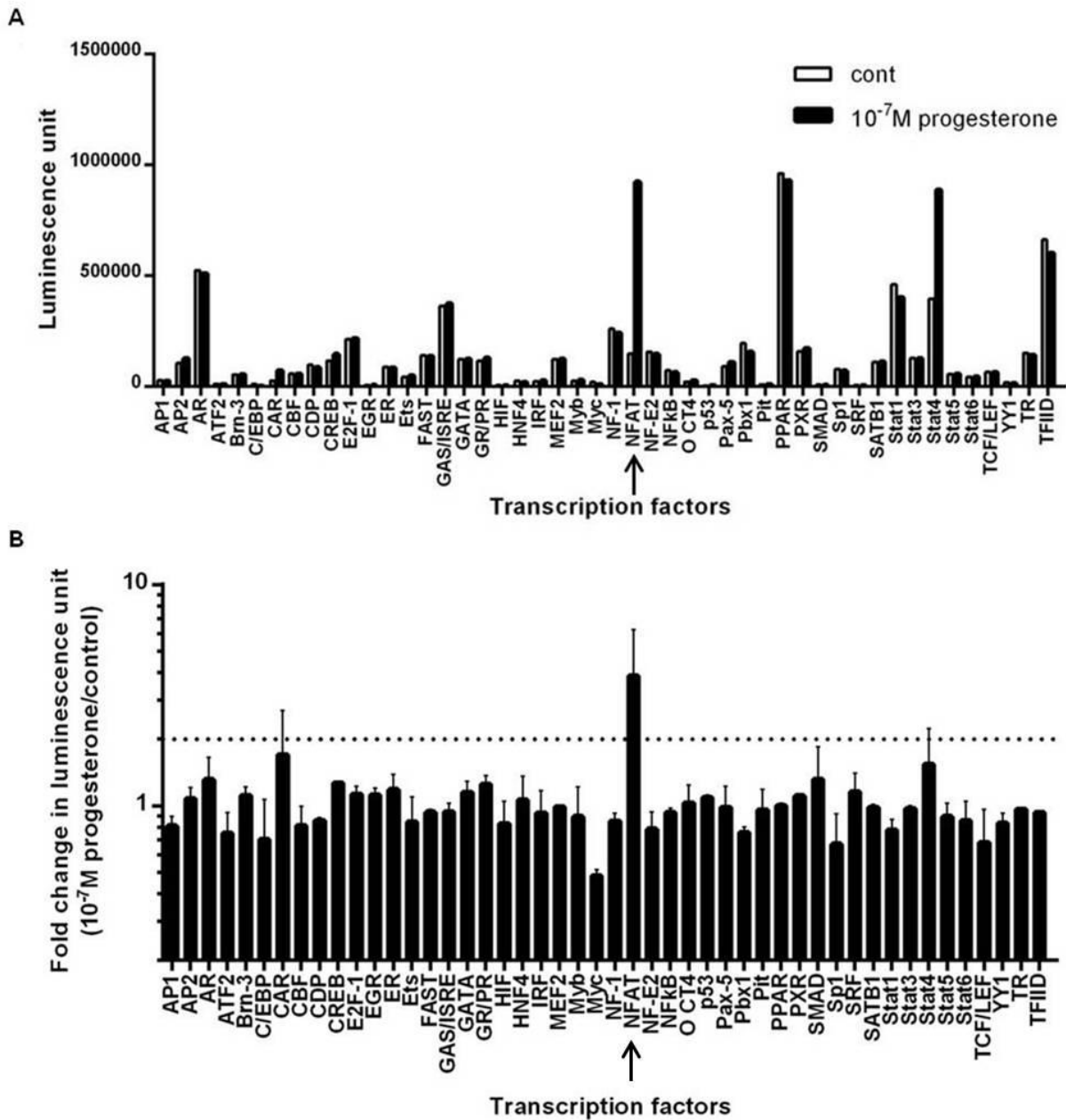


Figure 6.3: Progesterone increases nuclear factor of activated T-cell protein (NFAT).

A) 10⁻⁷M progesterone treatment for 24h increased total activated NFAT protein in the nuclear fraction of primary female NHBE cells. Data were expressed as A) absolute and B) relative fold change in luminescence unit over vehicle control (N=2 female NHBE cell donors). Dotted line represents a minimal threshold (2 fold increase) for statistical significance according to the manufacturer.

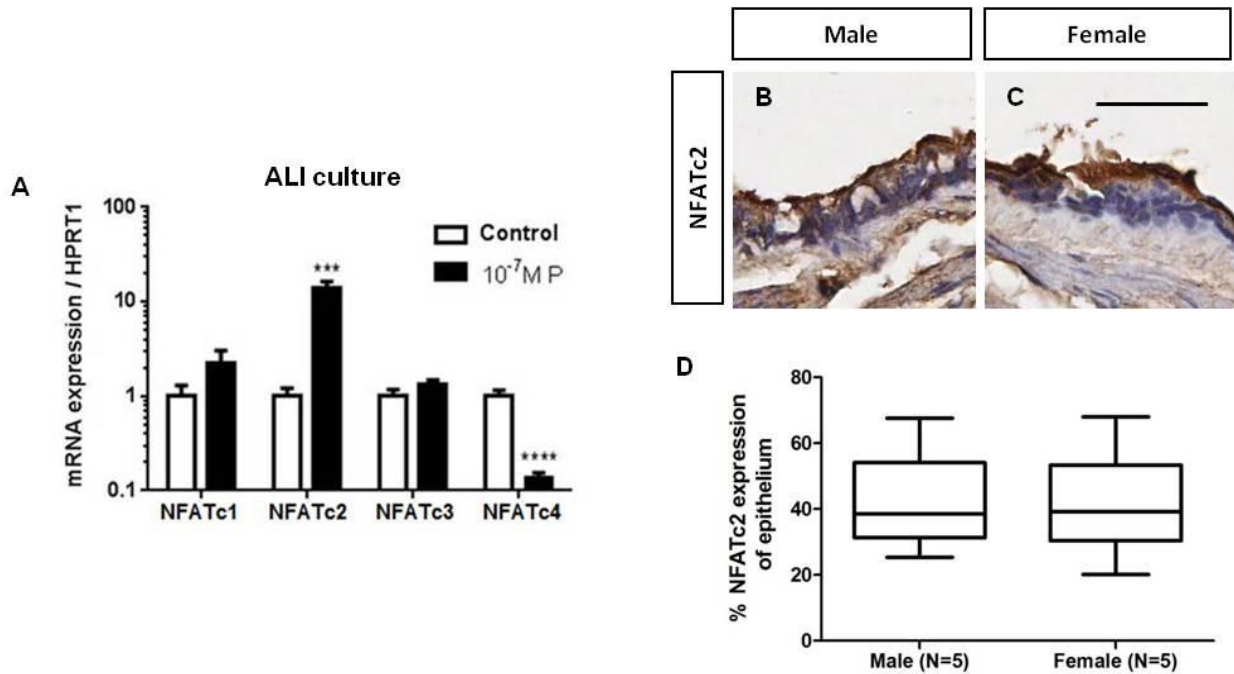


Figure 6.4: Progesterone differentially increased NFATc2 mRNA expression in ALI cultures.

NFAT (c1-c4) mRNA expression was normalized to HPRT1 in ethanol vehicle-treated (control) A) ALI cultures. B) NFAT (c1-c4) mRNA expression was normalized to HPRT1 in ALI cultures treated with ethanol vehicle (control) or 10⁻⁷M progesterone for 2 weeks. Values were expressed as mean ± SEM from N=4 female donors. NFATc2 protein was expressed in the airway epithelium of human C) male and D) female lung tissue sections with quantification of total NFATc2 protein expressed as percentage of the cross-sectional area of the epithelium in panel E. Non-parametric t-test was used in panel B and E.

6.3.4 Progesterone differentially increased NFATc2 mRNA in 1HAE₀ cells

To investigate whether NFATc2 plays any role in progesterone-stimulated MUC5AC expression, we silenced NFATc2 using siRNA in 1HAE₀ cell line to ensure uniform gene silencing. To elucidate the kinetic response of progesterone on the transcription of NFATc2, we showed a transient and differential increase in NFATc2 at 4h but not NFATc1, c3 or c4 mRNA expression (Figure 6.5A-D).

6.3.5 NFATc2 siRNA blunted progesterone-induced increase in MUC5AC mRNA

To confirm whether NFATc2 is involved in the regulation of MUC5AC mRNA expression, 1HAE₀ cells were pre-treated with NFATc2 siRNA (siNFATc2) for 48h followed by 10⁻⁷M progesterone stimulation. We confirmed that siNFATc2 selectively attenuated NFATc2 but not NFATc1, c3 or c4 mRNA expression (Figure 6.6A). Treatment of 1HAE₀ cells with progesterone alone for 4h, or scramble control siRNA (siCon) + progesterone increased NFATc2 mRNA by 1.5±0.2 and 1.6±0.3 folds over vehicle controls, respectively (Figure 6.6B). The use of siNFATc2 significantly attenuated progesterone-induced increase in NFATc2 mRNA expression. Treatment of 1HAE₀ cells with progesterone alone for 24h, or siCon + progesterone increased MUC5AC mRNA by 1.6±0.2 and 1.9±0.1 folds over control, respectively (Figure 6.6C). The use of siNFATc2 significantly attenuated progesterone-induced increase in MUC5AC mRNA expression. Primer specificities for NFATc1-c4, MUC5B and MUC5AC were confirmed by the presence of single DNA product in 1.1% agarose gel (Figure 6.6D). Collectively, we demonstrated that NFATc2 may be a novel regulator of progesterone-stimulated increase in MUC5AC expression.

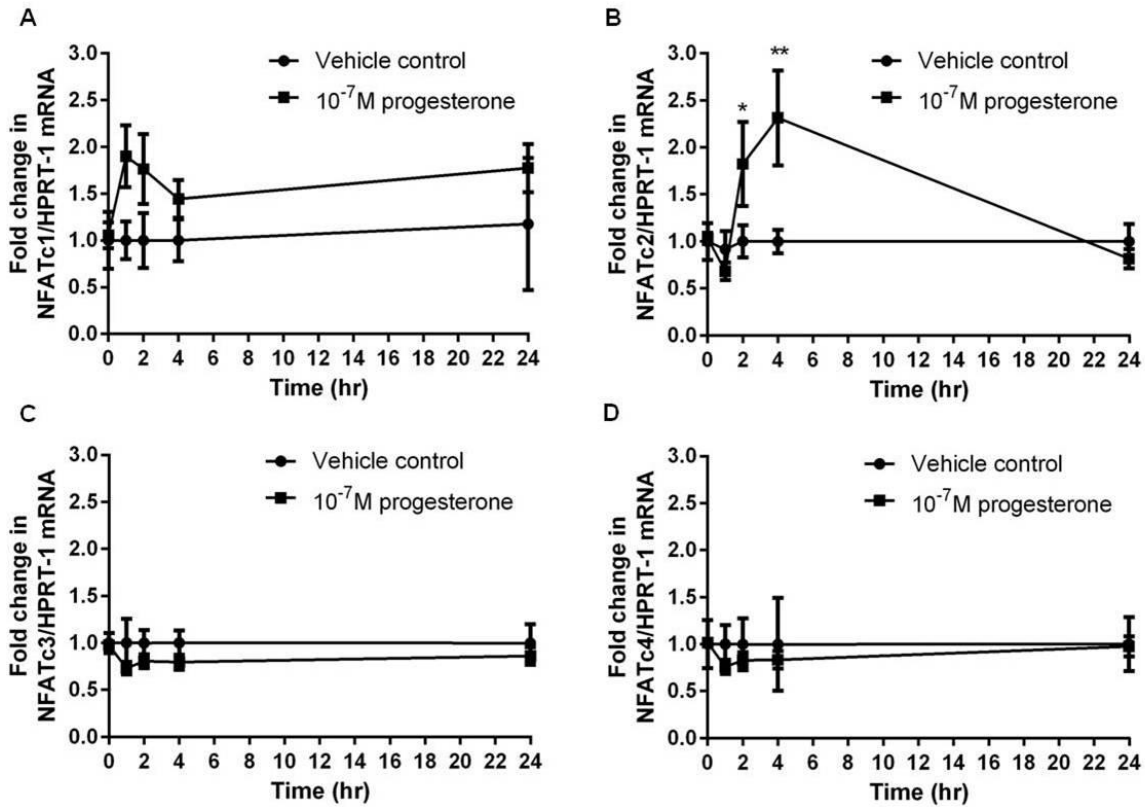


Figure 6.5: Progesterone stimulation transiently and differentially increased NFATc2 mRNA expression in 1HAE₀ cells.

Kinetic responses of a single dose of 10⁻⁷M progesterone at time 0h on A) NFATc1, B) NFATc2, C) NFATc3 and D) NFATc4 mRNA expression over time were shown. All 4 genes were measured from the same sample and values were expressed as mean ± SEM from 3 independent experimental replicates in 1HAE₀ cells. *p < 0.05, **p < 0.01 compared with vehicle controls. Two-way ANOVA with Bonferroni's multiple comparisons tests were used in all analyses.

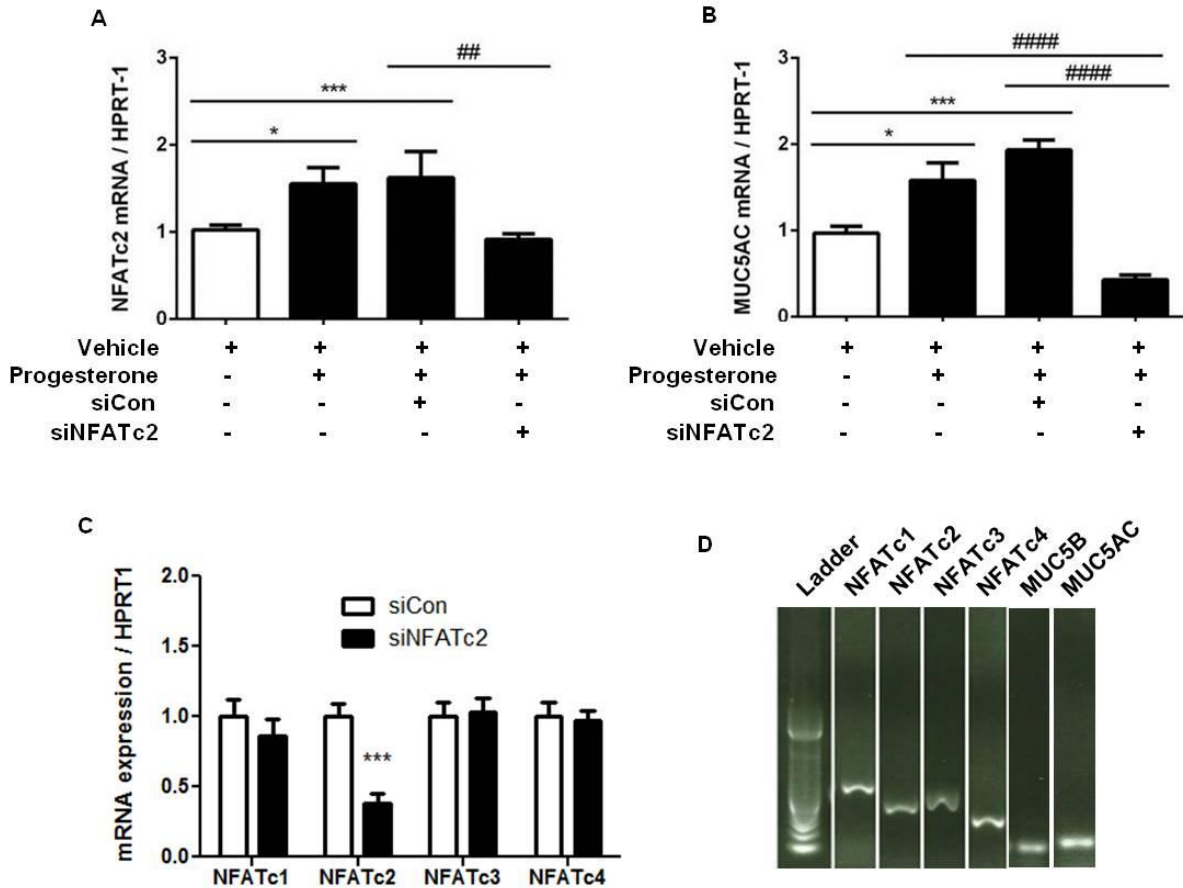


Figure 6.6: NFATc2 siRNA blunted progesterone-induced increase in NFATc2 and MUC5AC mRNA expression.

A) NFATc2 mRNA expression were increased with 10^{-7} M progesterone (P) and (siCon+P) stimulation, but was attenuated with (siNFATc2+P) treatment at 4h. B) MUC5AC mRNA expression were increased with 10^{-7} M P and (siCon+P), but was attenuated with (siNFATc2+P) treatment. C) siNFATc2 attenuated NFATc2 but not NFATc1, c3 or c4 mRNA expression compared to control siRNA (siCon) treatment. D) NFATc1-c4, MUC5B and MUC5AC primer specificities were confirmed in a DNA gel with single product. A 100bp DNA ladder was indicated. Values were expressed as mean \pm SEM from 3 experimental replicates in 1HAE₀ cells. One-way ANOVA with Bonferroni's multiple comparisons test was used in panels A and B. Non-parametric t-test was used in panel C.

6.4 Discussion

The effect of sex steroids on the airway epithelium is largely unexplored relative to current knowledge in other non-reproductive organs such as the brain, heart and the systemic vasculature [9, 10]. In this present study, we demonstrated that inhibition of the progesterone receptor with mifepristone attenuated progesterone-stimulated increase in PAS-positive cells in NHBE cells cultured in ALI. The corresponding increase in PAS-positive cells was associated with an increase in MUC5AC but not MUC5B mRNA expression. Gene silencing siNFATc2 treatment revealed that progesterone regulates MUC5AC gene expression through the transcription factor NFATc2.

Progesterone has been recognized as the second major female sex hormone that is involved in important physiological changes associated with embryogenesis, menstrual cycle and pregnancy [10]. Despite large epidemiologic studies showing that women may be more vulnerable to chronic lung diseases such as asthma, COPD and cystic fibrosis, very few studies have examined the biological effects of sex steroids in normal and diseased airways [10]. One important pathologic link to these conditions is mucus hypersecretion with plugging of the airways, leading to increased morbidity and mortality [25]. In this study, we used a cell culture model raised in air liquid interface, which has been widely used for the study of mucociliary clearance and barrier functions [239, 240]. ALI culture is a pseudostratified epithelium that consists of ciliated cells, goblet cells and basal cells [241]. Progesterone receptors were expressed in the cytoplasm of ciliated cells in the human airway epithelium of resected lung donors and in ALI cultures [242]. Jain and colleagues have showed that mifepristone, a progesterone receptor antagonist, prevented progesterone-induced decrease in ciliary beat frequency, whereas estrogen can also prevent this effect, suggesting a natural opposing

interaction of female sex hormones on the airway epithelium [242]. In this study, we showed that mifepristone attenuated progesterone-induced increase in MUC5AC protein expression, which is an indicator of goblet cells. There was a shift from a predominant PAS-negative cell population to PAS-positive cell predominance after two weeks of progesterone treatment, and this effect was attenuated by the use of mifepristone. The origin of progesterone-induced increase in PAS-positive cells is unknown. However, Tyner and colleagues revealed that goblet cells were derived from ciliated-cell lineage [243]. A similar study demonstrated that IL13 induces ciliated-cell differentiation into secretory cells via downregulation of actin-binding protein ezrin [244]. Collectively, although data suggest that progesterone-stimulated decrease in ciliary beat frequency and increase in MUC5AC protein synthesis may overwhelm the mucociliary clearance function in ALI cultures, the precise physiologic effect of mucociliary clearance with respect to the oscillating concentrations of estradiol and progesterone *in-vivo*, and their receptor interactions over the menstrual cycle is complex and incompletely known.

To determine a potential transcriptional regulator by which progesterone increases MUC5AC protein expression, we showed that total NFAT protein was increased in the nuclear fraction of NHBE cells. The luminescence signal from the protein transcription factor array essentially reflected the amount of activated NFAT protein binding on the NFAT response elements. Translocation of activated NFAT protein into the nucleus requires calcium-dependent activation of calcineurin, which is a phosphatase that activates NFAT protein in the cytosol via a dephosphorylation mechanism [245]. In this study, we showed that progesterone transiently and differentially induced NFATc2 in 1HAE₀ cells, which peaked at 4h. Similarly, Lee and colleagues also showed that the transcriptional activity of an NFAT promoter-luciferase

construct was transiently peaked at 4h after platelet-derived growth factor (PDGF) stimulation, which was abolished with cyclosporin A, an inhibitor of calcineurin activity [246].

To bridge the connection between NFATc2 and MUC5AC, we showed that silencing NFATc2 mRNA using siNFATc2 blunted progesterone-stimulated increase in MUC5AC mRNA expression, suggesting that NFATc2 may be a potent regulator of MUC5AC. It is not known whether there is an NFAT-specific response element on the promoter of MUC5AC gene. However, it is known that the human MUC5AC gene consists of DNA binding response elements for the binding of transcription factors including nuclear factor kappa-light-chain-enhancer of activated B cells (NFκB), Forkhead box protein A2 (FOXA2), activating protein 1 (AP1), specificity protein (SP1) and cyclic AMP response element binding (CREB) protein [60]. All protein from the NFAT family have unusually similar DNA-binding motive as the NFκB/Rel family [245]. NFATc2 protein dimers have been shown to bind on κB sites of the human IL-8 and HIV-1 LTR promoter regions [247, 248]. The identification of a putative NFκB binding site on the promoter of human MUC5AC gene [249] is a predicted binding site for NFATc2. Collectively, these data showed that estrogen receptor and progesterone receptor activation differentially increased NFATc1 and NFATc2 mRNA expression, respectively; both of which can individually increase MUC5AC protein expression in the human bronchial epithelium.

It is important to note several limitations in our study. First, we used constant physiologic concentrations of progesterone throughout the experiment, rather than allowing the cells to experience the fluctuating concentrations that truly reflects the menstrual cycle. Second, there is a lack of a commercially available progesterone receptor-specific inhibitor (PR-A vs. PR-B). Although mifepristone is a proven antagonist in both progesterone receptor and glucocorticoid receptor (GR) [250], there may be minor off-target effects in our culture model that could not be

fully accounted for in our analysis. Finally, total mucins and water content are important factors in determining the overall viscoelastic property of mucus and mucociliary clearance in the airways. We have not determined whether progesterone plays any role in water transport and overall mucus rheology because our main objective was to determine the transcriptional regulation of MUC5AC in the bronchial epithelium. Notwithstanding these limitations, our study demonstrated a novel mechanism by which progesterone modulates mucus expression, which may partially explain the contribution of female sex hormones on mucus production in the human bronchial epithelium.

Chapter 7: Conclusion

Emerging clinical studies revealed that women may be biologically more susceptible to the toxic effects from cigarette smoke, and have proposed that circulating female sex hormones, estrogen in particular, may play an important role in these processes [7-10]. Women with severe COPD have thickened airway walls, and narrowed luminal area than men [12]. In a large meta-analysis, female smokers also experienced an accelerated decline in lung function compared to male smokers after 45 years of age [13, 14]. However, the biological mechanisms associated with these changes are unknown. Here, we selected C57BL/6 mice as a model of COPD because we have repeatedly demonstrated emphysema and small airway remodelling after 6 months of smoke exposure [41, 42, 44]. In chapter 2 and 3, we showed that female C57BL/6 mice have histological evidence of increased small airway remodelling and functional evidence of increased distal airway resistance than male mice after 6 months of smoke exposure, and ovariectomy attenuated these effects. In chapter 4, we have proposed that these observations may be derived from an increase in lung oxidative stress. An increase in airway-specific superoxide expression and Nox4 mRNA expression was accompanied by a reduction in Nrf2 mRNA expression and antioxidant capacity in the lungs of female mice. Wang and colleagues have showed that cigarette smoke exposure directly oxidizes the latency-associated peptide (LAP) of TGF β 1 by oxidizing cysteine or methionine residues, causing the active form of TGF β 1 protein to be released into *in vitro* and rat tracheal explants [149, 212]. Using an *in vivo* mouse model of COPD, we showed that 6 months of smoke exposure liberated the release of active TGF β in whole lung homogenates and in airway-specific tissues of female but not in male mice. Products downstream of TGF β activation including Nox4 and α sma mRNA expression, and total collagen expression were disproportionately increased in female but not in male mice. Interestingly,

ovariectomy at maturity attenuated all of these changes after chronic smoke exposure compared to ovary-intact mice, suggesting the contribution of female sex hormones on the modulation of lung-specific antioxidant capacity in response to the cigarette smoke. Furthermore, as a therapeutic intervention, subcutaneous implantation of tamoxifen attenuated the excess smoke-induced increase in *Cyp1a1*, *Nox3* and *Nox4* mRNA expression in the airways of female than male mice, suggesting that estrogen may be involved in these biological processes. Our data is in agreement with clinical findings where female smokers have increased level of *Cyp1a1* expression than male smokers. However, we must be cautious of this interpretation because these mice were only exposed to sub-chronic duration of smoke exposure for 1 month and the antioxidant gene responses were all blunted in female mice after 6 months of smoke exposure. Although this may seem to be conflicting, it may simply reflect the kinetics of a duration-dependent smoke response on the regulation of antioxidant genes in the airways. In support with this hypothesis, Malhotra and colleagues showed that advanced COPD patients have decreased Nrf2-regulated *Nqo1*, glutamate-cysteine ligase, modifier subunit (*GCLM*) and *Hmox1* mRNA expression in the lungs, which were associated with a decrease in glutathione and an increase in thiobarbituric acid-reactive substance (TBARS) compared to non-COPD subjects [251]. To detect phenotypic and functional changes, further studies are required to show whether tamoxifen can attenuate chronic smoke-induced increase in airway remodelling and distal airway resistance in female mice over 6 months. Collectively, our data demonstrated a sexual dimorphism in smoke-induced airway remodelling that is in agreement with clinical observations discussed earlier, and a potential link between oxidative stress and airway remodelling. Nox4 inhibitors and sulforaphane (Nrf2 activator) have been identified and are currently in clinical trial for COPD [252].

As we have identified that smoke exposure did not affect goblet cell productions on the distal airway epithelium, the effect of sex hormones on mucus expression in a mouse model of COPD could not be explored. Therefore, we used an air liquid interface (ALI) cell culture model to explore the effects of estrogen and progesterone on mucus synthesis in normal human bronchial epithelial cells. Choi and colleagues showed that estrogen increased MUC5B expression in human nasal epithelial cells in ALI culture via non-genomic activation CREB signalling [240]. In chapter 5, we showed that two weeks of estrogen treatment on ALI cultures increased the number of PAS-positive cells via ER β activation. Interesting, ER β stimulation transiently and differentially increased NFATc1 but not the other isoforms of NFAT genes. Treatment with NFATc1 siRNA attenuated estrogen-induced increase in MUC5AC mRNA expression at the transcriptional level in 1HAE₀ cells. Next we showed that physiologic progesterone concentration also increased PAS-positive cells via PR-A/B activation. Interesting, unlike ER β , PR-A/B stimulation transiently and differentially increased NFATc2 but not the other isoforms of NFAT genes. Treatment with NFATc2 siRNA also attenuated progesterone-induced increase in MUC5AC mRNA in 1HAE₀ cells. Collectively, these data suggest that estradiol or progesterone stimulation uniquely activates its own downstream target; however, the exact biochemistry in these processes requires further studies. It is interesting that Fonseca and colleagues showed that mice deficient in NFATc2 attenuated ovalbumin-induced increase in mucus cells in the central airways, suggesting potential link between NFATc2 and mucus expression.

7.1 Limitations and strengths of the studies

The strength of this study is that we have a mouse model of COPD that recapitulated two of three important phenotypes of COPD using mainstream cigarette smoke. We are able to

provide a histologic evidence of small airway remodelling and emphysema, and coupling these with lung mechanics. Our data is congruent with clinical evidence that women with severe COPD have thicker airway walls and narrowed airway lumens than men. Morissette and colleagues have shown translational potential of animal models by demonstrating similar genes, pathways and biological functions affected by cigarette smoke in the lungs of mice and human [38]. However, it is important to note that smoke-induced emphysema requires at least 6 months in mice and is less severe than those observed in human, which takes many years for this process to occur. Although the use of specific genetic deficiencies such as ER α or ER β may be more attractive in determining the specific sex hormone receptor contributions on chronic smoke-induced lung abnormalities, development abnormalities resulting in improper formation of alveoli and reduced elastic recoil properties have been shown in ER α or ER β knockout mice. The confounding effect arising from developmental alterations may significantly impact lung function measurements and the interpretation of the data. In our study, ovariectomy and therapeutic administration of tamoxifen in mice more closely resemble the natural biological system.

7.2 Future directions

Owing largely to the overwhelming amount of reactive oxygen species (10^{15}) per puff of cigarette smoke, it is inevitable that there is build-up of oxidative stress in the lungs of smokers with COPD. An increase in oxidative stress has been proposed to be associated with small airway remodelling. Interesting, we showed that female mice are more susceptible to chronic smoke-induced airway remodelling and this largely affected by estrogen receptor-mediated disruption of antioxidant capacity and TGF β -mediated activation. To further strength the argument whether estrogen is a major culprit for the excess build-up of oxidative and airway

remodelling, therapeutic administration of estrogen in ovariectomized mice at pharmacologic doses is required in chronically smoke-exposed female and male mice. Even if data can support that estrogen is likely involved in this sex-related differences, it is almost impossible to administer female smokers with tamoxifen or other estrogen receptor-antagonizing drugs, given the counter-intuitive argument on therapy without symptoms early on in their fertile smoking years. However, it is possible, despite difficulty with recruitment of subjects, to determine the longitudinal effects of tamoxifen on oxidative stress and airway remodelling in female smokers who are on tamoxifen therapy.

Alternatively, other downstream therapeutic target such as Nrf2 protein in the airway epithelium may be an attractive target in the resolution of chronic smoke-induced increase in emphysema and airway remodelling. Malhotra and colleagues showed that advanced COPD patients have reduced Nrf2-regulated antioxidants, which are associated with a decrease in glutathione and an increase in lipid peroxidation in the lungs [251]. Furthermore, these Nrf2-regulated antioxidant mRNA expressions were positively associated with FEV1/FVC. Rangasamy and colleagues showed that genetic ablation of Nrf2 exacerbates smoke-induced emphysema in mice, which is accompanied by increased cell death and oxidative stress in Type II alveolar epithelial cells in parenchymal tissues [185]. Collectively, these data provide compelling evidence that Nrf2 activation may be able to reverse chronic smoke-induced emphysema and airway remodelling in female C57BL/6 mice.

Bibliography

1. Barnes PJ, SD Shapiro, and RA Pauwels: **Chronic obstructive pulmonary disease: molecular and cellular mechanisms.** *Eur Respir J* 2003. **22**: p. 672-88.
2. Pierce JP and EA Gilpin: **A historical analysis of tobacco marketing and the uptake of smoking by youth in the United States: 1890-1977.** *Health Psychol* 1995. **14**: p. 500-8.
3. MMWR. Deaths from Chronic Obstructive Pulmonary Disease. www.cdc.gov/mmwr/preview/mmwrhtml/mm5745a4.htm#tab1. Last date updated: Nov 13 2008. Last date accessed: Mar 3 2010.
4. Clayton JA and FS Collins: **Policy: NIH to balance sex in cell and animal studies.** *Nature* 2014. **509**: p. 282-3.
5. Beery AK and I Zucker: **Sex bias in neuroscience and biomedical research.** *Neurosci Biobehav Rev* 2011. **35**: p. 565-72.
6. Mogil JS and ML Chanda: **The case for the inclusion of female subjects in basic science studies of pain.** *Pain* 2005. **117**: p. 1-5.
7. Card JW and DC Zeldin: **Hormonal influences on lung function and response to environmental agents: lessons from animal models of respiratory disease.** *Proc Am Thorac Soc* 2009. **6**: p. 588-95.
8. Carey MA, JW Card, JW Voltz, SJ Arbes, Jr., DR Germolec, KS Korach, and DC Zeldin: **It's all about sex: gender, lung development and lung disease.** *Trends Endocrinol Metab* 2007. **18**: p. 308-13.
9. Townsend EA, VM Miller, and YS Prakash: **Sex differences and sex steroids in lung health and disease.** *Endocr Rev* 2012. **33**: p. 1-47.
10. Sathish V, YN Martin, and YS Prakash: **Sex steroid signaling: Implications for lung diseases.** *Pharmacol Ther* 2015.
11. Tam A, D Morrish, S Wadsworth, D Dorscheid, SF Man, and DD Sin: **The role of female hormones on lung function in chronic lung diseases.** *BMC Womens Health* 2011. **11**: p. 24.
12. Martinez FJ, JL Curtis, F Sciruba, J Mumford, ND Giardino, G Weinmann, E Kazerooni, S Murray, GJ Criner, DD Sin, J Hogg, AL Ries, M Han, AP Fishman, B Make, EA Hoffman, Z Mohsenifar, and R Wise: **Sex differences in severe pulmonary emphysema.** *Am J Respir Crit Care Med* 2007. **176**: p. 243-52.
13. Prescott E, AM Bjerg, PK Andersen, P Lange, and J Vestbo: **Gender difference in smoking effects on lung function and risk of hospitalization for COPD: results from a Danish longitudinal population study.** *Eur Respir J* 1997. **10**: p. 822-7.
14. Gan WQ, SF Man, DS Postma, P Camp, and DD Sin: **Female smokers beyond the perimenopausal period are at increased risk of chronic obstructive pulmonary disease: a systematic review and meta-analysis.** *Respir Res* 2006. **7**: p. 52.
15. Gillum RF: **Frequency of attendance at religious services and cigarette smoking in American women and men: the Third National Health and Nutrition Examination Survey.** *Prev Med* 2005. **41**: p. 607-13.
16. Celli B, J Vestbo, CR Jenkins, PW Jones, GT Ferguson, PM Calverley, JC Yates, JA Anderson, LR Willits, and RA Wise: **Sex differences in mortality and clinical expressions of patients with chronic obstructive pulmonary disease. The TORCH experience.** *Am J Respir Crit Care Med* 2011. **183**: p. 317-22.

17. Han MK, D Postma, DM Mannino, ND Giardino, S Buist, JL Curtis, and FJ Martinez: **Gender and chronic obstructive pulmonary disease: why it matters.** *Am J Respir Crit Care Med* 2007. **176**: p. 1179-84.
18. Silverman EK, ST Weiss, JM Drazen, HA Chapman, V Carey, EJ Campbell, P Denish, RA Silverman, JC Celedon, JJ Reilly, LC Ginns, and FE Speizer: **Gender-related differences in severe, early-onset chronic obstructive pulmonary disease.** *Am J Respir Crit Care Med* 2000. **162**: p. 2152-8.
19. Kanner RE, JE Connett, MD Altose, AS Buist, WW Lee, DP Tashkin, and RA Wise: **Gender difference in airway hyperresponsiveness in smokers with mild COPD. The Lung Health Study.** *Am J Respir Crit Care Med* 1994. **150**: p. 956-61.
20. Tam A and DD Sin: **Why are women more vulnerable to chronic obstructive pulmonary disease?** *Expert Rev Respir Med* 2013. **7**: p. 197-9.
21. Standards for the diagnosis and care of patients with chronic obstructive pulmonary disease. American Thoracic Society. *Am J Respir Crit Care Med* 1995; 152(5 Pt 2):S77-121.
22. Barnes PJ: **Chronic obstructive pulmonary disease.** *N Engl J Med* 2000. **343**: p. 269-80.
23. Rennard SI: **COPD: overview of definitions, epidemiology, and factors influencing its development.** *Chest* 1998. **113**: p. 235S-241S.
24. **Standards for the diagnosis and care of patients with chronic obstructive pulmonary disease. American Thoracic Society.** *Am J Respir Crit Care Med* 1995. **152**: p. S77-121.
25. Hogg JC, FS Chu, WC Tan, DD Sin, SA Patel, PD Pare, FJ Martinez, RM Rogers, BJ Make, GJ Criner, RM Cherniack, A Sharafkhaneh, JD Luketich, HO Coxson, WM Elliott, and FC Sciruba: **Survival after lung volume reduction in chronic obstructive pulmonary disease: insights from small airway pathology.** *Am J Respir Crit Care Med* 2007. **176**: p. 454-9.
26. Kilburn KH: **A hypothesis for pulmonary clearance and its implications.** *Am Rev Respir Dis* 1968. **98**: p. 449-63.
27. Hogg JC, PT Macklem, and WM Thurlbeck: **Site and nature of airway obstruction in chronic obstructive lung disease.** *N Engl J Med* 1968. **278**: p. 1355-60.
28. Hogg JC, F Chu, S Utokeaparch, R Woods, WM Elliott, L Buzatu, RM Cherniack, RM Rogers, FC Sciruba, HO Coxson, and PD Pare: **The nature of small-airway obstruction in chronic obstructive pulmonary disease.** *N Engl J Med* 2004. **350**: p. 2645-53.
29. Downs SH, O Brandli, JP Zellweger, C Schindler, N Kunzli, MW Gerbase, L Burdet, R Bettschart, E Zemp, M Frey, R Keller, JM Tschopp, P Leuenberger, and U Ackermann-Liebrich: **Accelerated decline in lung function in smoking women with airway obstruction: SAPALDIA 2 cohort study.** *Respir Res* 2005. **6**: p. 45.
30. Martin TR, RG Castile, JJ Fredberg, ME Wohl, and J Mead: **Airway size is related to sex but not lung size in normal adults.** *J Appl Physiol (1985)* 1987. **63**: p. 2042-7.
31. Sheel AW, JA Guenette, R Yuan, L Holy, JR Mayo, AM McWilliams, S Lam, and HO Coxson: **Evidence for dysanapsis using computed tomographic imaging of the airways in older ex-smokers.** *J Appl Physiol (1985)* 2009. **107**: p. 1622-8.
32. Ferguson GT: **Why does the lung hyperinflate?** *Proc Am Thorac Soc* 2006. **3**: p. 176-9.
33. Global Initiative for Chronic Obstructive Lung Disease. Pocket guide to COPD diagnosis, management, and prevention. A Guide for Health Care Professionals. 2003.

34. Mannino DM, A Sonia Buist, and WM Vollmer: **Chronic obstructive pulmonary disease in the older adult: what defines abnormal lung function?** *Thorax* 2007. **62**: p. 237-41.
35. Leith DE and R Brown: **Human lung volumes and the mechanisms that set them.** *Eur Respir J* 1999. **13**: p. 468-72.
36. Nishimura K, T Izumi, M Tsukino, and T Oga: **Dyspnea is a better predictor of 5-year survival than airway obstruction in patients with COPD.** *Chest* 2002. **121**: p. 1434-40.
37. Casanova C, C Cote, JP de Torres, A Aguirre-Jaime, JM Marin, V Pinto-Plata, and BR Celli: **Inspiratory-to-total lung capacity ratio predicts mortality in patients with chronic obstructive pulmonary disease.** *Am J Respir Crit Care Med* 2005. **171**: p. 591-7.
38. Morissette MC, M Lamontagne, JC Berube, G Gaschler, A Williams, C Yauk, C Couture, M Laviolette, JC Hogg, W Timens, S Halappanavar, MR Stampfli, and Y Bosse: **Impact of cigarette smoke on the human and mouse lungs: a gene-expression comparison study.** *PLoS One* 2014. **9**: p. e92498.
39. Drazen JM, PW Finn, and GT De Sanctis: **Mouse models of airway responsiveness: physiological basis of observed outcomes and analysis of selected examples using these outcome indicators.** *Annu Rev Physiol* 1999. **61**: p. 593-625.
40. Gelfand EW: **Pro: mice are a good model of human airway disease.** *Am J Respir Crit Care Med* 2002. **166**: p. 5-6; discussion 7-8.
41. Churg A, H Tai, T Coulthard, R Wang, and JL Wright: **Cigarette smoke drives small airway remodeling by induction of growth factors in the airway wall.** *Am J Respir Crit Care Med* 2006. **174**: p. 1327-34.
42. Churg A, S Zhou, O Preobrazhenska, H Tai, R Wang, and JL Wright: **Expression of profibrotic mediators in small airways versus parenchyma after cigarette smoke exposure.** *Am J Respir Cell Mol Biol* 2009. **40**: p. 268-76.
43. Zhou S, JL Wright, J Liu, DD Sin, and A Churg: **Aging does not enhance experimental cigarette smoke-induced COPD in the mouse.** *PLoS One* 2013. **8**: p. e71410.
44. Hackett TL, F Shaheen, S Zhou, JL Wright, and A Churg: **Fibroblast signal transducer and activator of transcription 4 drives cigarette smoke-induced airway fibrosis.** *Am J Respir Cell Mol Biol* 2014. **51**: p. 830-9.
45. Hautamaki RD, DK Kobayashi, RM Senior, and SD Shapiro: **Requirement for macrophage elastase for cigarette smoke-induced emphysema in mice.** *Science* 1997. **277**: p. 2002-4.
46. Belaouaj A, R McCarthy, M Baumann, Z Gao, TJ Ley, SN Abraham, and SD Shapiro: **Mice lacking neutrophil elastase reveal impaired host defense against gram negative bacterial sepsis.** *Nat Med* 1998. **4**: p. 615-8.
47. Churg A, S Zhou, X Wang, R Wang, and JL Wright: **The role of interleukin-1beta in murine cigarette smoke-induced emphysema and small airway remodeling.** *Am J Respir Cell Mol Biol* 2009. **40**: p. 482-90.
48. Massaro D and GD Massaro: **Estrogen regulates pulmonary alveolar formation, loss, and regeneration in mice.** *Am J Physiol Lung Cell Mol Physiol* 2004. **287**: p. L1154-9.
49. Massaro D and GD Massaro: **Estrogen receptor regulation of pulmonary alveolar dimensions: alveolar sexual dimorphism in mice.** *Am J Physiol Lung Cell Mol Physiol* 2006. **290**: p. L866-70.

50. Sisson TH, JM Hansen, M Shah, KE Hanson, M Du, T Ling, RH Simon, and PJ Christensen: **Expression of the reverse tetracycline-transactivator gene causes emphysema-like changes in mice.** *Am J Respir Cell Mol Biol* 2006. **34**: p. 552-60.
51. Haas TL, JL Doyle, MR Distasi, LE Norton, KM Sheridan, and JL Unthank: **Involvement of MMPs in the outward remodeling of collateral mesenteric arteries.** *Am J Physiol Heart Circ Physiol* 2007. **293**: p. H2429-37.
52. McBride JT. Architecture of the Tracheobronchial Tree. In: Comparative Biology of the Normal Lung, edited by Parent RA. Boca Raton: CRC, 1991, p. 49–62.
53. Wright JL, M Cosio, and A Churg: **Animal models of chronic obstructive pulmonary disease.** *Am J Physiol Lung Cell Mol Physiol* 2008. **295**: p. L1-15.
54. Rabe KF, S Hurd, A Anzueto, PJ Barnes, SA Buist, P Calverley, Y Fukuchi, C Jenkins, R Rodriguez-Roisin, C van Weel, and J Zielinski: **Global strategy for the diagnosis, management, and prevention of chronic obstructive pulmonary disease: GOLD executive summary.** *Am J Respir Crit Care Med* 2007. **176**: p. 532-55.
55. Wright JL and JP Sun: **Effect of smoking cessation on pulmonary and cardiovascular function and structure: analysis of guinea pig model.** *J Appl Physiol (1985)* 1994. **76**: p. 2163-8.
56. Bates JH and CG Irvin: **Measuring lung function in mice: the phenotyping uncertainty principle.** *J Appl Physiol (1985)* 2003. **94**: p. 1297-306.
57. Irvin CG and JH Bates: **Measuring the lung function in the mouse: the challenge of size.** *Respir Res* 2003. **4**: p. 4.
58. Pillow JJ, GL Hall, KE Willet, AH Jobe, Z Hantos, and PD Sly: **Effects of gestation and antenatal steroid on airway and tissue mechanics in newborn lambs.** *Am J Respir Crit Care Med* 2001. **163**: p. 1158-63.
59. Lumsden AB, A McLean, and D Lamb: **Goblet and Clara cells of human distal airways: evidence for smoking induced changes in their numbers.** *Thorax* 1984. **39**: p. 844-9.
60. Voynow JA and BK Rubin: **Mucins, mucus, and sputum.** *Chest* 2009. **135**: p. 505-12.
61. Boers JE, AW Ambergen, and FB Thunnissen: **Number and proliferation of basal and parabasal cells in normal human airway epithelium.** *Am J Respir Crit Care Med* 1998. **157**: p. 2000-6.
62. Evans MJ, LS Van Winkle, MV Fanucchi, and CG Plopper: **Cellular and molecular characteristics of basal cells in airway epithelium.** *Exp Lung Res* 2001. **27**: p. 401-15.
63. Evans MJ, RA Cox, SG Shami, B Wilson, and CG Plopper: **The role of basal cells in attachment of columnar cells to the basal lamina of the trachea.** *Am J Respir Cell Mol Biol* 1989. **1**: p. 463-9.
64. Rock JR, MW Onaitis, EL Rawlins, Y Lu, CP Clark, Y Xue, SH Randell, and BL Hogan: **Basal cells as stem cells of the mouse trachea and human airway epithelium.** *Proc Natl Acad Sci U S A* 2009. **106**: p. 12771-5.
65. Evans MJ and CG Plopper: **The role of basal cells in adhesion of columnar epithelium to airway basement membrane.** *Am Rev Respir Dis* 1988. **138**: p. 481-3.
66. Knight DA and ST Holgate: **The airway epithelium: structural and functional properties in health and disease.** *Respirology* 2003. **8**: p. 432-46.
67. Hong KU, SD Reynolds, S Watkins, E Fuchs, and BR Stripp: **In vivo differentiation potential of tracheal basal cells: evidence for multipotent and unipotent subpopulations.** *Am J Physiol Lung Cell Mol Physiol* 2004. **286**: p. L643-9.

68. Sallenave JM, J Shulmann, J Crossley, M Jordana, and J Gauldie: **Regulation of secretory leukocyte proteinase inhibitor (SLPI) and elastase-specific inhibitor (ESI/elafin) in human airway epithelial cells by cytokines and neutrophilic enzymes.** *Am J Respir Cell Mol Biol* 1994. **11**: p. 733-41.
69. De Water R, LN Willems, GN Van Muijen, C Franken, JA Fransen, JH Dijkman, and JA Kramps: **Ultrastructural localization of bronchial antileukoprotease in central and peripheral human airways by a gold-labeling technique using monoclonal antibodies.** *Am Rev Respir Dis* 1986. **133**: p. 882-90.
70. Hong KU, SD Reynolds, A Giangreco, CM Hurley, and BR Stripp: **Clara cell secretory protein-expressing cells of the airway neuroepithelial body microenvironment include a label-retaining subset and are critical for epithelial renewal after progenitor cell depletion.** *Am J Respir Cell Mol Biol* 2001. **24**: p. 671-81.
71. Spina D: **Epithelium smooth muscle regulation and interactions.** *Am J Respir Crit Care Med* 1998. **158**: p. S141-5.
72. You Y, T Huang, EJ Richer, JE Schmidt, J Zabner, Z Borok, and SL Brody: **Role of foxj1 in differentiation of ciliated airway epithelial cells.** *Am J Physiol Lung Cell Mol Physiol* 2004. **286**: p. L650-7.
73. Ayers MM and PK Jeffery: **Proliferation and differentiation in mammalian airway epithelium.** *Eur Respir J* 1988. **1**: p. 58-80.
74. Harkema JR, Mariassy A., St. George J., Hyde D.M., Plopper C.G., *Epithelial cells of the conducting airways: a species comparison.* Farmer S.G., Hay D.W.P. (eds) ed. 1991, New York.
75. Jeffery PK: **Morphologic features of airway surface epithelial cells and glands.** *Am Rev Respir Dis* 1983. **128**: p. S14-20.
76. Hovenberg HW, JR Davies, and I Carlstedt: **Different mucins are produced by the surface epithelium and the submucosa in human trachea: identification of MUC5AC as a major mucin from the goblet cells.** *Biochem J* 1996. **318 (Pt 1)**: p. 319-24.
77. Thornton DJ, K Rousseau, and MA McGuckin: **Structure and function of the polymeric mucins in airways mucus.** *Annu Rev Physiol* 2008. **70**: p. 459-86.
78. Sheehan JK, DJ Thornton, M Somerville, and I Carlstedt: **Mucin structure. The structure and heterogeneity of respiratory mucus glycoproteins.** *Am Rev Respir Dis* 1991. **144**: p. S4-9.
79. Rogers DF: **Airway goblet cells: responsive and adaptable front-line defenders.** *Eur Respir J* 1994. **7**: p. 1690-706.
80. Yates GT, TY Wu, RE Johnson, AT Cheung, and CL Frand: **A theoretical and experimental study on tracheal muco-ciliary transport.** *Biorheology* 1980. **17**: p. 151-62.
81. Sheehan JK, M Kesimer, and R Pickles: **Innate immunity and mucus structure and function.** *Novartis Found Symp* 2006. **279**: p. 155-66; discussion 167-9, 216-9.
82. Lazarowski ER, RC Boucher, and TK Harden: **Mechanisms of release of nucleotides and integration of their action as P2X- and P2Y-receptor activating molecules.** *Mol Pharmacol* 2003. **64**: p. 785-95.
83. Tarran R, BR Grubb, JT Gatzky, CW Davis, and RC Boucher: **The relative roles of passive surface forces and active ion transport in the modulation of airway surface liquid volume and composition.** *J Gen Physiol* 2001. **118**: p. 223-36.

84. Reverdin N, G Gabbiani, and Y Kapanci: **Actin in tracheo-bronchial ciliated epithelial cells.** *Experientia* 1975. **31**: p. 1348-50.
85. Jeffery PK and L Reid: **New observations of rat airway epithelium: a quantitative and electron microscopic study.** *J Anat* 1975. **120**: p. 295-320.
86. Boucher RC: **Human airway ion transport. Part one.** *Am J Respir Crit Care Med* 1994. **150**: p. 271-81.
87. Zeitlin PL: **Cystic fibrosis and estrogens: a perfect storm.** *J Clin Invest* 2008. **118**: p. 3841-4.
88. Terranova VP, DH Rohrbach, and GR Martin: **Role of laminin in the attachment of PAM 212 (epithelial) cells to basement membrane collagen.** *Cell* 1980. **22**: p. 719-26.
89. Boudreau N, Z Werb, and MJ Bissell: **Suppression of apoptosis by basement membrane requires three-dimensional tissue organization and withdrawal from the cell cycle.** *Proc Natl Acad Sci U S A* 1996. **93**: p. 3509-13.
90. Wadsworth SJ, AM Freyer, RL Corteling, and IP Hall: **Biosynthesized matrix provides a key role for survival signaling in bronchial epithelial cells.** *Am J Physiol Lung Cell Mol Physiol* 2004. **286**: p. L596-603.
91. Paulsson M: **Basement membrane proteins: structure, assembly, and cellular interactions.** *Crit Rev Biochem Mol Biol* 1992. **27**: p. 93-127.
92. Burns AR, CW Smith, and DC Walker: **Unique structural features that influence neutrophil emigration into the lung.** *Physiol Rev* 2003. **83**: p. 309-36.
93. Kapanci Y, C Ribaux, C Chaponnier, and G Gabbiani: **Cytoskeletal features of alveolar myofibroblasts and pericytes in normal human and rat lung.** *J Histochem Cytochem* 1992. **40**: p. 1955-63.
94. Leslie KO, J Mitchell, and R Low: **Lung myofibroblasts.** *Cell Motil Cytoskeleton* 1992. **22**: p. 92-8.
95. Follonier Castella L, G Gabbiani, CA McCulloch, and B Hinz: **Regulation of myofibroblast activities: calcium pulls some strings behind the scene.** *Exp Cell Res* 2010. **316**: p. 2390-401.
96. Haeryfar SM and DW Hoskin: **Thy-1: more than a mouse pan-T cell marker.** *J Immunol* 2004. **173**: p. 3581-8.
97. Saalbach A, R Kraft, K Herrmann, UF Haustein, and U Anderegg: **The monoclonal antibody AS02 recognizes a protein on human fibroblasts being highly homologous to Thy-1.** *Arch Dermatol Res* 1998. **290**: p. 360-6.
98. Saalbach A, T Wetzig, UF Haustein, and U Anderegg: **Detection of human soluble Thy-1 in serum by ELISA. Fibroblasts and activated endothelial cells are a possible source of soluble Thy-1 in serum.** *Cell Tissue Res* 1999. **298**: p. 307-15.
99. Craig W, R Kay, RL Cutler, and PM Lansdorp: **Expression of Thy-1 on human hematopoietic progenitor cells.** *J Exp Med* 1993. **177**: p. 1331-42.
100. Ramirez G, JS Hagood, Y Sanders, R Ramirez, C Becerril, L Segura, L Barrera, M Selman, and A Pardo: **Absence of Thy-1 results in TGF-beta induced MMP-9 expression and confers a profibrotic phenotype to human lung fibroblasts.** *Lab Invest* 2011. **91**: p. 1206-18.
101. Hinz B, G Celetta, JJ Tomasek, G Gabbiani, and C Chaponnier: **Alpha-smooth muscle actin expression upregulates fibroblast contractile activity.** *Mol Biol Cell* 2001. **12**: p. 2730-41.

102. Skalli O, MF Pelte, MC Pecelet, G Gabbiani, P Gugliotta, G Bussolati, M Ravazzola, and L Orci: **Alpha-smooth muscle actin, a differentiation marker of smooth muscle cells, is present in microfilamentous bundles of pericytes.** *J Histochem Cytochem* 1989. **37**: p. 315-21.
103. Howarth PH, AJ Knox, Y Amrani, O Tliba, RA Panettieri, Jr., and M Johnson: **Synthetic responses in airway smooth muscle.** *J Allergy Clin Immunol* 2004. **114**: p. S32-50.
104. John M, BT Au, PJ Jose, S Lim, M Saunders, PJ Barnes, JA Mitchell, MG Belvisi, and KF Chung: **Expression and release of interleukin-8 by human airway smooth muscle cells: inhibition by Th-2 cytokines and corticosteroids.** *Am J Respir Cell Mol Biol* 1998. **18**: p. 84-90.
105. Pype JL, LJ Dupont, P Menten, E Van Coillie, G Opdenakker, J Van Damme, KF Chung, MG Demedts, and GM Verleden: **Expression of monocyte chemotactic protein (MCP)-1, MCP-2, and MCP-3 by human airway smooth-muscle cells. Modulation by corticosteroids and T-helper 2 cytokines.** *Am J Respir Cell Mol Biol* 1999. **21**: p. 528-36.
106. Chung KF: **The role of airway smooth muscle in the pathogenesis of airway wall remodeling in chronic obstructive pulmonary disease.** *Proc Am Thorac Soc* 2005. **2**: p. 347-54; discussion 371-2.
107. Hirst SJ, CH Twort, and TH Lee: **Differential effects of extracellular matrix proteins on human airway smooth muscle cell proliferation and phenotype.** *Am J Respir Cell Mol Biol* 2000. **23**: p. 335-44.
108. Wylam ME, V Sathish, SK VanOosten, M Freeman, D Burkholder, MA Thompson, CM Pabelick, and YS Prakash: **Mechanisms of Cigarette Smoke Effects on Human Airway Smooth Muscle.** *PLoS One* 2015. **10**: p. e0128778.
109. Freyer AM, SR Johnson, and IP Hall: **Effects of growth factors and extracellular matrix on survival of human airway smooth muscle cells.** *Am J Respir Cell Mol Biol* 2001. **25**: p. 569-76.
110. Oltmanns U, MB Sukkar, S Xie, M John, and KF Chung: **Induction of human airway smooth muscle apoptosis by neutrophils and neutrophil elastase.** *Am J Respir Cell Mol Biol* 2005. **32**: p. 334-41.
111. Farha S, K Asosingh, D Laskowski, J Hammel, RA Dweik, HP Wiedemann, and SC Erzurum: **Effects of the menstrual cycle on lung function variables in women with asthma.** *Am J Respir Crit Care Med* 2009. **180**: p. 304-10.
112. Johannesson M, D Ludviksdottir, and C Janson: **Lung function changes in relation to menstrual cycle in females with cystic fibrosis.** *Respir Med* 2000. **94**: p. 1043-6.
113. Koehler KF, LA Helguero, LA Haldosen, M Warner, and JA Gustafsson: **Reflections on the discovery and significance of estrogen receptor beta.** *Endocr Rev* 2005. **26**: p. 465-78.
114. Kuiper GG, E Enmark, M Pelto-Huikko, S Nilsson, and JA Gustafsson: **Cloning of a novel receptor expressed in rat prostate and ovary.** *Proc Natl Acad Sci U S A* 1996. **93**: p. 5925-30.
115. Tremblay GB, A Tremblay, NG Copeland, DJ Gilbert, NA Jenkins, F Labrie, and V Giguere: **Cloning, chromosomal localization, and functional analysis of the murine estrogen receptor beta.** *Mol Endocrinol* 1997. **11**: p. 353-65.
116. Mosselman S, J Polman, and R Dijkema: **ER beta: identification and characterization of a novel human estrogen receptor.** *FEBS Lett* 1996. **392**: p. 49-53.

117. Culig Z: **Role of the androgen receptor axis in prostate cancer.** *Urology* 2003. **62**: p. 21-6.
118. Couse JF, J Lindzey, K Grandien, JA Gustafsson, and KS Korach: **Tissue distribution and quantitative analysis of estrogen receptor-alpha (ERalpha) and estrogen receptor-beta (ERbeta) messenger ribonucleic acid in the wild-type and ERalpha-knockout mouse.** *Endocrinology* 1997. **138**: p. 4613-21.
119. Ivanova MM, W Mazhawidza, SM Dougherty, JD Minna, and CM Klinge: **Activity and intracellular location of estrogen receptors alpha and beta in human bronchial epithelial cells.** *Mol Cell Endocrinol* 2009. **305**: p. 12-21.
120. Fleisher B, MV Kulovich, M Hallman, and L Gluck: **Lung profile: sex differences in normal pregnancy.** *Obstet Gynecol* 1985. **66**: p. 327-30.
121. Dammann CE, SM Ramadurai, DD McCants, LD Pham, and HC Nielsen: **Androgen regulation of signaling pathways in late fetal mouse lung development.** *Endocrinology* 2000. **141**: p. 2923-9.
122. Doershuk CF, BJ Fisher, and LW Matthews: **Specific airway resistance from the perinatal period into adulthood. Alterations in childhood pulmonary disease.** *Am Rev Respir Dis* 1974. **109**: p. 452-7.
123. Thurlbeck WM: **Postnatal human lung growth.** *Thorax* 1982. **37**: p. 564-71.
124. Carey MA, JW Card, JW Voltz, DR Germolec, KS Korach, and DC Zeldin: **The impact of sex and sex hormones on lung physiology and disease: lessons from animal studies.** *Am J Physiol Lung Cell Mol Physiol* 2007. **293**: p. L272-8.
125. Payne AH and DB Hales: **Overview of steroidogenic enzymes in the pathway from cholesterol to active steroid hormones.** *Endocr Rev* 2004. **25**: p. 947-70.
126. Mendelsohn ME and RH Karas: **Molecular and cellular basis of cardiovascular gender differences.** *Science* 2005. **308**: p. 1583-7.
127. Hewitt SC, JC Harrell, and KS Korach: **Lessons in estrogen biology from knockout and transgenic animals.** *Annu Rev Physiol* 2005. **67**: p. 285-308.
128. Ellmann S, H Sticht, F Thiel, MW Beckmann, R Strick, and PL Strissel: **Estrogen and progesterone receptors: from molecular structures to clinical targets.** *Cell Mol Life Sci* 2009. **66**: p. 2405-26.
129. Giannopoulos G and SK Smith: **Androgen receptors in fetal rabbit lung and the effect of fetal sex on the levels of circulating hormones and pulmonary hormone receptors.** *J Steroid Biochem* 1982. **17**: p. 461-5.
130. de Ronde W, YT van der Schouw, M Muller, DE Grobbee, LJ Gooren, HA Pols, and FH de Jong: **Associations of sex-hormone-binding globulin (SHBG) with non-SHBG-bound levels of testosterone and estradiol in independently living men.** *J Clin Endocrinol Metab* 2005. **90**: p. 157-62.
131. Cheng CY, NA Musto, GL Gunsalus, J Frick, and CW Bardin: **There are two forms of androgen binding protein in human testes. Comparison of their protomeric variants with serum testosterone-estradiol binding globulin.** *J Biol Chem* 1985. **260**: p. 5631-40.
132. French FS and EM Ritzen: **A high-affinity androgen-binding protein (ABP) in rat testis: evidence for secretion into efferent duct fluid and absorption by epididymis.** *Endocrinology* 1973. **93**: p. 88-95.

133. Grishkovskaya I, GV Avvakumov, G Sklenar, D Dales, GL Hammond, and YA Muller: **Crystal structure of human sex hormone-binding globulin: steroid transport by a laminin G-like domain.** *EMBO J* 2000. **19**: p. 504-12.
134. Siiteri PK, JT Murai, GL Hammond, JA Nisker, WJ Raymoure, and RW Kuhn: **The serum transport of steroid hormones.** *Recent Prog Horm Res* 1982. **38**: p. 457-510.
135. Dunn JF, BC Nisula, and D Rodbard: **Transport of steroid hormones: binding of 21 endogenous steroids to both testosterone-binding globulin and corticosteroid-binding globulin in human plasma.** *J Clin Endocrinol Metab* 1981. **53**: p. 58-68.
136. Mendel CM: **The free hormone hypothesis. Distinction from the free hormone transport hypothesis.** *J Androl* 1992. **13**: p. 107-16.
137. Rosner W: **Plasma steroid-binding proteins.** *Endocrinol Metab Clin North Am* 1991. **20**: p. 697-720.
138. Nakhla AM, MS Khan, NP Romas, and W Rosner: **Estradiol causes the rapid accumulation of cAMP in human prostate.** *Proc Natl Acad Sci U S A* 1994. **91**: p. 5402-5.
139. General US. The health consequences of smoking: chronic obstructive lung disease. In. Edited by General US: US Gov Press Office; 1984.
140. Hoidal JR, RB Fox, PA LeMarbe, R Perri, and JE Repine: **Altered oxidative metabolic responses in vitro of alveolar macrophages from asymptomatic cigarette smokers.** *Am Rev Respir Dis* 1981. **123**: p. 85-9.
141. Ghosh S, AJ Janocha, MA Aronica, S Swaidani, SA Comhair, W Xu, L Zheng, S Kaveti, M Kinter, SL Hazen, and SC Erzurum: **Nitrotyrosine proteome survey in asthma identifies oxidative mechanism of catalase inactivation.** *J Immunol* 2006. **176**: p. 5587-97.
142. Pryor WA and K Stone: **Oxidants in cigarette smoke. Radicals, hydrogen peroxide, peroxyxynitrate, and peroxyxynitrite.** *Ann N Y Acad Sci* 1993. **686**: p. 12-27; discussion 27-8.
143. Van Winkle LS, AD Gunderson, JA Shimizu, GL Baker, and CD Brown: **Gender differences in naphthalene metabolism and naphthalene-induced acute lung injury.** *Am J Physiol Lung Cell Mol Physiol* 2002. **282**: p. L1122-34.
144. Chichester CH, AR Buckpitt, A Chang, and CG Plopper: **Metabolism and cytotoxicity of naphthalene and its metabolites in isolated murine Clara cells.** *Mol Pharmacol* 1994. **45**: p. 664-72.
145. Han W, BT Pentecost, RL Pietropaolo, MJ Fasco, and SD Spivack: **Estrogen receptor alpha increases basal and cigarette smoke extract-induced expression of CYP1A1 and CYP1B1, but not GSTP1, in normal human bronchial epithelial cells.** *Mol Carcinog* 2005. **44**: p. 202-11.
146. Etter JF, T Vu Duc, and TV Perneger: **Saliva cotinine levels in smokers and nonsmokers.** *Am J Epidemiol* 2000. **151**: p. 251-8.
147. Benowitz NL, CN Lessov-Schlaggar, GE Swan, and P Jacob, 3rd: **Female sex and oral contraceptive use accelerate nicotine metabolism.** *Clin Pharmacol Ther* 2006. **79**: p. 480-8.
148. Sin DD, SB Cohen, A Day, H Coxson, and PD Pare: **Understanding the biological differences in susceptibility to chronic obstructive pulmonary disease between men and women.** *Proc Am Thorac Soc* 2007. **4**: p. 671-4.

149. Barcellos-Hoff MH and TA Dix: **Redox-mediated activation of latent transforming growth factor-beta 1.** *Mol Endocrinol* 1996. **10**: p. 1077-83.
150. Wang RD, JL Wright, and A Churg: **Transforming growth factor-beta1 drives airway remodeling in cigarette smoke-exposed tracheal explants.** *Am J Respir Cell Mol Biol* 2005. **33**: p. 387-93.
151. Rubio ML, MV Sanchez-Cifuentes, M Ortega, G Peces-Barba, JD Escolar, S Verbanck, M Paiva, and N Gonzalez Mangado: **N-acetylcysteine prevents cigarette smoke induced small airways alterations in rats.** *Eur Respir J* 2000. **15**: p. 505-11.
152. Blobel GC, WP Schiemann, and HF Lodish: **Role of transforming growth factor beta in human disease.** *N Engl J Med* 2000. **342**: p. 1350-8.
153. Wu MY and CS Hill: **Tgf-beta superfamily signaling in embryonic development and homeostasis.** *Dev Cell* 2009. **16**: p. 329-43.
154. Lyons RM, J Keski-Oja, and HL Moses: **Proteolytic activation of latent transforming growth factor-beta from fibroblast-conditioned medium.** *J Cell Biol* 1988. **106**: p. 1659-65.
155. Allen DM, LE Chen, AV Seaber, and JR Urbaniak: **Pathophysiology and related studies of the no reflow phenomenon in skeletal muscle.** *Clin Orthop Relat Res* 1995: p. 122-33.
156. Schultz-Cherry S, H Chen, DF Mosher, TM Misenheimer, HC Krutzsch, DD Roberts, and JE Murphy-Ullrich: **Regulation of transforming growth factor-beta activation by discrete sequences of thrombospondin 1.** *J Biol Chem* 1995. **270**: p. 7304-10.
157. Yu Q and I Stamenkovic: **Cell surface-localized matrix metalloproteinase-9 proteolytically activates TGF-beta and promotes tumor invasion and angiogenesis.** *Genes Dev* 2000. **14**: p. 163-76.
158. Sato Y and DB Rifkin: **Inhibition of endothelial cell movement by pericytes and smooth muscle cells: activation of a latent transforming growth factor-beta 1-like molecule by plasmin during co-culture.** *J Cell Biol* 1989. **109**: p. 309-15.
159. Hausser H, A Groning, A Hasilik, E Schonherr, and H Kresse: **Selective inactivity of TGF-beta/decorin complexes.** *FEBS Lett* 1994. **353**: p. 243-5.
160. Markmann A, H Hausser, E Schonherr, and H Kresse: **Influence of decorin expression on transforming growth factor-beta-mediated collagen gel retraction and biglycan induction.** *Matrix Biol* 2000. **19**: p. 631-6.
161. Kolb M, PJ Margetts, PJ Sime, and J Gauldie: **Proteoglycans decorin and biglycan differentially modulate TGF-beta-mediated fibrotic responses in the lung.** *Am J Physiol Lung Cell Mol Physiol* 2001. **280**: p. L1327-34.
162. Noordhoek JA, DS Postma, LL Chong, L Menkema, HF Kauffman, W Timens, JF van Straaten, and YM van der Geld: **Different modulation of decorin production by lung fibroblasts from patients with mild and severe emphysema.** *COPD* 2005. **2**: p. 17-25.
163. Gerwin BI, J Keski-Oja, M Seddon, JF Lechner, and CC Harris: **TGF-beta 1 modulation of urokinase and PAI-1 expression in human bronchial epithelial cells.** *Am J Physiol* 1990. **259**: p. L262-9.
164. Hu B, Z Wu, and SH Phan: **Smad3 mediates transforming growth factor-beta-induced alpha-smooth muscle actin expression.** *Am J Respir Cell Mol Biol* 2003. **29**: p. 397-404.
165. Jiang F, GS Liu, GJ Dusting, and EC Chan: **NADPH oxidase-dependent redox signaling in TGF-beta-mediated fibrotic responses.** *Redox Biol* 2014. **2**: p. 267-72.

166. Kenyon NJ, RW Ward, G McGrew, and JA Last: **TGF-beta1 causes airway fibrosis and increased collagen I and III mRNA in mice.** *Thorax* 2003. **58**: p. 772-7.
167. Hecker L, R Vittal, T Jones, R Jagirdar, TR Luckhardt, JC Horowitz, S Pennathur, FJ Martinez, and VJ Thannickal: **NADPH oxidase-4 mediates myofibroblast activation and fibrogenic responses to lung injury.** *Nat Med* 2009. **15**: p. 1077-81.
168. Amara N, D Goven, F Prost, R Muloway, B Crestani, and J Boczkowski: **NOX4/NADPH oxidase expression is increased in pulmonary fibroblasts from patients with idiopathic pulmonary fibrosis and mediates TGFbeta1-induced fibroblast differentiation into myofibroblasts.** *Thorax* 2010. **65**: p. 733-8.
169. Shapiro SD: **Proteinases in chronic obstructive pulmonary disease.** *Biochem Soc Trans* 2002. **30**: p. 98-102.
170. Saetta M, A Di Stefano, G Turato, FM Facchini, L Corbino, CE Mapp, P Maestrelli, A Ciaccia, and LM Fabbri: **CD8+ T-lymphocytes in peripheral airways of smokers with chronic obstructive pulmonary disease.** *Am J Respir Crit Care Med* 1998. **157**: p. 822-6.
171. Dhami R, B Gilks, C Xie, K Zay, JL Wright, and A Churg: **Acute cigarette smoke-induced connective tissue breakdown is mediated by neutrophils and prevented by alpha1-antitrypsin.** *Am J Respir Cell Mol Biol* 2000. **22**: p. 244-52.
172. Rennard SI: **Cigarette smoke in research.** *Am J Respir Cell Mol Biol* 2004. **31**: p. 479-80.
173. Erjefalt JS, I Erjefalt, F Sundler, and CG Persson: **In vivo restitution of airway epithelium.** *Cell Tissue Res* 1995. **281**: p. 305-16.
174. Horiba K and Y Fukuda: **Synchronous appearance of fibronectin, integrin alpha 5 beta 1, vinculin and actin in epithelial cells and fibroblasts during rat tracheal wound healing.** *Virchows Arch* 1994. **425**: p. 425-34.
175. Rickard KA, J Taylor, SI Rennard, and JR Spurzem: **Migration of bovine bronchial epithelial cells to extracellular matrix components.** *Am J Respir Cell Mol Biol* 1993. **8**: p. 63-8.
176. Park KS, JM Wells, AM Zorn, SE Wert, VE Laubach, LG Fernandez, and JA Whitsett: **Transdifferentiation of ciliated cells during repair of the respiratory epithelium.** *Am J Respir Cell Mol Biol* 2006. **34**: p. 151-7.
177. Sirianni FE, A Milaninezhad, FS Chu, and DC Walker: **Alteration of fibroblast architecture and loss of Basal lamina apertures in human emphysematous lung.** *Am J Respir Crit Care Med* 2006. **173**: p. 632-8.
178. Zandvoort A, DS Postma, MR Jonker, JA Noordhoek, JT Vos, YM van der Geld, and W Timens: **Altered expression of the Smad signalling pathway: implications for COPD pathogenesis.** *Eur Respir J* 2006. **28**: p. 533-41.
179. Mannino DM, Homa DM, Akinbami LJ, Ford ES, Redd SC. Chronic obstructive pulmonary disease surveillance — United States, 1971 – 2000. Morbidity and Mortality Weekly Report. 2002;51(SS-6):1–16.
180. Centers for Disease Control and Prevention. National Center for Health Statistics. National Hospital Discharge Survey, 2010. Analysis performed by American Lung Association Research and Health Education using SPSS and SUDAAN software.
181. Churg A, R Wang, X Wang, PO Onnervik, K Thim, and JL Wright: **Effect of an MMP-9/MMP-12 inhibitor on smoke-induced emphysema and airway remodelling in guinea pigs.** *Thorax* 2007. **62**: p. 706-13.

182. Hogg JC: **Pathophysiology of airflow limitation in chronic obstructive pulmonary disease.** *Lancet* 2004. **364**: p. 709-21.
183. Gosselink JV, S Hayashi, WM Elliott, L Xing, B Chan, L Yang, C Wright, D Sin, PD Pare, JA Pierce, RA Pierce, A Patterson, J Cooper, and JC Hogg: **Differential expression of tissue repair genes in the pathogenesis of chronic obstructive pulmonary disease.** *Am J Respir Crit Care Med* 2010. **181**: p. 1329-35.
184. Podowski M, C Calvi, S Metzger, K Misono, H Poonyagariyagorn, A Lopez-Mercado, T Ku, T Lauer, S McGrath-Morrow, A Berger, C Cheadle, R Tudor, HC Dietz, W Mitzner, R Wise, and E Neptune: **Angiotensin receptor blockade attenuates cigarette smoke-induced lung injury and rescues lung architecture in mice.** *J Clin Invest* 2012. **122**: p. 229-40.
185. Rangasamy T, CY Cho, RK Thimmulappa, L Zhen, SS Srisuma, TW Kensler, M Yamamoto, I Petrache, RM Tudor, and S Biswal: **Genetic ablation of Nrf2 enhances susceptibility to cigarette smoke-induced emphysema in mice.** *J Clin Invest* 2004. **114**: p. 1248-59.
186. Jeffery PK: **Remodeling in asthma and chronic obstructive lung disease.** *Am J Respir Crit Care Med* 2001. **164**: p. S28-38.
187. Roos AB, C Sanden, M Mori, L Bjermer, MR Stampfli, and JS Erjefalt: **IL-17A is Elevated in End-stage COPD and Contributes to Cigarette Smoke-induced Lymphoid Neogenesis.** *Am J Respir Crit Care Med* 2015.
188. March TH, JA Wilder, DC Esparza, PY Cossey, LF Blair, LK Herrera, JD McDonald, MJ Campen, JL Mauderly, and J Segrave: **Modulators of cigarette smoke-induced pulmonary emphysema in A/J mice.** *Toxicol Sci* 2006. **92**: p. 545-59.
189. Pack RJ, LH Al-Ugaily, and G Morris: **The cells of the tracheobronchial epithelium of the mouse: a quantitative light and electron microscope study.** *J Anat* 1981. **132**: p. 71-84.
190. Ionescu C, E Derom, and R De Keyser: **Assessment of respiratory mechanical properties with constant-phase models in healthy and COPD lungs.** *Comput Methods Programs Biomed* 2010. **97**: p. 78-85.
191. Battig K, R Buzzi, and R Nil: **Smoke yield of cigarettes and puffing behavior in men and women.** *Psychopharmacology (Berl)* 1982. **76**: p. 139-48.
192. Tam A, A Churg, JL Wright, S Zhou, M Kirby, HO Coxson, S Lam, SF Man, and DD Sin: **Sex Differences in Airway Remodeling in a Mouse Model of Chronic Obstructive Pulmonary Disease.** *Am J Respir Crit Care Med* 2015.
193. De Langhe E, G Vande Velde, J Hostens, U Himmelreich, B Nemery, FP Luyten, J Vanoirbeek, and RJ Lories: **Quantification of lung fibrosis and emphysema in mice using automated micro-computed tomography.** *PLoS One* 2012. **7**: p. e43123.
194. Counter WB, IQ Wang, TH Farncombe, and NR Labiris: **Airway and pulmonary vascular measurements using contrast-enhanced micro-CT in rodents.** *Am J Physiol Lung Cell Mol Physiol* 2013. **304**: p. L831-43.
195. Church DF and WA Pryor: **Free-radical chemistry of cigarette smoke and its toxicological implications.** *Environ Health Perspect* 1985. **64**: p. 111-26.
196. Mollerup S, D Ryberg, A Hewer, DH Phillips, and A Haugen: **Sex differences in lung CYP1A1 expression and DNA adduct levels among lung cancer patients.** *Cancer Res* 1999. **59**: p. 3317-20.

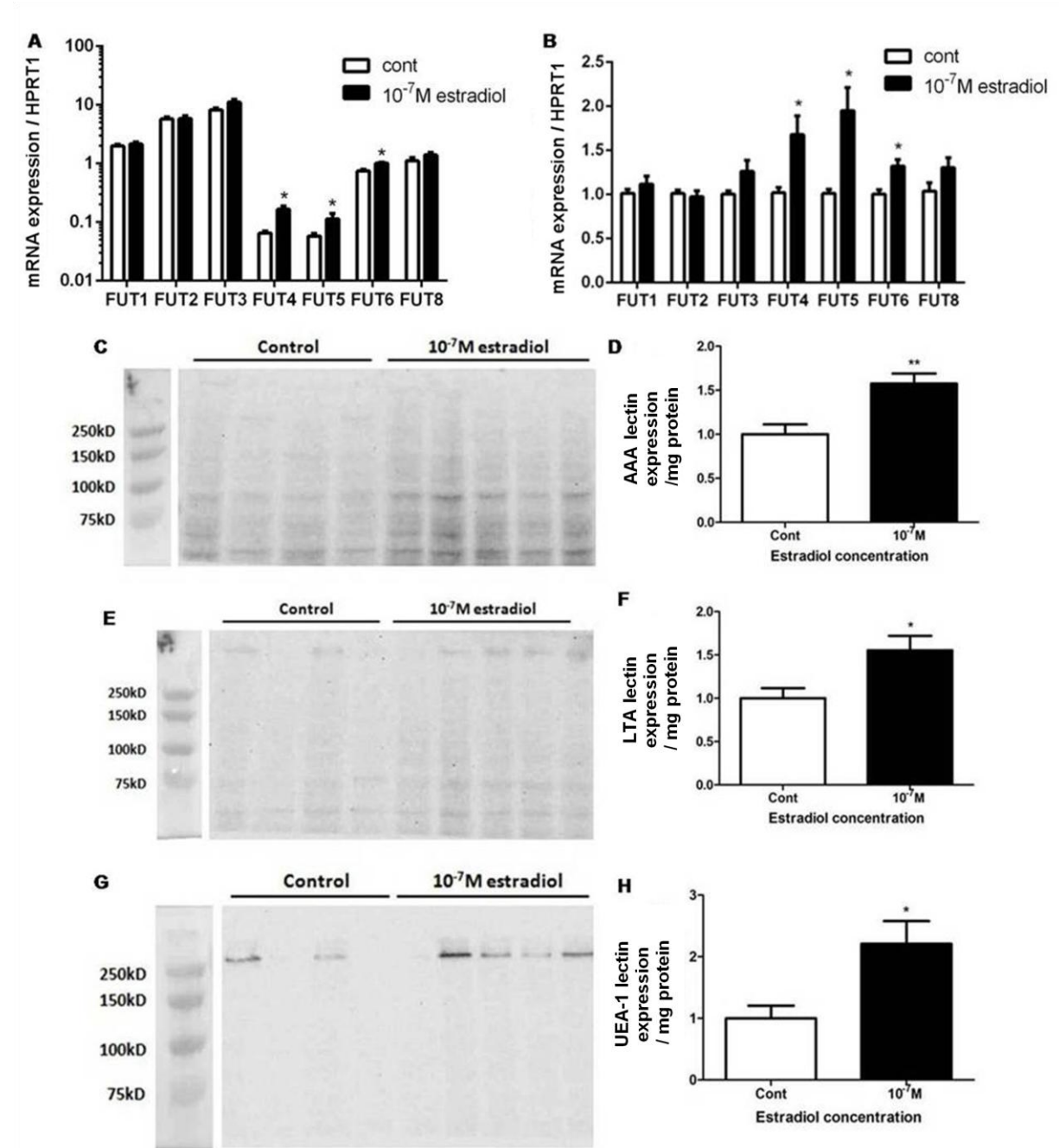
197. Zhang H, SW Sunnarborg, KK McNaughton, TG Johns, DC Lee, and JE Faber: **Heparin-binding epidermal growth factor-like growth factor signaling in flow-induced arterial remodeling.** *Circ Res* 2008. **102**: p. 1275-85.
198. Bourdeau V, J Deschenes, R Metivier, Y Nagai, D Nguyen, N Bretschneider, F Gannon, JH White, and S Mader: **Genome-wide identification of high-affinity estrogen response elements in human and mouse.** *Mol Endocrinol* 2004. **18**: p. 1411-27.
199. Kwak MK, K Itoh, M Yamamoto, TR Sutter, and TW Kensler: **Role of transcription factor Nrf2 in the induction of hepatic phase 2 and antioxidative enzymes in vivo by the cancer chemoprotective agent, 3H-1, 2-dimethiole-3-thione.** *Mol Med* 2001. **7**: p. 135-45.
200. Cho HY and SR Kleeberger: **Nrf2 protects against airway disorders.** *Toxicol Appl Pharmacol* 2010. **244**: p. 43-56.
201. Kharat I and F Saatcioglu: **Antiestrogenic effects of 2,3,7,8-tetrachlorodibenzo-p-dioxin are mediated by direct transcriptional interference with the liganded estrogen receptor. Cross-talk between aryl hydrocarbon- and estrogen-mediated signaling.** *J Biol Chem* 1996. **271**: p. 10533-7.
202. Ansell PJ, C Espinosa-Nicholas, EM Curran, BM Judy, BJ Philips, M Hannink, and DB Lubahn: **In vitro and in vivo regulation of antioxidant response element-dependent gene expression by estrogens.** *Endocrinology* 2004. **145**: p. 311-7.
203. Ansell PJ, SC Lo, LG Newton, C Espinosa-Nicholas, DD Zhang, JH Liu, M Hannink, and DB Lubahn: **Repression of cancer protective genes by 17beta-estradiol: ligand-dependent interaction between human Nrf2 and estrogen receptor alpha.** *Mol Cell Endocrinol* 2005. **243**: p. 27-34.
204. Montano MM and BS Katzenellenbogen: **The quinone reductase gene: a unique estrogen receptor-regulated gene that is activated by antiestrogens.** *Proc Natl Acad Sci U S A* 1997. **94**: p. 2581-6.
205. Lind C, E Cadenas, P Hochstein, and L Ernster: **DT-diaphorase: purification, properties, and function.** *Methods Enzymol* 1990. **186**: p. 287-301.
206. Siegel D, EM Bolton, JA Burr, DC Liebler, and D Ross: **The reduction of alpha-tocopherolquinone by human NAD(P)H: quinone oxidoreductase: the role of alpha-tocopherolhydroquinone as a cellular antioxidant.** *Mol Pharmacol* 1997. **52**: p. 300-5.
207. Siegel D, DL Gustafson, DL Dehn, JY Han, P Boonchoong, LJ Berliner, and D Ross: **NAD(P)H:quinone oxidoreductase 1: role as a superoxide scavenger.** *Mol Pharmacol* 2004. **65**: p. 1238-47.
208. Chan TS, S Teng, JX Wilson, G Galati, S Khan, and PJ O'Brien: **Coenzyme Q cytoprotective mechanisms for mitochondrial complex I cytopathies involves NAD(P)H: quinone oxidoreductase 1(NQO1).** *Free Radic Res* 2002. **36**: p. 421-7.
209. Winski SL, Y Koutalos, DL Bentley, and D Ross: **Subcellular localization of NAD(P)H:quinone oxidoreductase 1 in human cancer cells.** *Cancer Res* 2002. **62**: p. 1420-4.
210. Poss KD and S Tonegawa: **Reduced stress defense in heme oxygenase 1-deficient cells.** *Proc Natl Acad Sci U S A* 1997. **94**: p. 10925-30.
211. Zhong J and M Roth: **Lung remodeling mechanisms in chronic lung diseases.** *Curr Opin Allergy Clin Immunol* 2014. **14**: p. 69-76.

212. Wang RD, H Tai, C Xie, X Wang, JL Wright, and A Churg: **Cigarette smoke produces airway wall remodeling in rat tracheal explants.** *Am J Respir Crit Care Med* 2003. **168**: p. 1232-6.
213. Borbely G, I Szabadkai, Z Horvath, P Marko, Z Varga, N Breza, F Baska, T Vantus, M Huszar, M Geiszt, L Hunyady, L Buday, L Orfi, and G Keri: **Small-molecule inhibitors of NADPH oxidase 4.** *J Med Chem* 2010. **53**: p. 6758-62.
214. Sheehan JK, S Kirkham, M Howard, P Woodman, S Kutay, C Brazeau, J Buckley, and DJ Thornton: **Identification of molecular intermediates in the assembly pathway of the MUC5AC mucin.** *J Biol Chem* 2004. **279**: p. 15698-705.
215. Wickstrom C, JR Davies, GV Eriksen, EC Veerman, and I Carlstedt: **MUC5B is a major gel-forming, oligomeric mucin from human salivary gland, respiratory tract and endocervix: identification of glycoforms and C-terminal cleavage.** *Biochem J* 1998. **334 (Pt 3)**: p. 685-93.
216. Smirnova MG, L Guo, JP Birchall, and JP Pearson: **LPS up-regulates mucin and cytokine mRNA expression and stimulates mucin and cytokine secretion in goblet cells.** *Cell Immunol* 2003. **221**: p. 42-9.
217. Yoon JH, KS Kim, HU Kim, JA Linton, and JG Lee: **Effects of TNF-alpha and IL-1 beta on mucin, lysozyme, IL-6 and IL-8 in passage-2 normal human nasal epithelial cells.** *Acta Otolaryngol* 1999. **119**: p. 905-10.
218. Chen Y, P Thai, YH Zhao, YS Ho, MM DeSouza, and R Wu: **Stimulation of airway mucin gene expression by interleukin (IL)-17 through IL-6 paracrine/autocrine loop.** *J Biol Chem* 2003. **278**: p. 17036-43.
219. Danahay H, H Atherton, G Jones, RJ Bridges, and CT Poll: **Interleukin-13 induces a hypersecretory ion transport phenotype in human bronchial epithelial cells.** *Am J Physiol Lung Cell Mol Physiol* 2002. **282**: p. L226-36.
220. Voynow JA, LR Young, Y Wang, T Horger, MC Rose, and BM Fischer: **Neutrophil elastase increases MUC5AC mRNA and protein expression in respiratory epithelial cells.** *Am J Physiol* 1999. **276**: p. L835-43.
221. Takeyama K, K Dabbagh, HM Lee, C Agusti, JA Lausier, IF Ueki, KM Grattan, and JA Nadel: **Epidermal growth factor system regulates mucin production in airways.** *Proc Natl Acad Sci U S A* 1999. **96**: p. 3081-6.
222. Shao MX, T Nakanaga, and JA Nadel: **Cigarette smoke induces MUC5AC mucin overproduction via tumor necrosis factor-alpha-converting enzyme in human airway epithelial (NCI-H292) cells.** *Am J Physiol Lung Cell Mol Physiol* 2004. **287**: p. L420-7.
223. Kohri K, IF Ueki, JJ Shim, PR Burgel, YM Oh, DC Tam, T Dao-Pick, and JA Nadel: **Pseudomonas aeruginosa induces MUC5AC production via epidermal growth factor receptor.** *Eur Respir J* 2002. **20**: p. 1263-70.
224. Dougherty SM, W Mazhawidza, AR Bohn, KA Robinson, KA Mattingly, KA Blankenship, MO Huff, WG McGregor, and CM Klinge: **Gender difference in the activity but not expression of estrogen receptors alpha and beta in human lung adenocarcinoma cells.** *Endocr Relat Cancer* 2006. **13**: p. 113-34.
225. Gruenert DC, CB Basbaum, MJ Welsh, M Li, WE Finkbeiner, and JA Nadel: **Characterization of human tracheal epithelial cells transformed by an origin-defective simian virus 40.** *Proc Natl Acad Sci U S A* 1988. **85**: p. 5951-5.

226. Dave V, T Childs, Y Xu, M Ikegami, V Besnard, Y Maeda, SE Wert, JR Neilson, GR Crabtree, and JA Whitsett: **Calcineurin/Nfat signaling is required for perinatal lung maturation and function.** *J Clin Invest* 2006. **116**: p. 2597-609.
227. Dave V, T Childs, and JA Whitsett: **Nuclear factor of activated T cells regulates transcription of the surfactant protein D gene (Sftpd) via direct interaction with thyroid transcription factor-1 in lung epithelial cells.** *J Biol Chem* 2004. **279**: p. 34578-88.
228. Smith PL, JT Myers, CE Rogers, L Zhou, B Petryniak, DJ Becker, JW Homeister, and JB Lowe: **Conditional control of selectin ligand expression and global fucosylation events in mice with a targeted mutation at the FX locus.** *J Cell Biol* 2002. **158**: p. 801-15.
229. Becker DJ and JB Lowe: **Fucose: biosynthesis and biological function in mammals.** *Glycobiology* 2003. **13**: p. 41R-53R.
230. Compton DR, S Sheng, KE Carlson, NA Rebacz, IY Lee, BS Katzenellenbogen, and JA Katzenellenbogen: **Pyrazolo[1,5-a]pyrimidines: estrogen receptor ligands possessing estrogen receptor beta antagonist activity.** *J Med Chem* 2004. **47**: p. 5872-93.
231. Sun J, YR Huang, WR Harrington, S Sheng, JA Katzenellenbogen, and BS Katzenellenbogen: **Antagonists selective for estrogen receptor alpha.** *Endocrinology* 2002. **143**: p. 941-7.
232. Rao A, C Luo, and PG Hogan: **Transcription factors of the NFAT family: regulation and function.** *Annu Rev Immunol* 1997. **15**: p. 707-47.
233. Seminario MC, J Guo, BS Bochner, LA Beck, and SN Georas: **Human eosinophils constitutively express nuclear factor of activated T cells p and c.** *J Allergy Clin Immunol* 2001. **107**: p. 143-52.
234. Yan F, W Li, H Zhou, Y Wu, S Ying, Z Chen, and H Shen: **Interleukin-13-induced MUC5AC expression is regulated by a PI3K-NFAT3 pathway in mouse tracheal epithelial cells.** *Biochem Biophys Res Commun* 2014. **446**: p. 49-53.
235. Takeda M, M Tanabe, W Ito, S Ueki, Y Konno, M Chihara, M Itoga, Y Kobayashi, Y Moritoki, H Kayaba, and J Chihara: **Gender difference in allergic airway remodelling and immunoglobulin production in mouse model of asthma.** *Respirology* 2013. **18**: p. 797-806.
236. Fonseca BP, PC Olsen, LP Coelho, TP Ferreira, HS Souza, MA Martins, and JP Viola: **NFAT1 transcription factor regulates pulmonary allergic inflammation and airway responsiveness.** *Am J Respir Cell Mol Biol* 2009. **40**: p. 66-75.
237. Tam A, S Wadsworth, D Dorscheid, SF Man, and DD Sin: **Estradiol increases mucus synthesis in bronchial epithelial cells.** *PLoS One* 2014. **9**: p. e100633.
238. Warner SM, TL Hackett, F Shaheen, TS Hallstrand, A Kicic, SM Stick, and DA Knight: **Transcription factor p63 regulates key genes and wound repair in human airway epithelial basal cells.** *Am J Respir Cell Mol Biol* 2013. **49**: p. 978-88.
239. Chung WC, SH Ryu, H Sun, DC Zeldin, and JS Koo: **CREB mediates prostaglandin F2alpha-induced MUC5AC overexpression.** *J Immunol* 2009. **182**: p. 2349-56.
240. Choi HJ, YS Chung, HJ Kim, UY Moon, YH Choi, I Van Seuning, SJ Baek, HG Yoon, and JH Yoon: **Signal pathway of 17beta-estradiol-induced MUC5B expression in human airway epithelial cells.** *Am J Respir Cell Mol Biol* 2009. **40**: p. 168-78.
241. Tam A, S Wadsworth, D Dorscheid, SF Man, and DD Sin: **The airway epithelium: more than just a structural barrier.** *Thorax* 2011. **5**: p. 255-73.

242. Jain R, JM Ray, JH Pan, and SL Brody: **Sex hormone-dependent regulation of cilia beat frequency in airway epithelium.** *Am J Respir Cell Mol Biol* 2012. **46**: p. 446-53.
243. Tyner JW, EY Kim, K Ide, MR Pelletier, WT Roswit, JD Morton, JT Battaile, AC Patel, GA Patterson, M Castro, MS Spoor, Y You, SL Brody, and MJ Holtzman: **Blocking airway mucous cell metaplasia by inhibiting EGFR antiapoptosis and IL-13 transdifferentiation signals.** *J Clin Invest* 2006. **116**: p. 309-21.
244. Laoukili J, E Perret, T Willems, A Minty, E Parthoens, O Houcine, A Coste, M Jorissen, F Marano, D Caput, and F Tournier: **IL-13 alters mucociliary differentiation and ciliary beating of human respiratory epithelial cells.** *J Clin Invest* 2001. **108**: p. 1817-24.
245. Hogan PG, L Chen, J Nardone, and A Rao: **Transcriptional regulation by calcium, calcineurin, and NFAT.** *Genes Dev* 2003. **17**: p. 2205-32.
246. Lee MY, SM Garvey, AS Baras, JA Lemmon, MF Gomez, PD Schoppee Bortz, G Daum, RC LeBoeuf, and BR Wamhoff: **Integrative genomics identifies DSCR1 (RCAN1) as a novel NFAT-dependent mediator of phenotypic modulation in vascular smooth muscle cells.** *Hum Mol Genet* 2010. **19**: p. 468-79.
247. Giffin MJ, JC Stroud, DL Bates, KD von Koenig, J Hardin, and L Chen: **Structure of NFAT1 bound as a dimer to the HIV-1 LTR kappa B element.** *Nat Struct Biol* 2003. **10**: p. 800-6.
248. Jin L, P Sliz, L Chen, F Macian, A Rao, PG Hogan, and SC Harrison: **An asymmetric NFAT1 dimer on a pseudo-palindromic kappa B-like DNA site.** *Nat Struct Biol* 2003. **10**: p. 807-11.
249. Fujisawa T, S Velichko, P Thai, LY Hung, F Huang, and R Wu: **Regulation of airway MUC5AC expression by IL-1beta and IL-17A; the NF-kappaB paradigm.** *J Immunol* 2009. **183**: p. 6236-43.
250. Afhuppe W, JM Beekman, C Otto, D Korr, J Hoffmann, U Fuhrmann, and C Moller: **In vitro characterization of ZK 230211--A type III progesterone receptor antagonist with enhanced antiproliferative properties.** *J Steroid Biochem Mol Biol* 2010. **119**: p. 45-55.
251. Malhotra D, R Thimmulappa, A Navas-Acien, A Sandford, M Elliott, A Singh, L Chen, X Zhuang, J Hogg, P Pare, RM Tuder, and S Biswal: **Expression of concern: Decline in NRF2-regulated antioxidants in chronic obstructive pulmonary disease lungs due to loss of its positive regulator, DJ-1.** *Am J Respir Crit Care Med* 2008. **178**: p. 592-604.
252. Barnes PJ: **New anti-inflammatory targets for chronic obstructive pulmonary disease.** *Nat Rev Drug Discov* 2013. **12**: p. 543-59.

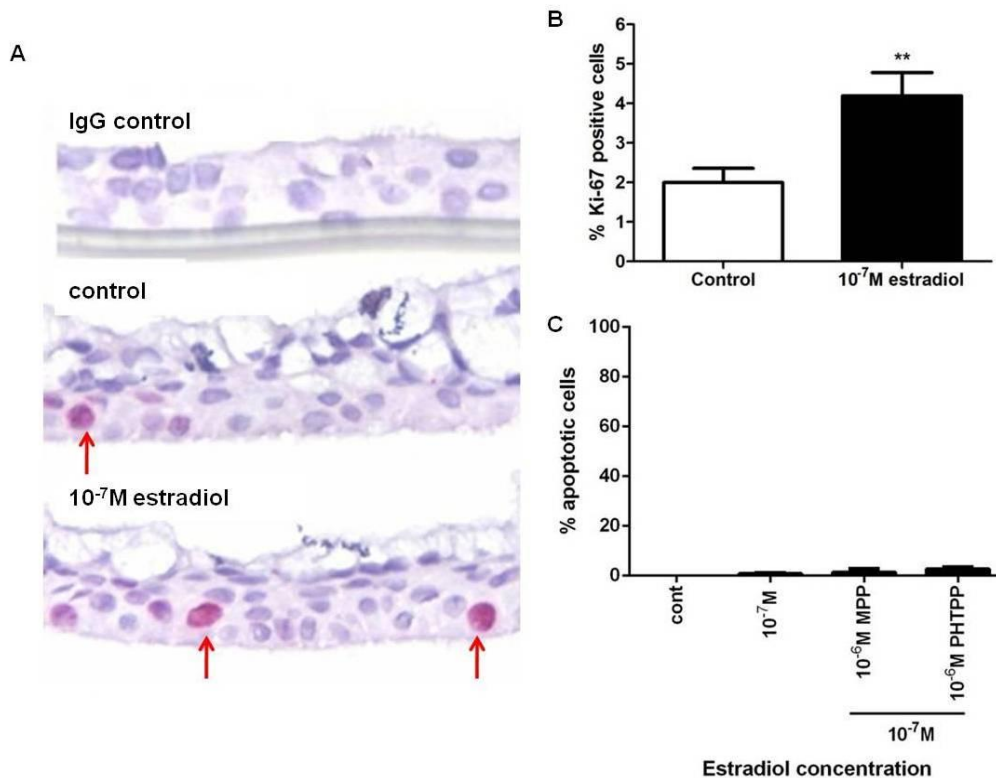
Appendices



Appendix 1: Effects of estradiol on fucosyltransferase mRNA expression in ALI cultures.

10^{-7} M estradiol (black bars) increased FUT-4, -5 and -6 mRNA expression compared with vehicle control (white bars). Data are expressed as A) absolute change in C_t value normalized to HPRT1 and B) fold increase in mRNA expression over vehicle control normalized using HPRT1. Total fucose sugar residues in the cytoplasmic protein fractions of ALI cultures were determined by lectin binding assays. Fucose residues were significantly increased with 10^{-7} M

estradiol using fucose binding lectins, C-D) AAA, E-F) LTA and G-H) UEA-1. D, F, and H are densitometric quantifications of C, E, and G, respectively. The intensity of all bands in each lane in detecting total fucose residues were quantified using the software program Image J and normalized to total protein loaded per lane in milligrams. Data is expressed as fold increase over vehicle control. Values shown are mean \pm SEM of experiments performed with N=4 donors. * $P < 0.05$, ** $P < 0.01$ compared against vehicle control. Non-parametric t-tests were used in all statistical analyses.



Appendix 2: Effects of estradiol on cell proliferation and apoptosis in ALI cultures.

A) Cell proliferation in ALI cultures was assessed by Ki-67 staining. B) Estradiol enhanced Ki67-positive cell staining in the basal epithelium. C) Quantification of % apoptotic cells by cell counting in ALI cultures counter-stained with methyl green for nuclei. Images are representative of 4 different donors. ** $P < 0.01$ represents statistical significance compared against control using non-parametric t-test in B. One-way ANOVA with Bonferroni's multiple comparisons test was used in C.